



**HAL**  
open science

# Autologous cell-laden hydrogel sheet for prevention of post-surgical abdominal adhesion

Lucie Bresson

► **To cite this version:**

Lucie Bresson. Autologous cell-laden hydrogel sheet for prevention of post-surgical abdominal adhesion. Human health and pathology. Université du Droit et de la Santé - Lille II, 2017. English. NNT : 2017LIL2S033 . tel-01835340

**HAL Id: tel-01835340**

**<https://theses.hal.science/tel-01835340>**

Submitted on 11 Jul 2018

**HAL** is a multi-disciplinary open access archive for the deposit and dissemination of scientific research documents, whether they are published or not. The documents may come from teaching and research institutions in France or abroad, or from public or private research centers.

L'archive ouverte pluridisciplinaire **HAL**, est destinée au dépôt et à la diffusion de documents scientifiques de niveau recherche, publiés ou non, émanant des établissements d'enseignement et de recherche français ou étrangers, des laboratoires publics ou privés.



COLLEGE DOCTORAL

École Doctorale  
BIOLOGIE SANTÉ



UNIVERSITE LILLE 2 DROIT ET SANTE  
ECOLE DOCTORALE BIOLOGIE SANTE DE LILLE

Année : 2017

THESE D'UNIVERSITE

Plaque d'hydrogel chargée de cellules autologues pour la prévention des adhérences postopératoires abdominales

Autologous cell-laden hydrogel sheet for prevention of post-surgical abdominal adhesion

Présentée et soutenue publiquement le 10 novembre 2017 par

Lucie BRESSON

Thèse dirigée par Madame le Docteur Feng Chai et Monsieur le Professeur Teru Okitsu

Travail de recherche réalisé au sein de l'Unité INSERM U1008- Biomatériaux

Dirigée par Monsieur le Professeur Juergen Siepmann

---

JURY

Rapporteurs :

Monsieur le Professeur Renaud de Tayrac

Membres du Jury

Madame le Docteur Feng Chai

Monsieur le Professeur Teru Okitsu

Madame le Professeur Joëlle Amédée

Madame le Professeur Chrystèle Rubod

Monsieur le Docteur Eric Leblanc

## **Acknowledgments**

To my thesis directors

Dr Feng Chai

INSERM U1008 Groupe Recherche en Biomatériaux, Faculté de Médecine, Lille

I would first like to thank you to accept to conduct this work three years ago, teaching me your knowledge and your rigor.

Pr Teru Okitsu

Center for International Research on Biomedical Systems (CIBiS), Institute of Industrial Science, The University of Tokyo, Meguro, Tokyo, Japan

SMMILE program, Institut pour la Recherche sur le Cancer de Lille, Boulevard du Pr. Jules Leclercq, Lille, France.

I would like to express my sincere gratitude to you for the support of my Ph.D study, for your guidance and your knowledge.

To the examiner

Professor Renaud de Tayrac

Chef de Service de Gynécologie-Obstétrique, CHRU de Nîmes

I want to express my gratitude to you for the review of the manuscript. Your knowledge and insights in the field of adhesion prevention and gynecology are essential for reviewing my work.

To the committee members

Professor Joëlle Amédée

Research Director Inserm U1026 BioTis « Tissue Bioengineering »

Director of Research Federative structure "Technology for Health"

University of Bordeaux.

I am glad to be judged by you as I appreciate your vast knowledge and skill in the field of regenerative therapies.

Professor Chrystèle Rubod dit Guillet

Professeur de Chirurgie Gynécologique, Hôpital Jeanne de Flandre, CHRU de Lille

My sincere thanks also goes to you for teaching me gynecology and surgery during my residence and fellowship, still offering me your knowledge and your patience. Once again, faithfully, you accepted to participate to my work during this three last years and to judge my final dissertation.

Doctor Eric Leblanc

Chef de service du Département de chirurgie et d'oncologie gynécologique,

Centre Oscar Lambret, Lille

Firstly I would like to thank you for giving me the wonderful opportunity to work with you. You are my teacher in the field of surgery and I thank you for all the advices, ideas, moral support and patience in guiding me through these last five years. Your wealth of knowledge in the field of gynecology, oncology and surgery is unbelievable. Thank you also for your enthusiasm for my PhD work. You suggested the topic to me, and still asking me about the advancement of the project. You and Fabrice gave me all the time needed to go to the laboratory. I'll never forget how you made me feel good in your team.

I would like to thank Pr Lartigau, Pr Collard, and Dr Leclercq who proposed me this challenge. My research would not have been possible without their continuous help and support.

I am also grateful to the Canceropole Nord Ouest for helping and providing the funding for the PhD research.

The collaboration with 3-D Matrix and the use of BD-Purastat® would not have been possible without Pr Yukiko Matsunaga and Marie Buffier.

A very special gratitude goes out to the following laboratory team: Nicolas Blanchemain, Mickaël Maton, Maria José Garcia Fernandez, Carla Palomino Durand, Alejandra Corina Mogrovejo Valdivia, Claudia Flores Vilca, Marco Lopez, Alice Gauzit, Adrien Hertault, Alexandra Machado, Monique Bonnier, for their unfailing support, advising and assistance, but also for providing me with an excellent atmosphere for doing research.

I am indebted to my many of my colleagues to support me.

First of all, I am grateful to my colleague and friend Fabrice Narducci who have still supported me along the way.

I am also grateful to Florence Bochu, Corinne Spatscheck, and all the nurses of the operating theater for helping me for the sampling of the human tissues and for providing me equipments for my work.

Thanks to the following persons for providing support for the clinical trial : my colleagues surgeons, Dr Marie Cecile Le Deley and Pr Nicolas Penel, Marie Vanseymortier, and Julien Thery, from the department of clinical research. A special note of thanks should also be given to Severine Marchant for all the articles provided and to Emmanuelle Tresch, Emilie Bogear, and Jennifer Wallet. Your patience while explaining statistics was greatly appreciated.

I would also like to express my appreciation to Dr Anne Sophie Lemaire, Dr Juliette Beaujot, and Dr Yves Marie Robin from the Department of Anatomopathology, that gave me technical support with the making of histological slides. Thank you for teaching me to read these histological sections.

I would never have been able to finish my dissertation without the support from Chann! During the three years of my work, you was always there whenever I had questions, trouble spots or doubts.

Lastly I would like to thank Abel, my sons Alix, Marceau, Martin, and my friends Aude, Alain, Agat', Ghislain, Anne, Mona, Catagay, Momoko san, Nina, Yves, Karine, Thomas and Nath'. Your love and support, sense of humour, patience, optimism and advice were more valuable than you could ever imagine...

## Plan

Abstract	8
Abbreviations	
1. Part 1: STATE OF THE ART	
1.1. STATE OF THE ART OF MESOTHELIUM HISTOPHYSIOLOGY REPAIR AND ADHESION FORMATION	
1.1.1. Macroscopical description of the peritoneum	12
1.1.2. Microscopical description of the peritoneum	13
1.1.3. Functions of the peritoneum	14
1.1.4. Peritoneum healing	15
1.1.5. Adhesion formation	16
1.1.6. Clinical impact	18
1.1.7. Adhesion prevention, existing strategies in clinical practice	19
1.1.8. Adhesion prevention, potential strategies	23
1.2. STATE OF THE ART OF THE ANIMAL MODELS OF ADHESION	
1.2.1. Introduction	24
1.2.2. Adhesion creation	24
1.2.3. Clinical relevancy	30
1.2.4. Adhesion assessment	30
1.2.5. Conclusions	35
OBJECTIVES OF THE PROJECT	36-37
2. Part 2: METHOD AND RESULTS OF THE PROJECT	
2.1. CHAPTER 1: VALIDATION OF THE ANIMAL MODEL	
2.1.1. Introduction	39
2.1.2. Method	42
2.1.3. Results and discussion	43
2.1.4. Conclusions	48

## 2.2. CHAPTER 2: CHOICE OF CELL SOURCE

### 2.2.1. Mesothelial cells (MCs)

2.2.1.1.	Method	52
2.2.1.2.	Results and discussion	55
2.2.1.3.	Conclusions	57
2.2.1.4.	Perspectives	57

### 2.2.2. Adipose stem cells (ASCs)

2.2.2.1.	Method	60
2.2.2.2.	Results and discussion	64
2.2.2.3.	Conclusions	69
2.2.2.4.	Perspectives	70

## 2.3. CHAPTER 3: COMPARISON BETWEEN CELL-THERAPY AND CELL-LADENED SCAFFOLDS OR TISSUE-THERAPY

### 2.3.1. Introduction

### 2.3.2. Cell therapy using IP injection of MCs

2.3.2.1.	Method	73
2.3.2.2.	Results and discussion	74
2.3.2.3.	Conclusions	74

### 2.3.3. Comparison between cell-sheet therapy and tissue therapy (peritoneal graft)

2.3.3.1.	Introduction	75
2.3.3.2.	Method	75
2.3.3.3.	Experimental design and induction of standardized peritoneal lesion	75
2.3.3.3.1.	Preparation and transplantation of autologous peritoneal graft	77
2.3.3.3.2.	Preparation and implantation of bilayer cell sheet	78
2.3.3.4.	Results	78
2.3.3.4.1.	Macroscopic evaluation	80
2.3.3.4.2.	Histological evaluation	81

### 2.3.4. Discussion

### 2.3.5. Conclusion

2.4. CHAPTER 4: CHOICE OF SCAFFOLD MATERIALS	
2.4.1. Introduction	85
2.4.2. BD-Purastat <sup>®</sup> choice	87
2.4.3. BD-Purastat <sup>®</sup> dilution and gelation assays	87
2.4.4. Viability of <i>in vitro</i> encapsulated cells	89
2.4.5. <i>In vivo</i> transplantation of 0.5% BD-Purastat <sup>®</sup> into an animal model of adhesion	90
2.4.6. Conclusions	92
2.5. CHAPTER 5: IN VIVO APPLICATION OF CELL-LADENED BD-PURASTAT <sup>®</sup> GELS	
2.5.1. Cell type comparisons	93
2.5.2. MC density comparison for MCs laden 0,5% BD-Purastat <sup>®</sup> applications	94
2.5.3. Discussion	95
2.5.4. Conclusions	96
2.5.5. Perspectives	97
3. Part 3: CONCLUSIONS and PERSPECTIVES	
3.1. Conclusions	99
3.2. Perspectives	100
REFERENCES	103
PUBLICATIONS	114
PRESENTATIONS	114

## **Abbreviations**

SVF Stromal vascular fraction

PBS phosphate buffered saline

FBS fetal bovin serum

ASC adipose stem cell

MC mesothelial cell

FB Fibroblast

MSC mesenchymal stem cell

TEM transmission electron microscopy

SEM scanning electron microscopy

EMT epithelial-to-mesenchymal transition

SMMIL-E seeding microsystems in medecin in Lille

ANSM agence nationale de securité du medicament

PLGA poly-lactic-co-glycolic acid

PEG poly-ethylene glycol

GAG glycosaminoglycane

ECM extra cellular matrix

## Abstract

Autologous cell-laden hydrogel sheet for prevention of post-operative abdominal adhesion

Introduction: Postoperative abdominal adhesions are a major complication leading to medical and economical problems. Replace injured peritoneum, which is composed of a monolayer of mesothelial cells (MC), using cell-therapy or cell-laden scaffold are two promising strategies to prevent adhesions. MC as functional and differentiated cells are crucial. However, adipose stem cells (ASCs) could replace MCs thanks to their potential of differentiation. Furthermore, hydrogel polymers are attractive scaffolds mimicking the properties of the native ECM. So, milestones of our project of regenerative medicine are comparison of cell-laden scaffolds and cell-therapy, choice of cell source and biomaterial, and finally transplantation of the cell-laden hydrogel scaffold, in a pre-established rat model of adhesion.

Material and Method: Firstly, models of adhesion were compared using different peritoneal injuries. Then, MCs and ASCs were compared for isolation, culture, characterization, and differentiation. Next, cell-therapy using MC intra peritoneal injection (IP) or cell-sheet technology was compared with tissue-therapy using peritoneal grafts through a *proof of concept* study. BD-Purastat<sup>®</sup> hydrogel was tested in collaboration with 3D Matrix firm. Cell-laden hydrogel gels were implanted and assessed on adhesion prevention.

Results: Two animal models of adhesion were validated and both techniques were effective and clinically relevant. MCs and ASCs were isolated from respectively tunica vaginalis and subcutaneous inguinal fat pad. MCs, with typical cobble-stone morphology and bright edges, were positively stained for vimentin and cytokeratin. Senescence arrived after only three passages for these adult well-differentiated cells. Spindle-shaped ASCs had a good capacity of expansion, were able to differentiate in osteocytes and adipocytes, and to form colonies as expected for stem cells. Autologous peritoneal grafts prevented postoperative abdominal adhesions in the rat model. As the mechanism of this prevention, the MC survived and contributed to reperitonealization, only when they were transplanted as a part of the autologous peritoneal grafts and were located on the surface exposed to the abdomen. Cell sheet technology and MCs IP injection failed in the adhesion prevention. BD-Purastat<sup>®</sup> presented good mechanical properties and biocompatibility. Alone, it reduced significantly adhesion extent. But, cell encapsulation into BD-Purastat<sup>®</sup> did not improve this prevention.

Conclusion and perspectives: Our study supported that MCs and scaffold are both needed to succeed in peritoneum's engineering to prevent adhesion. ASCs differentiation into MCs phenotype has still to be shown. BD- Purastat<sup>®</sup> decreases adhesion extent and behavior of the cell into this scaffold needs to be studied to improve the effectiveness of the cell-laden hydrogel application.

**Key words:**

Post-operative abdominal adhesion, prevention, tissue therapy, autologous cells, hydrogel

1. Part 1

STATE OF THE ART

The abdominal surgery, from minimally invasive procedures to laparotomies, can cause damages on the peritoneum, the serous membrane covering all the abdominal cavity (1). One of the most common consequence is abdominal adhesion, which occurs in ~90% of patients after abdominal surgery and can result in complications, e.g. intestinal obstructions, infertility in women, and chronic lower abdominal pain. It is reported in a cohort study that 32.6% of patients who had lower abdominal surgery required re-admissions due to potential adhesion-related problems. Managing adhesions and their related complications impose an enormous economic burden.

Gynecologic surgery is interested in healing patients with ovarian, uterine, vulvae and peritoneal diseases. As a part of abdominal surgery, most of gynecologic surgery is performed in the abdominal cavity. In the case of young women suffering from endometriosis or myomas, surgeon needs to preserve the fertility and adhesion prevention is crucial. Furthermore, re-intervention rate, especially in endometriosis management, is high and involves also being efficient in adhesion prevention. For oncological practice, surgeon deals with the same objectives in an additional context of associated treatments such as radiotherapy and chemotherapy, which could already have damaged peritoneum.

## 1.1. State of the art of mesothelium, histophysiology, repair and adhesion formation

### 1.1.1. Macroscopical description of the peritoneum

The mesothelium extends as a monolayer over the entire surface of the three serosal cavities (pleural, pericardial and peritoneal) and, in the males, it also lines the sac that surrounds the testes. During fetal development, the part of the peritoneum, which descends with the testes into the scrotum, is called tunica vaginalis. The peritoneum is the largest serous membrane of the human body. Parietal peritoneum lines the inner surface of the abdominal walls. Visceral peritoneum integrates with the outer serosal layers of organs, thereby covering the visceral organs (Figure 1). In particular, peritoneum adjacent to the female reproductive organs forms deep supportive parallel folds over the entire length of the fallopian tube. Whereas the peritoneum lining the abdominal walls and the visceral organs is similar throughout the abdomen, the peritoneum around the ovaries is slightly different and is composed of the mesovarium, the mesosalpinx, and the mesometrium (2). The peritoneum is discontinuous at the fimbrial openings of the Fallopian tubes in females, whereas it is a totally closed sac in males.

Macroscopically similar all around the abdominal cavity, peritoneum permits frictionless movements of the intraabdominal organs, and maintains equilibrium in the abdominal cavity. Morphological studies of the mesothelium of several mammalian species, including rat, mouse, dog, hamster, rabbit, horse and humans, have demonstrated, with minor exceptions, that mammalian mesothelium is essentially similar, irrespective of species or anatomical site (3).

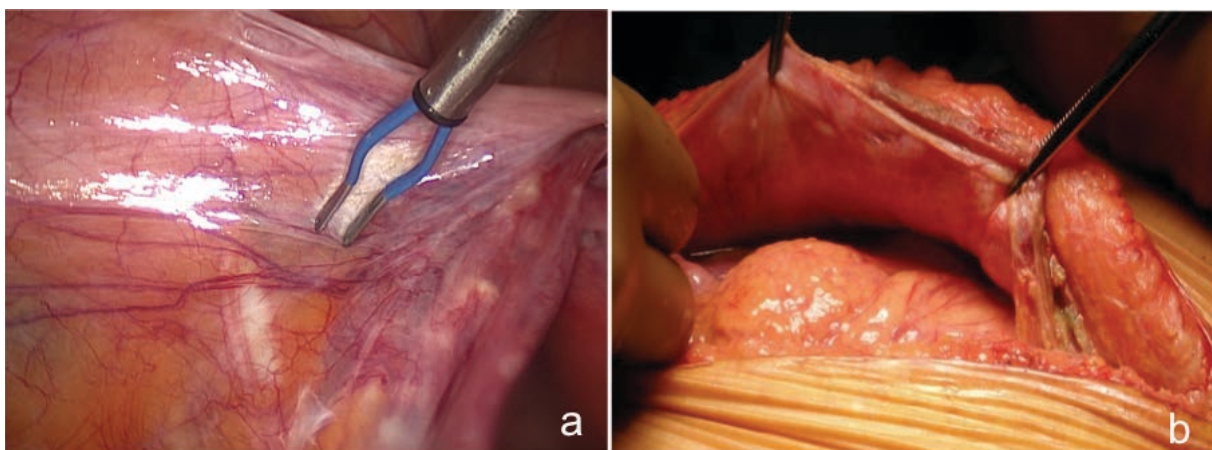


Figure 1 : Macroscopic views of the peritoneum by laparoscopy (a) and laparotomy (b)

### 1.1.2. Microscopical description of the peritoneum

The mesothelium forms a monolayer of predominantly elongated, flattened, squamous-like mesothelial cells, approximately 25  $\mu\text{m}$  in diameter, with the cytoplasm raising over a central round or oval nucleus. Surface specialization, in the form of characteristic microvilli and occasional cilia, is also seen (Figure 2).



Figure 2: from Mutsaers *et al.*: Transmission electronic micrograph (TEM) showing normal testicular MC with a thin attenuated cytoplasm (large arrow) and surface microvilli (medium arrow) resting on a basement membrane (small arrow). Elongated fibroblast-like cells (F) are located beneath the basement membrane within the tunica albuginea, surrounded by collagen (arrow heads) and other connective tissue. Bar, 1.4  $\mu\text{m}$ .

Although the mesothelium is composed predominantly of squamous-like cells, cuboidal MC can be found in various areas, including the septal folds of the mediastinal pleura, the parenchymal organs (liver, spleen), the 'milky spots' of the omentum and the peritoneal side of the diaphragm overlying the lymphatic lacunae. These lymphatic lacunae or stomatal openings are present between MC enabling communication between peritoneal cavity and lymphatic system, allowing rapid removal of fluid, cells, bacteria and particles from the serosal cavities. They are also providing a direct link between the pleural and peritoneal cavities (4).

MC also have a well-developed system of vesicles and vacuoles; most are micropinocytic, but multivesicular bodies and large vacuoles can be found. These vesicles are involved in transport of fluids and particulates across the mesothelium, because experimental studies have shown that tracer particles up to 100 nm can traverse the cell by pinocytic transport.

The boundaries between MC are tortuous, with adjacent cells often overlapping. They have well-developed cell-cell junctional complexes, including tight junctions, adherens junctions, gap junctions and desmosomes. Tight junctions are crucial for the development of cell surface polarity and the

establishment and maintenance of a semi-permeable diffusion barrier. Mesothelium displayed wide intercellular expression of E-, N- and P-cadherins, and although, unlike the epithelium, N-cadherin and membrane associative occludines such as zonula occludens ZO-1 (5).

MC are unique as although they are derived from the mesoderm and express the mesenchymal intermediate actin filaments vimentin and desmin, they also express cytokeratins, which are intermediate filaments characteristic of epithelial cells (6). Cytokeratins 8 and 18 are exclusive markers of MC (7). However, MC have the ability to change their phenotype comparable to changes seen in epithelial-to-mesenchymal transition (EMT). Via EMT, the post-natal mesothelium retains differentiative potential of the embryonic mesothelium, which generates fibroblasts and vascular smooth muscle cells (8). This has implications both in normal repair and pathological processes. This includes that after several passages in culture, MC lose their cytokeratin expression and adopt a fibroblast-like phenotype, consistent with ultrastructural observations in healing serosa (3). But also it implies that the mesothelium is a likely source of fibrogenic cells during serosal inflammation and wound healing and may play an important role in serosal fibrosis and adhesion formation.

**Basal lamina:** At the basal surface, a thin basal lamina consisting of a layer of extra cellular matrix (ECM), mainly composed of type IV collagen, offering a stable network, and laminin, permitting adhesion, with a thickness less than 100 nm.

**Submesothelial stroma:** Stroma is the connective tissue that supports mesothelial layer and basal lamina. Its thickness varies according to the location, and it consists of collagen fibers, mostly type I, fibronectin, proteoglycans, glycosaminoglycans (GAG), fibroblast (FB), adipocytes and lymphatic and blood vessels. It also includes a deep layer of elastin, more prominent in organs with peristaltic movements such as intestines.

#### 1.1.3. Functions of the peritoneum are exposed thereafter (Figure 3) (4).

MC produce both tissue-type and urokinase-type plasminogen activators (tPA and uPA), which are proteases that contribute to fibrinolysis, by converting plasminogen into plasmin. This conversion is inhibited by the glycoproteins plasminogen activator inhibitors PAI-1 and PAI-2, which are also produced by MC for the balance between fibrin deposition and degradation.

Transport of fluids and solutes across the peritoneum occurs passively via intercellular junctions (tight junctions) and stomata. Active transport occurs transcellularly via pinocytotic vesicles.

A slippery, non-adhesive surface is formed by the glycocalyx. This friction-free surface is considered to prevent tumor adhesion and dissemination across the peritoneum.

MC contribute to the induction of inflammatory responses by their antigen-presenting function. Antigen presentation by the MC enables recognition of foreign materials by T-helper cells via MHC-II molecules and secretion of inflammatory mediators.

An inflammatory response of the peritoneum in response to foreign material is also initiated by leukocytes (mainly monocytes) that are attracted to the peritoneal cavity. Monocytes produce cytokines such as IL-1, IFN- and TNF-, which activate MC to secrete inflammatory mediators that enhance inflammation (prostaglandins, cytokines, chemokines, nitric oxide, growth factors, phospholipids and proteoglycan species). A chemotactic gradient promotes migration of inflammatory cells towards the apical surface of the MC, where the glycocalyx interacts with the recruited immune cells.

To initiate tissue repair and to stabilize the peritoneal microenvironment, MC are able to transform into cells with a mesenchymal phenotype. Loss of cell-cell junctions, reorganization of the cytoskeleton and disappearance of apical and basal cell surface polarity characterize this EMT.

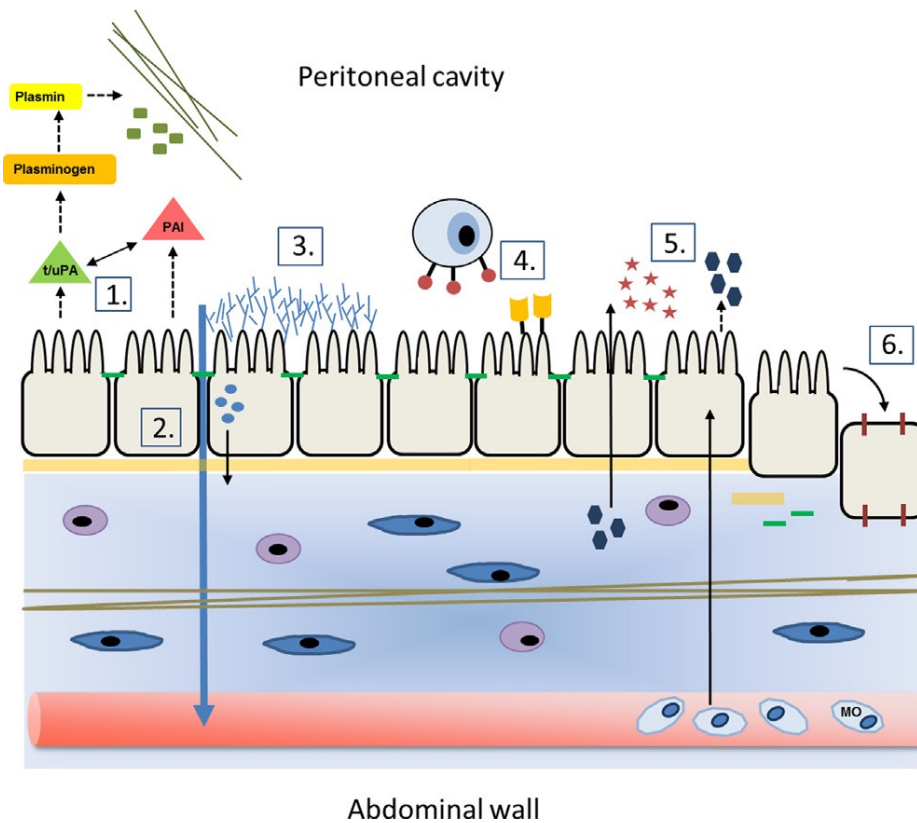


Figure 3 from van Baal *et al.*: Functions of the peritoneum: (1) Balance between fibrin deposition and degradation. (2) Transport of fluids (3) Glycocalyx non-adhesive surface (4) Antigen presentation. (5) Inflammatory response (6) Epithelial-to-mesenchymal-like transition

#### 1.1.4. Peritoneum healing

Natural healing process of mesothelium includes centripetal migration and incorporation of MC coming from the exfoliation of mature or proliferating MC from: adjacent or opposing surfaces; of pre-existing free-floating serosal reserve cells (9); of transformed serosal macrophages; of submesothelial mesenchymal precursors; and bone marrow-derived circulating precursors (10).

MC have the capacity to secrete a variety of growth factors and ECM molecules, analogous to that of epithelial cells. Growth factors initiate cell proliferation and migration at the edge of a lesion and repair cells migrate over ECM molecules that are exposed or deposited at the wound site to cover the injury (10).

During normal repair, fibrin, which is deposited between closely apposed injured surfaces, is removed by the action of PAs secreted by regenerating MC. Within days the fibrin is absorbed and by day 7 there is a complete regeneration of the mesothelial layer.

#### 1.1.5. Adhesion formation

Adhesions develop following direct trauma to the mesothelium, if the normal healing process is impaired. Trauma induces a leakage of a serosanguinous exudate from injured serosa that is rich in fibrin and thereafter a release of cytokines and chemokines within the peritoneal cavity. These are chemotactic for neutrophils and activate MC and macrophages, leading to the secretion of vasodilatory factors that in turn lead to the leakage of more fibrin. The fibrinous exudate allows adjacent surfaces to adhere to each other and, if the fibrin is not cleared, provides a scaffold for infiltration of endothelial cells and FBs. The fibrin mesh then begins to be replaced by ECM, increasing the tensile strength of the adhesion (11). In addition, MCs undergo EMT and become fibrogenic cells (12).

Postoperative adhesions are initiated as rapidly as 2 hours after surgical intervention in rodent model (13), at 8 hours, angiogenesis and fibrin deposition are identified, at 24 hours, significant cellular proliferation in the area of the adhesion is observed. Fibronectin is detectable after one week as well as fibrin deposition, angiogenesis, and tissue proliferation that remained stable throughout the second and third week after peritoneum trauma (13).

The process of matrix remodeling is a continuation of the previous stage of matrix deposition. The resultant changes in the structure of the adhesion band cause an increase in tensile strength over time. Throughout the first week after injury, the initial fibrin matrix is gradually replaced by collagen, concurrent with its population by fibroblastic or mesothelial cells. As the matrix is remodeled, water is slowly reabsorbed, which allows the tension and firmness of the adhesion to increase with time.

#### 1.1.6. Clinical impact

After abdominal and pelvic surgeries, adhesions develop over 90 % of the time (14,15). Adhesions are commonly reported after upper and lower abdominal surgeries. For the patients, complications such as bowel obstruction or women infertility may appear overtime and may require reoperations (16–20). Indirect complications of peritoneal adhesions, such as difficult reoperations, prolonged operative time, pre- and postoperative complications, are also often encountered at surgical reoperations. The overall

risk of adhesion-related readmission following either laparoscopic or open surgery is comparable (20). Over one third of patients who undergo extensive open surgery seem to be readmitted with adhesion-related complications within 10 years (21) and adhesions are involved in 56 % of reintervention complications (22). Seventy-four percent of cases of bowel obstruction are due to post-surgical adhesions (23). Adhesions are associated with a marked risk of enterotomy jeopardising 19 % and 10–25 % of patients undergoing open and laparoscopic surgery, respectively (24,25). Adhesions are responsible for 20–40 % of secondary infertility cases in women (18).

Finally, managing adhesions and their related complications impose an enormous economic burden. In the UK, the cost of adhesion-related readmissions was estimated at £24.2 and £95.2 million at 2 and 5 years after surgery, respectively (26).

#### 1.1.7. Adhesion prevention, existing strategies in clinical practice

Strategies targeting the pathophysiological mechanisms involved in dysregulated serosal repair, such as the coagulation and inflammatory pathways, have also been trialed in an effort to prevent adhesion formation, including the inhibition of inflammation (27–30), prevention of fibrin formation and promotion of fibrinolysis (31–35), anti-angiogenesis (36,37) and tissue separation using hyaluronan-based membranes (38). During the past years, addition of surgical barriers - biologically derived meshes (e.g. Surgisis®, Permacol®, Alloderm®) - that provide anti-adhesive separation of denuded serosal tissues have proved beneficial but none completely prevent adhesion development in all patients (39,40). All of them, in common, are decellularized human or animal tissue, and act as a collagen scaffold for fibroblastic ingrowth and collagen deposition. The recent tendency is to develop nanofibers, nanosheets or composite matrix to decrease the quantity of synthetic biomaterial (30,32,33) and reduce the side effects or to use natural hydrogels as chitosan, pullulan, and carboxymethyl cellulose (32,34,35). For example, Xia developed a biodegradable trilayered barrier membrane composed of sponge and electrospun layers offering hemostasis and antiadhesion features thanks to the biomaterials chosen. On one side, a poly-lactic-co-glycolic acid (PLGA) / polyethylene glycol (PEG) electrospun layer promoted the growth of epithelial cells, and exhibited inhibition on the adhesion and spread of FBs. On the other side, a chitosan sponge and glycerin took away the blood clots during the swelling and dissolution stages. With this strategy, on a rat model of cecum and parietal

peritoneum abrasion, the author showed an effective reduction of the severity and the occurrence of adhesions (32). Up to now, none of these recent strategies suppressed totally the formation of adhesion. Despite certain anti-adhesion effect, the limitations for clinical applications lie in the difficulty of treatment due to their lack of flexibility, loose contact with applied tissue; and need for suture fixation that can lead additional tissue damage. Moreover, the disease itself (pelvic cancer, endometriosis) can induce adhesion. The prevention of tissue adhesion after surgery is still considered as a big challenge in clinical fields.

Thus, there is an emerging need for tissue-engineering methods that can restore the functions of the mesothelial cells, rather than providing simple physical barrier (12,41).

#### 1.1.8. Adhesion prevention, potential strategies

Tissue engineering is a concept whereby cells are taken from a patient, their number expanded and seeded on a scaffold. The appropriate stimuli (chemical, biological, and/or mechanical) are applied and over a relatively short time new tissue is formed. The cells are another important factor in tissue engineering approach. Mesothelial cells, as other specialized cells, have their limitations, such as the invasive nature of cell collection, low proliferation capacity and the potential for cells to be in a diseased state.

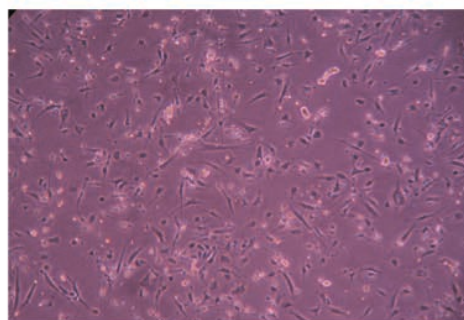
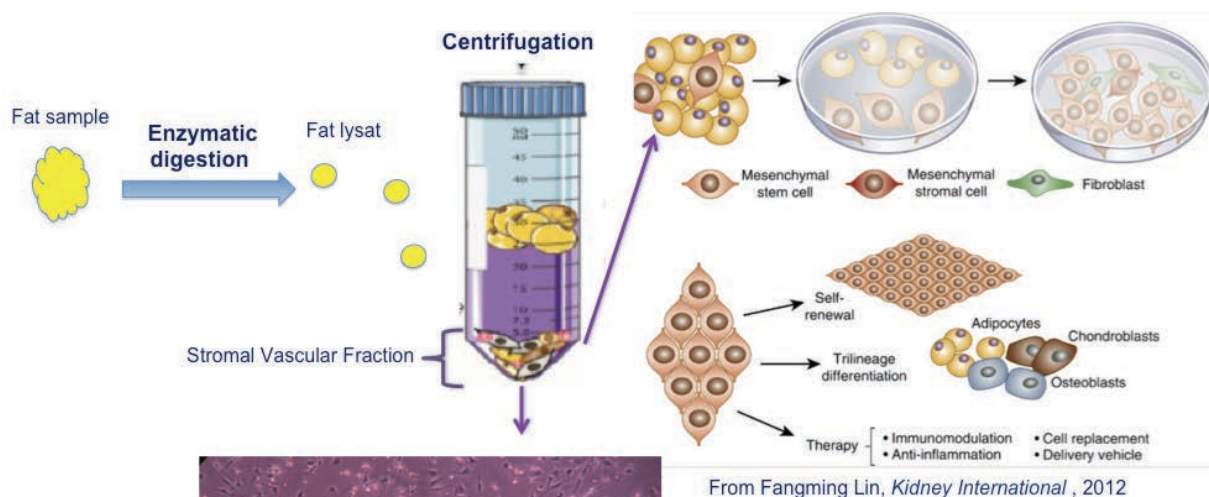
To overcome these limitations, attention has become focused upon the use of stem cells, notably adult mesenchymal stem cells (MSCs). Among MSCs, adipose stem cells (ASCs) are capable of multilineage differentiation and rapid cultivation, could directly differentiate into or activate the mesothelial progenitor cells, and could eventually facilitate the regeneration of the mesothelium when they are transplanted into the damaged peritoneum (42). Kim *et al.* transplanted human ASCs on a rabbit model for repairing damaged visceral pleura, and showed that ASCs contributed to the regeneration of MCs, although the mechanism is not yet clear (43). These ASCs are largely available and easy to get by transcutaneous suction (44–46).

#### 1.1.9. Adipose stem cells

In mammals, adipose tissue is composed of adipose stem cells (the precursor cells that give rise to new adipocytes), adipocytes (the fat-storing cells) and various other cell types, which include mural, endothelial and neuronal cells. Fat tissue is located in various depots such as inguinal, interscapular,

perigonadal, retroperitoneal and mesenteric depots, that have distinct morphologies (47). Moreover, two main classes of adipose tissue are characterized histologically, molecularly and functionally. White adipose tissue is designed for energy storage and coordination of the systemic metabolism whereas brown adipose tissue dissipates energy and generates heat. Finally, adipocytes are positioned throughout the skin and the bone marrow to regulate stem cell biology by controlling for example epidermal and hematopoietic lineage decisions (48).

As we already said, adipose tissue development, formation and maintenance is linked to adipose stem cells. Recent literature identifies and characterizes adipose stem cells. Fat tissue dissociation found them in the stromal vascular fraction (SVF), which is the remaining cell pellet obtained after digestion and centrifugation and separation from the floating adipocytes. This heterogeneous mixture of cells is composed of fibroblasts, endothelial cells, hematopoietic cells and neural cells. Among these myriad of cells, the SVF seems to contain adipose stem cells that proliferate, self renew, and differentiate (49–51) (Figure 4). The concept of vascular niche raised to describe the presence of adipose stem cells residing as a subset of perivascular mural cells within adipose depots (47). Stem and precursor cells in the freshly isolated SVF count for at least 3% (52). Stem cells are selected by their ability to adhere to the plastic support of culture.



Microscopic observation in culture after 24 H: debris, floating cells and coexisting adherent cell populations of red blood cells, elongated spindle shaped cells and round cells.

Figure 4: Schematic representation of SVF and ASC isolation.

#### 1.1.10. Cell therapy

Foley et al. reported that serosal healing involved implantation, proliferation and incorporation of free-floating MCs into the regenerating mesothelium in small animal models (9). The injection of that free floating mesothelial cells has been reported to reduce the formation of adhesion, but the ratio of implanted cells is very low and the loss of mesothelial cells very high (53). Bertram showed on an visceral and parietal peritoneal abrasion model, a reduction of the extent of the adhesion through an intraperitoneal injection of MCs (53). Lucas *et al.* used another rat model based on a parietal peritoneum and muscular excision associated with sutures to show a reduction of adhesion formation using intraperitoneal injection of mesenchymal stem cells isolated from new born rats. The loss of cells and thereafter the very small fraction of injected cells retained on the place of interest are the main limit of these therapies (54). Moreover, the transplanted cells enhance the inflammation via increased release of proinflammatory factors (55), and the optimal moment for performing such transplantation cannot yet be precisely determined (56). Di Paolo reviewed 15 years of research on MCs transplantation to highlight that MCs have been effective in reducing the formation of adhesions, and in remodeling the area of mesothelial denudation especially after peritonitis or chronic peritoneal dialysis (7). He also found that autologous MCs, after injection into the peritoneal cavity, arranged themselves in a variable pattern on the peritoneal surface and were attracted by negatively charged areas where cells and cell residues are few. Finally, the time of cells injection, the location of cells implantation and the cells loss are the main limits of cell injection as a technique of cell-therapy.

#### 1.1.11. Cell-sheets engineering or scaffold-free tissue engineering:

To overcome this limits, Asano *et al.* proposed to apply a temperature-responsive culture surface, which permitted harvesting the cultured cell-sheet without proteolytic processing and retaining cell-to-cell junctions as well as the deposited ECM of the basal membrane of the sheet (41). Moreover, it makes it possible to transplant the sheet with no support or substrates. In his first study, MC-sheets were obtained from isologous rats by enzymatic disaggregation of mesentery and cultured on fibrin gel. He showed in a rat and a canine model a significant and promising prevention of adhesion formation (57,58). Thereafter, he developed a new method of isolating autologous MCs from the

tunica vaginalis- the membrane covering the testicle easily obtained and generally free from the influence of abdominal cancer (59). Despite these interesting described qualities, cell-sheet therapy presents unfortunately limitations like the mechanical weakness of the sheet and the difficulties of handleability.

#### 1.1.12. Tissue engineering - Scaffold

Improving the mechanical properties of cell-therapy by adding a scaffold leads us to use tissue therapy in place of cell therapy. Among the materials, hydrogels are receiving increasing attention due to their ability to entrap large amount of water, good biocompatibility, low interfacial tension, minimal mechanical and frictional irritation to tissue (46,60) and their ability to mimic tissue environment. Considering the composition and the feature of all the existing hydrogels, we could choice one of them offering anti adhesion properties (61).

Basing on above state of art in the domain of mesothelium regeneration, we aim at developing an autologous ASCs laden hydrogel sheet, which can perfectly replace the damaged peritoneal membrane and prevent post-operative abdominal adhesion.

## 1.2. State of the art of the animal models of adhesion

### 1.1. Introduction

We carried out a literature review to establish and validate an animal model for adhesion and evaluate strategies of prevention. We have identified several key-points: choice of the injured organ and location of adhesion in the abdominal cavity; adhesion formation process, reproducibility, efficiency, clinical relevancy, method of assessment of adhesion and histological examination. These were chosen based on the underlying cell signaling pathways that promote adhesion formation or that are targeted by the strategy of prevention studied.

Although experimental studies have been extensively published in the literature, there is an apparent lack of uniformity in the design. In animal studies, various experimental techniques used to create adhesion have been described. Similar discrepancies can be observed in the classification and measurement of adhesions. Based on these facts, it is not easy to draw definitive conclusions from anti-adhesive proposals. The aim of this review is to report methods used to induce adhesion, measurement techniques, and classification methods employed in experimental studies.

### 1.2. Methods

#### Literature search

We searched the Pubmed database limited to the final search date (30/09/2016) and not limited to English language publications. We used the search terms “model” or “prevention” in combination with the terms “abdominal adhesions” or “abdominal adherences”. We selected publications from the past ten years (2005-2016), but did not exclude commonly referenced and highly regarded older publications.

We also searched the reference lists of articles identified by this search strategy and selected those we judged relevant.

### 1.3. Adhesion creation

#### 1.3.1. Choice of organ and location

The location and access to the injured organ depend on the treatment used to prevent adhesion. A number of authors choose the cecum (13,53,62–73) due to ease of access and of external delivery,

opposed to the parietal peritoneum of the flank, which requires two forceps on the abdominal wall to be exposed (73). In the parietal peritoneum model, parietal excision or ligation enables suturing meshes or membrane barriers (53,62,63,67,69–71,74–79), whereas in cecum, sutures could perforate the digestive lumen resulting in peritonitis. In the challenge of infertility, uterine horns models are also often used to study adhesion formation in lumen horns or between horns and the surrounding organs (76,80–83). A number of authors choose to increase the efficiency of their model by inflicting a trauma on neighboring areas like cecum and parietal peritoneum or horns and sidewall peritoneum (53,62,63,67,69–71,75–77). Others propose to injure several spots on the same organ as suggested by Oncel et al., who induced adhesions located on the small bowel (very commonly observed in clinical practice) (84).

### 1.3.2. Adhesion formation process, reproducibility and efficiency

Various techniques have been reported to induce adhesion formation including thermal effect or burn, abrasion, sutures and mechanical excisions. In the first part of our review, we discuss these techniques as well as their relative efficiency and reproducibility. The effect of adding liquid such as serum, buffer, culture medium or blood will also be examined.

#### 1.3.2.1. Thermal effect or burn

Burn can be obtained by different electro-surgery methods the most widely used being bipolar and monopolar electro-coagulation. In bipolar electro-coagulation, the electrical current passes between two tips of a handpiece whereas in monopolar electro-coagulation, the electrical current passes from the handpiece to a ground plate, passing through the patient or the animal. The power (Watts) and the strength (ranging from 0 to 6) inducing fulguration, section, coagulation or desiccation can be changed according to the need (Table 1) (85).

Table 1. Forms of electro-surgery

Electro-surgery type	Features
Electro-fulguration	Uses a high voltage, dampened waveform to produce a spark that arcs from the probe tip to the skin lesion, causing superficial charring of the lesion surface.
Electro-section	Uses an undampened or mildly damped current in conjunction with a very fine emitting electron to produce a cutting effect through soft tissue.
Electro-coagulation	Uses an intermittent damped current in conjunction with a larger emitting electrode to produce less intense heat over a larger area to induce coagulation and thereby haemostasis.
Electro-desiccation	Uses an intermittent damped waveform with high voltage and a lower current emitted from a ball electrode to induce cell dehydration and tissue shrinkage.

Whereas settings for coagulation can be easily reproduced, the strength of the direct mechanical contact with the injured area is the only non-controllable parameter. Wallwiener et al., standardized the applied pressure using electronic scales, and detailed the duration and the technique of application of bipolar coagulation. The distance of opened forceps branches was 5 mm and each sweeping was carried out exactly below the previous one for 1-3 seconds with pressure ranging from 15 to 45 × g and the generator set to 60 W. They compared different coagulation protocols and added groups with suturing or mechanical denuding (78). Adhesion rate was 0% in the mechanical denuding group, 14% in the minimal electrocoagulation group and 100% in the extensive electro-coagulation and in the two groups with suturing. Extent of adhesion induction was 0% for the minimal and 50% for the extensive electro-coagulation groups, to 73% in the coagulation + suture group, and 64% in the suture + mechanical denuding group. Electro-coagulation trauma resulted in only dense adhesions highlighting the importance and additive effect of suturing on adhesion formation.

Kraemer *et al.*, compared in a rat model the formation of Monopolar Contact Coagulation (MCC) versus non-contact Argon Plasma Coagulation (APC) adhesion. APC - a non-contact method initially introduced for the hemostasis of parenchymatous tissue- is a plasma scalpel that simultaneously cuts tissue and cauterizes blood vessels measuring 3 mm in diameter with a small, hot (3000 C) gas jet (79,86). With a similar energy intake, contact coagulation induced a significantly higher rate of

adhesion formation. APC-induced adhesions were significantly less vascularized compared to MCC-induced adhesions. Besides, the higher thermal effect of APC compared to MCC (151±33°C versus 117±14°C, p<0.04), the direct mechanical contact of the MCC electrode with the highly sensitive peritoneum was thus hypothesized to be a pivotal additional stimulus for adhesion formation (79).

Keskin *et al.*, showed that induction of adhesion by coagulation of uterine horns is efficient. They compared, in the same animal, the effect of monopolar cautery on one side and incision with a scalpel and suturing on the other side on uterine horns (82). The scalpel incision with suturing and cautery had similar effect and induced the formation of severe and high tenacity adhesion. Kelecki *et al.*, published similar results using their uterine horn model with 95 % of adhesions being severe (83). They created standard lesions on both sides of rats' horns using bipolar cautery at 20 W power, one second on each of the 7 spots associated with same coagulations (1.5 × 1.5 cm) opposite the parietal peritoneum. Using another type of monopolar device, mostly used by dentists, Kawanishi *et al.*, applied a disposable electrosurgical cauterizer (Acu-Tip; Practicon Dental, Greenville, OH, USA) applied for 5 min on the cecum. They obtained severe adhesion however, they did not provide details on the size or extent. Finally, a simple heated metal probe, as seen in Foley *et al.*'s study, can also lead to adhesion formation (87). The limitation of this technique seems to be the reproducibility due to the difficulty in maintaining the probe's temperature.

Monopolar electrocoagulation has demonstrated a good efficiency in the induction of dense, severe adhesions on visceral and parietal peritoneum. However, its drawback is the size of the ground plate, which is usually too big for small animals such as rats or mice. On the other hand, bipolar electrocoagulation achieves adhesion efficiently only if the forceps is applied for more than 3 seconds (78). Thermal damage can be limited by controlling the time of application and upon seeing a change in the color of the tissue (turns white). It is easy to perform with rare side effects owing to the minimal thermal effect with the current passing only between the tips of the forceps and not through the animal till the ground plate. Both these techniques are commonly used in human surgery all around the world.

#### 1.3.2.2. Abrasion

A number of experimental studies have used cecal or uterine horn or sidewall peritoneum abrasion models (13,53,62–72,75,77). Yelian *et al.*, found a reproducible and efficient rat model of cecal

abrasion (13). The abrading device was precisely described as well as the surface abraded, the time, and the strength of the application. At least 96% of the rats developed adhesion however, neither the severity nor the extent of the adhesion was reported. Bertram et al., have described a parietal and visceral peritoneum abrasion model in which the ventral abdominal wall and the cecum were abraded using a stamp calibrated to 4 kPa pressure with an emery paper (260 grains per cm<sup>2</sup>) mounted on a curved plate (53). Bayan et al., recently validated this model (28). Other authors performed abrasion on cecum using sand paper, toothbrush, dry or soaked gauze with less precision until punctuate bleeding occurred on the injured area, not guaranteeing their reproducibility (70,72). De Clercq et al., and Sakai et al., in a peritoneal wall-cecal abrasion mice model, added saline or phosphate buffered serum after replacing the cecum in the cavity and before closure (67). The adhesions obtained were frequent, dense, extended. Bove et al., using the same model adapted for rats, described 70% adhesion occurrence even though the combined area represented approximately 7 cm<sup>3</sup> (69). Gaertner et al., obtained only 50% adhesion after cecal and parietal peritoneum abrasion (71). Abrasion alone seems to be less efficient in inducing formation of extended adhesions. Furthermore, reproducibility needs to be guaranteed using a specific protocol.

#### 1.3.2.3. Excision

With regard to the effects of peritoneal excision, two research teams reported contrasting findings in the 1970s (22, 23). They showed that parietal peritoneal excision made by mechanical denuding whilst not damaging the underlying muscular layer self-healed without adhesion. This suggests that excision of peritoneum is able to induce adhesion formation only if the underlying muscle is damaged: excised, sutured, or coagulated. Furthermore, muscle is known to be extremely vulnerable to ischemia (12), and ischemic muscle would contribute to the adhesion formation.

#### 1.3.2.4. Combined effects

Gaertner et al., combined suture excision with additional biomaterial and concluded that suturing adds an ischemic effect that was a strong stimulus for adhesion formation (71). In their model, they highlighted the limited efficiency of abrasion alone. Four combinations were compared: cecal-parietal peritoneum abrasion, cecal abrasion + peritoneum excision (leaving the underlying muscle exposed), full-thickness abdominal wall + overlying skin closure, and full-thickness abdominal wall removal + polypropylene mesh sewn with sutures. Excision increased the rate of adhesion formation to 59%

compared to cecal abrasion alone (50%). Furthermore, full abdominal wall excision induced extended adhesions when combined with sutures or non-absorbable mesh.

Whang et al., compared four different techniques that lead to the formation of adhesions: parietal peritoneum excision, parietal peritoneum abrasion, peritoneal button creation (which associated coagulation with suturing), and cecal abrasion (70). Following analysis of the performance of each model, coagulation associated with suturing clearly showed the best results in terms of both quantity and quality of adhesion, whereas the excision group exhibited the best quality of adhesion.

#### 1.3.2.5. Chemical agents

During any surgery, glove powders (magnesium silicate, talc etc.) applied to the abdominal cavity induce adhesion formation (88–90). Other chemical irritants such as iodine, chlorhexidine, hydrogen peroxide, or alcohol, often used during the preparation of the patient for a surgical procedure, applied over a damaged serosal surface, are known to aggravate adhesion formation (91).

#### 1.3.2.6. Sutures, meshes

We previously reported ischemic effect of sutures leading to the formation of adhesion following surgery. Sutures induce adhesion because of the foreign-body reaction induced by the composition of the thread. Polyglycolic acid and polyglactin sutures induce only mild foreign-body reactions compared to catgut, silk, and prolene sutures (92). Meshes used for hernia ventral repair, by open approach or laparoscopy, are debatable as these composite materials (absorbable or not) induce intra-abdominal adhesion formation (93,94).

#### 1.3.2.7. Other traumas

Other traumas such as cooling and drying of peritoneal serosa by carbon dioxide insufflation during laparoscopy induced adhesion formation by itself as well as through damage to the serosa (95).

#### 1.3.2.8. Serum, blood infusion on serosa damage

Blood, important source of fibrin, encourages adhesion formation combined with the previous methods of adhesion induction (96,97). On the contrary, intraperitoneal injection (IP) of saline serum or buffers such as phosphate buffered serum reduce adhesion formation. IP infusion is widely used (62,64,68,74,75), however, the volume injected varies significantly (ranging from 2-50 ml/kg body weight) (64,66,67). As Sahbaz et al., reported that severity of adhesions reduced in a group of rats that were administered 1 mL IP injection of isoserum daily during the 10 post-operative days following a cecal abrasion (64). In an anterior cecal wall abrasion combined with silk sutures rat model, a cold infusion of isoserum reduced adhesion formation (66).

#### 1.4. Clinical relevancy

Both location and mechanisms of induction of adhesions need to be addressed to answer the clinical problem studied. First, concerning the location, Oncel *et al.*, mimicked small bowel occlusion in their multiple small intestine adhesions model to reflect their clinical practice. Indeed, the small bowel which occupies most of the space in the center of the abdominal cavity and vulnerable during abdominal surgical procedures, is the most frequently observed location of adhesion formation (84).

Second, the mechanism for adhesion formation needs to reflect clinical practice. Whilst addition of blood, tissue excision, burn and sutures are common approaches to mimic clinical reality, abrasion of trauma is less common. Models by Wallwiener *et al.*, replicated the different aspects of peritoneal trauma during surgery like electrocautery, suturing, sharp incision, and mechanical damage (78). Butz et al., compared addition of blood and saline serum due to high frequency of bleedings during all surgical procedures (96). Kraemer et al., compared monopolar coagulation-the most common coagulation used by surgeons irrespective of the kind of surgery- and the emerging argon plasma coagulation (79).

#### 1.5. Adhesion assessment

##### 1.5.1. Macroscopic adhesion assessment time

There has been no consistency in the assessment of adhesion formation, varying in many experimental studies from post-operative day 14 (28,70,76,78,80,83), day 7 or 10 (53,64,65,69,74), or 21 (62), day 30 (77), or several times on days 1 or 2, 7, 14, 21, 30 (13,66–68,75).

Adhesions are thought to form as a result of serosanguinous exudate leakage from injured fibrin-rich serosa. Trauma also induces release of cytokines and chemokines within the peritoneal cavity. These are chemotactic for neutrophils and activate mesothelial cells and macrophages, leading to the secretion of vasodilatory factors that in turn lead to more fibrin leakage. The fibrinous exudate allows adjacent surfaces to adhere to each other and, if the fibrin is not cleared, provides a scaffold for infiltration of endothelial cells and fibroblasts. The fibrin mesh then begins to be replaced by the extracellular matrix, increasing the tensile strength of the adhesion (11). In addition, mesothelial cells undergo mesothelial-to-mesenchymal transition, a process analogous to epithelial-to-mesenchymal transition, and become fibrogenic cells (12). Yelian et al, detailed these different steps at 0, 2, 4, 8, 16, 24, 48, 72, 96, 168, 336, and 504 hours after the appearance of adhesions. In their rodent model, post-operative adhesions initiated as rapidly as 2 hours following surgical intervention. At 8 hours, angiogenesis and fibrin deposition were observed. At 24 hours, significant cellular proliferation in the adhesion area was observed. Cellular fibronectin -an adhesive glycoprotein that is an important component of extracellular matrix- was not detectable until 1 week after cecal abrasion. Fibrin deposition, angiogenesis and tissue proliferation remained stable throughout second and third week after cecal abrasion (13).

The matrix remodeling is a continuation of the matrix deposition process. Over time, the resultant changes in the structure of the adhesion band increase its tensile strength. Throughout the first week following injury, the initial fibrin matrix is gradually replaced by collagen with fibroblastic or mesothelial cell population. As the matrix is remodeled, water is slowly reabsorbed, which allows increasing the tension and firmness of the adhesion over time. This suggests that assessment should not be made before the day 7 following the initial peritoneal damage and could be scheduled during the first few weeks.

#### 1.5.2.Surgical approach

Surgical evaluation could be made through a transverse subcostal or an upper abdominal transverse incision. Adhesions could be macroscopically assessed by the surgeon who performed the initial surgery or by another observer blinded to the initial procedure (70,72).

### 1.5.3. Macroscopic scoring of adhesions

Adhesions are defined as bands (a thin film of connective tissue or a thick fibrous bridge) or as direct contact between two organ surfaces. The presence or absence of adhesion is the more basic assessment completed by quantitative and qualitative parameters. These parameters could provide more objective measures taking into account the number, strength and distribution, and compare extent and severity of an adhesion. Furthermore, these parameters are grouped and organized into scoring systems that have been validated.

Qualitative scoring systems include the description of site, tenacity, and vascularization of adhesion. According to the classification used, tenacity could be replaced by the description of the facility of adhesion dissection or by the severity. Vascularization could be apart from the other criteria or included in another criterion such as severity or tenacity. Several adapted scoring systems exist, the most commonly used being Zühlke's adhesions classification system. According to Zühlke, score is 0 if no adhesion is seen, 1 for one adhesion band without vessel and easily separated, 2 for two thin adhesion bands without vessels and easily separated so on and so forth (Table 2).

Table 2: Zuhlke's adhesion classification system

	Score
Macroscopic observation	
No adhesion	0
Filmy adhesions: easy to separate by blunt dissection; no vascularization	1
Stronger adhesions: blunt dissection sufficient but partly sharp dissection possible (beginning of vascularization)	2
Strong adhesions: lysis possible but sharp dissection only; clear vascularization	3
Very strong adhesions: lysis possible by sharp dissection only (organ strongly attached with severe adhesions and damage of organs hardly preventable)	4
Histological observation	
Inflammation and fibrosis	
absent	0
mild	1
moderate	2
severe	3
Granulation	
absent	1
present	2

Another system of assessment is based only on the description of density and severity of the adhesion and no information on either the extent or size. Based on this, an adhesion is scored as: no adhesion (score 0); one thin filmy adhesion (score 1); more than one thin adhesion (score 2); thick adhesion with focal point (score 3); thick adhesion with plantar attachment or more than one thick adhesion with focal point (score 4); and very thick vascularized adhesion or more than one plantar adhesion (score 5) (76).

Binda et al., proposed both qualitative and quantitative assessment (47). The qualitative scoring system was similar to systems previously reported: type of adhesion (0: no adhesion; 1: filmy; 2: dense; 3: capillaries present), tenacity (0: no adhesion; 1: easily fall apart; 2: require traction; 3: require sharp dissection). The quantitative scoring system assesses the extent of the adhesion as the proportion of the lesions covered by adhesions using the following formula: adhesion (%) = (sum of the length of the individual attachments/length of the lesion) × 100. Extent was scored as following : 0: no adhesion; 1: 1%–25%; 2: 26%–50%; 3: 51%–75%; 4: 76%–100% of the injured surface involved. The total (extent + type + tenacity) was presented as the average of the adhesions formed at four sites, right- and left-, visceral and parietal peritoneum, which were individually scored (95).

In the specific case of uterine horns model, the extent of adhesions across each uterine horn was defined according to the criteria of Leach et al.,: no adhesion (score 0); 1–25% involvement (score 1); 26–50% involvement (score 2); 51–75% involvement (score 3); 76–100% involvement (score 4) (98).

Even though Yelian *et al.*, proposed a thorough adhesion scoring group to improve inter-observer reproducibility (21), there are still discrepancies in adhesion assessment which could limit objective comparisons between studies results. Contrary to the aforementioned scoring systems, Bertram et al., proposed a quantitative method to measure adhesion formation. Ten days post operation, adhesions were planimetrically measured by an investigator unaware of the previous treatment of the animal. The specimens were placed on the plain surface of a digitiser board connected to a personal computer. Custom-made software was used to define every single area up to 500 points and the total area/ animal was computed (53).

#### 1.5.4. Histology

Two classifications are commonly used for histological examination, based on the cellular infiltrate, to describe the degree of inflammation and the foreign body reaction namely, fibrosis and neovascularization. Zühlke's adhesions classification system integrates macroscopic assessment and histological examination (Table 2). This system included four fibrosis and inflammation severity scores ranging from 0 to 3: no fibrosis or inflammation (grade 0); minimal and loose fibrosis, giant cells, occasional scattered lymphocytes, and plasma cells (grade 1); moderate fibrosis, giant cells with

increased numbers of admixed lymphocytes, plasma cells, eosinophils, and neutrophils (grade 2); florid and dense fibrosis, many admixed inflammatory cells, and microabscesses (grade 3).

Adhesion formation could also be assessed indirectly, by studying the implicated pathways. For example, Lee *et al.*, and Cassidy *et al.*, measured the tissue plasminogen activator (tPA) and its inhibitor secretion in the peritoneal fluid to assess the imbalance in fibrin formation. They studied the fibrinolytic activity as fibrinolysis activators and inhibitors are major regulators that could, after an imbalance, facilitate adhesion formation (66,74). Other adhesion markers such as fibronectin, type I collagen, vascular endothelial growth factor (VEGF), transforming growth factor (TGF)- $\beta$ 1 and cyclooxygenase-2, and matrix metalloproteinase-1/ tissue inhibitor of metalloproteinase ratios could be measured to establish which signaling pathway(s) is/are involved (13,99).

#### 1.6. Conclusions

Various models of post-operative adhesions are already proposed and commonly used for experimental studies assessing prevention therapies. The choice of the organ, the location of adhesion creation, and the process of adhesion induction should be chosen in accordance with the clinical issue but also with the strategy of prevention studied. Reproducibility, efficiency of the model are almost as important as clinical relevancy. Assessment methods should be based upon published and well-established scoring systems in order to be able to compare the results to the literature.

## OBJECTIVES OF THE PROJECT

The ultimate objective of the project was to develop an autologous cell laden scaffold to prevent adhesion formation during abdominal surgery. The milestones of the thesis work were exposed thereafter (Figure 5):

1. Validation of the animal model of post-operative abdominal adhesion with quantitative, qualitative and histological assessments
2. Comparison of cell sources: efficiency of isolation, culture and characterization of functional MCs and ASCs and demonstration of ASC transdifferentiation.
3. Comparison between cell-therapy and cell-laden scaffolds or tissue-therapy through a *proof of concept* study to validate the need of the scaffold;
4. Choice of the hydrogel scaffold biomaterial
5. *In vivo* application of the cell laden hydrogel.

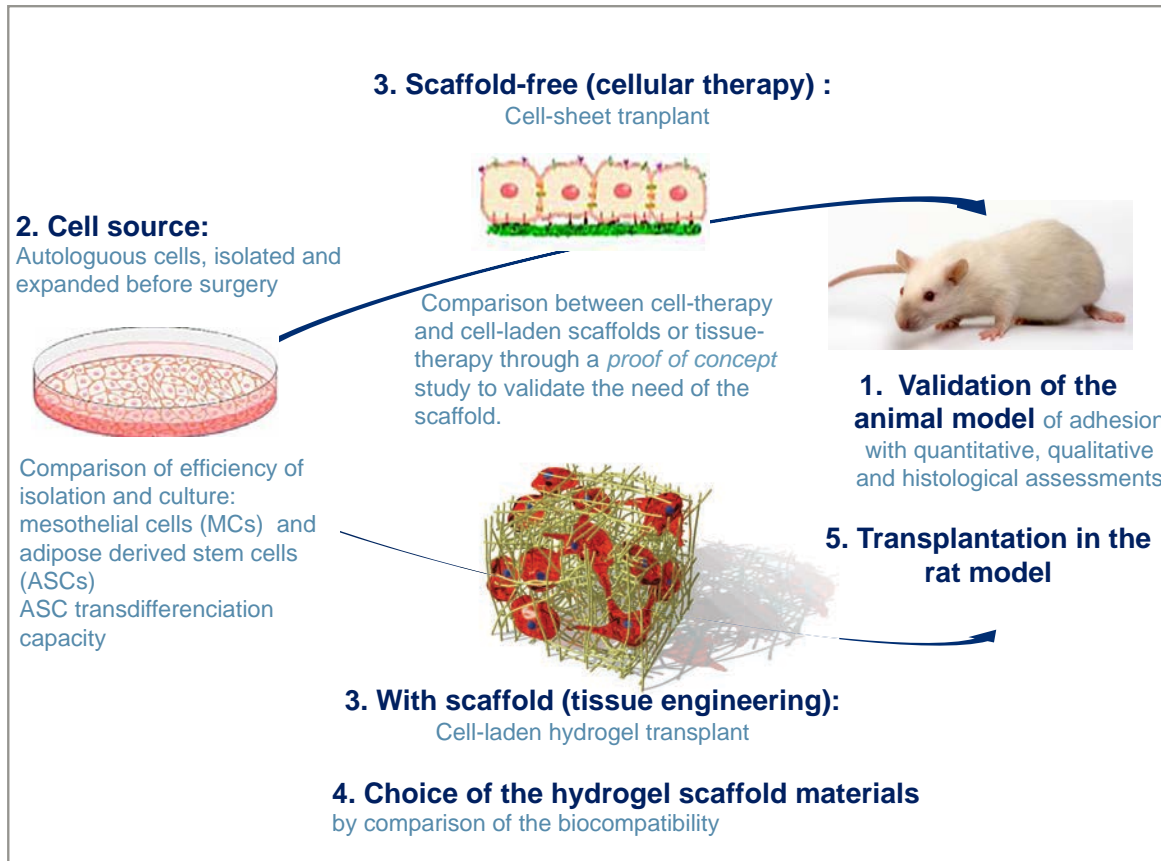


Figure 5: Milestones of the project

## 2. Part 2

### METHOD AND RESULTS OF THE PROJECT

## 2.1. CHAPTER 1: VALIDATION OF THE ANIMAL MODEL

### 2.1.1. Introduction

As shown in the literature review, we needed an efficient, reproducible and clinically relevant animal model. For our project, both cell and tissue therapies were tested after validating the model. Cell therapy included intraperitoneal injection (IP) of a cell suspension, including the injection of a volume of liquid. Furthermore, different types of grafts had to be transplanted into the model and had, based on the scaffold used, different methods of use, mechanical resistances, and capacities for adhesion to the injured area. Based on these requirements, two models of peritoneal lesions were tested, because each model presented advantages and disadvantages. In the first model, a parietal peritoneal lesion was created by bipolar electrocoagulation and suturing the right flank. In the second model, a visceral peritoneal lesion was created by bipolar electrocoagulation of the cecum. The choice of model used was made based on the features of the therapy to be tested, such as shape, size, adhesion capacity, and viscosity. The parietal peritoneum model was a more convenient support for fixing a graft with sutures, whereas an auto-adherent gel could be easily applied and grafted onto both types of models. The visceral cecal peritoneum model was more convenient for all injected therapies because it is simple to perform. Furthermore, in most of the cell therapy studies reported in the literature, an IP injection is performed after creation of the model, at least for the control group. To report the effects of IP injections of saline solution and culture media on the visceral peritoneum lesion model, we had to determine what volume and type of solution were optimal for IP injections.

Little is known about the optimal bipolar coagulation settings on the generator to burn the peritoneum and limit adverse effects. We conducted a pilot experiment to choose the settings of the generator, i.e., power (Watts) and strength to electrocoagulate the peritoneum (inducing fulguration, section, coagulation or desiccation).

## 2.1.2. Method

### 2.1.2.1. Animals

Male Sprague-Dawley rats, weighing 350 to 400 g (Charles River Laboratories, Saint-Germain-Nuelles, France) were used for all the experiments. The animals were housed in standard rodent cages under the conventional laboratory conditions of a constant temperature (22°C) with a 12 h light/dark cycle, and free access to laboratory chow and tap water. The Ethics Review Committee for Animal Experimentation (C2EA-75) at the Lille Faculty of Medicine approved the experimental study protocol (No. 2015112511478105).

### 2.1.2.2. Study Design

The pilot study was divided into two parts. The first part, "Immediate Tissue Effects", included three rats and was used to study the immediate histological effects of the settings of the bipolar generator on the visceral peritoneum. The second part, "Long-term Tissue Effects", was based on the results of the first part and included 29 rats that were used to assess the effects of the settings of the bipolar generator two weeks after thermal injury.

Finally, the last part of the pilot study compared the two models of peritoneal lesion and, in the second model, compared different IP injections. This last part was entitled "Choice of the standardized peritoneal lesion". Twenty-seven rats were included and allocated randomly to one of the following:

- Parietal Peritoneum Group, which received electrocoagulation combined with interrupted sutures on the right flank (n= 5, Figure 6a).
- Visceral Peritoneum Group, which received electrocoagulation on the cecum without IP injection (n=5, Figure 6b).
- Cecum NaCl low volume IP injection Group, which received visceral peritoneum electrocoagulation on the cecum with an IP injection of 1.5 ml of NaCl solution (n=5).
- Cecum NaCl high volume IP injection Group, which received visceral peritoneum electrocoagulation on the cecum with an IP injection of 3 ml of NaCl solution (n=6).
- Cecum DMEM IP injection Group, which received visceral peritoneum electrocoagulation on the cecum with an IP injection of 3 ml of Dulbecco's Modified Eagle Medium (DMEM) (n=6).



Figure 6 a, b: Immediate post-operative macroscopic view of parietal peritoneum electrocoagulation combined with interrupted sutures on the right flank (a) and visceral peritoneum electrocoagulation on the cecum (b).

#### 2.1.2.3. Surgical procedure

##### 2.1.2.3.1. Immediate Tissue Effects

To re-use rats coming from other protocols (no previous history of abdominal experiments) and follow the 3R guidelines of INSERM, we used three 250 g female Sprague Dawley rats from the DHURE. Under general anesthesia, mask inhalation of Isoflurane<sup>®</sup> (Santa Cruz Technology, Dallas, USA), the ventral hair was shaved using electrical clippers, and a 2 to 3 cm midline incision on the inferior part of the abdominal wall was made to open the abdomen. The cecum was delivered externally. A standardized burn lesion, 1 cm in diameter (0.8 cm<sup>2</sup>) was made on the visceral cecal round surface, using sweeping bipolar forceps (Valleylab<sup>™</sup>, Medtronic, Minneapolis, USA) with the power settings on 10, 20, 30 or 40 W, and a strength level of 1, 2, 3, or 4. The damaged surface was harvested immediately and fixed in 4% formalin solution. All tissue specimens were embedded in paraffin, sectioned into 5 µm-thick slices, and stained with hematoxylin phloxine saffron (HPS) using standardized methods. Rats were immediately sacrificed using a single intracardiac injection of 0.3 mg/kg T61<sup>®</sup> (INTERVET, Beaucouze, France).

##### 2.1.2.3.2. Long-term Tissue Effects

Twenty-nine male Sprague Dawley rats, each weighing 350 g, were included in the Long-term Tissue Effects study. Under the same conditions of anesthesia and surgical preparation as the first part of the

study, a standardized burn lesion was inflicted on the visceral cecal round surface, in a diameter of 1 cm (0.8 cm<sup>2</sup>) using sweeping bipolar forceps. A power setting of 40 W on the bipolar generator was used for all the rats and the strength level varied based on the randomly assigned group the rat was in: strength level 2 (n=7), strength level 3 (n=5), strength level 4 (n=7), and strength level 5 (n=11). The cecum was then gently replaced in the abdominal cavity and an IP injection (3 ml) of saline solution was dispersed dropwise into the abdominal cavity before closure.

#### 2.1.2.3.3. Choice of the standardized peritoneal lesion

Under general anesthesia and through an incision in the inferior part of the abdominal wall, the rats in each group were given peritoneal lesions as listed below.

- Parietal peritoneum group: the right abdominal wall of the peritoneum was exposed and a standardized burn lesion was inflicted on the peritoneal surface 1.5 cm dorsal to and parallel with the midline incision in an area of 0.5 x 1.0 cm using sweeping bipolar forceps (Valleylab™, Medtronic, Minneapolis, USA) set to 40 W and strength level 4 for 6 s. To further induce ischemia in the burn area, three interrupted sutures made with Vicryl® 3.0 (Ethicon, Somerville, USA) were placed at regular intervals on the cranial, caudal, and middle parts of the burn area.
- Visceral peritoneum group: the cecum was easily delivered externally. A standardized burn lesion with a diameter of 1 cm (0.8 cm<sup>2</sup>) was inflicted on the visceral cecal round surface using sweeping bipolar forceps (Valleylab™, Medtronic, Minneapolis, USA) set at 40 W and strength level 4 for 6 s. The tissues immediately turned white, and each sweep was done exactly below the previous one. The cecum was gently replaced into the abdominal cavity. Rats in this group then had either a volume of saline solution or culture medium dispersed dropwise into the abdominal cavity.

Subsequently, all rats except those in the immediate effect study had the midline incision closed in two layers with a running suture, using Vicryl® 3.0 (Ethicon, Somerville, USA), on the muscle and by simple knots, using Ethibond® 2.0 (Ethicon, Somerville, USA), on the skin. All animals received 10 µg/kg buprenorphine (Vetergesic®, CEVA santé animale, Libourne, France) by subcutaneous injection postoperatively and every 24 hours for the following two days for pain management purposes.

#### 2.1.2.3.4. Assessment

##### 2.1.2.3.4.1. Macroscopic assessment of postoperative peritoneal adhesion

Fourteen days after the peritoneal lesion was made, two blinded investigators used inverted U-shaped laparotomies to macroscopically assess the formation of postoperative peritoneal adhesions in rats under general anesthesia. Then, the rats were sacrificed using a single intravascular injection of 0.3 mg/kg T61<sup>®</sup> (INTERVET, Beaucouze, France). To qualitatively evaluate the postoperative adhesion, the presence or absence of peritoneal adhesion was recorded and the status of the peritoneal adhesion was scored based on the following criteria: 0 = no adhesion, 1 = filmy avascular adhesion, 2 = filmy vascular adhesion, and 3 = dense and vascular adhesion. The peritoneal adhesion was defined as “filmy” when the scale of a ruler was visible through the tissue and it was defined as “dense” when the scale of a ruler was invisible. To quantitatively evaluate the postoperative adhesion, the percentage of the area covered with adhering tissue versus the whole area of the standardized peritoneal lesion was calculated.

##### 2.1.2.3.4.2. Histological assessment of postoperative peritoneal adhesions

During the second-look laparotomy, to determine whether postoperative adhesion existed, the tissue around the standard peritoneal lesion was excised completely, rinsed with isotonic solution, and fixed in a 4% formalin solution. All tissue specimens were embedded in paraffin, sectioned into 5- $\mu$ m-thick slices, and stained with hematoxylin phloxine saffron (HPS) using standardized methods.

#### 2.1.2.3.5. Statistical analyses

Data are presented as raw values or median (range) values. The groups were compared with each other to assess differences in the quality and quantity of the adhesions. The frequencies, such as scores of postoperative abdominal adhesions, were compared using the chi-squared test with Yates' correction, or for  $n \leq 5$ , Fisher's exact test. The medians, such as the amount of the injured area covered by adhesion, were compared using a non-parametric t-test or a Wilcoxon Mann-Whitney test.  $p < 0.05$  was considered statistically significant but for small size groups, the Bonferroni correction was applied. GraphPad Prism for Windows XP, version 6.0 (GraphPad Software Inc., La Jolla, CA, USA) was used for the statistical analyses.

### 2.1.3. Results and discussion

#### 2.1.3.1.1. Immediate Tissue Effects

All three layers of the cecum (serosa, muscularis and mucosa) were damaged when strength levels 2, 3, and 4 on the bipolar generator were used. Only the serosa was damaged when the bipolar generator was used at strength level 1 although the orientation of the cells, which were wrinkled, changed (Figure 7). The change in power from 10 to 40 W did not affect the amount of tissue damage. No differences in histology were found in the lesions created using strength levels 2, 3 and 4.

Figure 6 shows the layers that make up the cecum: the serosa (replaced in the rectum by perimuscular tissue), the muscularis propria (also called the externa), the submucosa, and the mucosa.

- The serosa is a single layer of flat to low cuboidal MCs and adjacent fibroelastic tissue
- The mucosa consists of low columnar to cuboidal cells. Crypts and tubules are tightly packed, have straight test-tube shapes (minimal branching), grow parallel to each other, have a straight luminal surface, rest on a thin basement membrane, extend to the muscularis mucosa, and contain absorptive cells and goblet cells.
- The muscularis propria or externa consists of an inner circular layer, the myenteric plexus of Auerbach, and an outer longitudinal layer.
- The submucosa or muscularis mucosa is thin and regular.

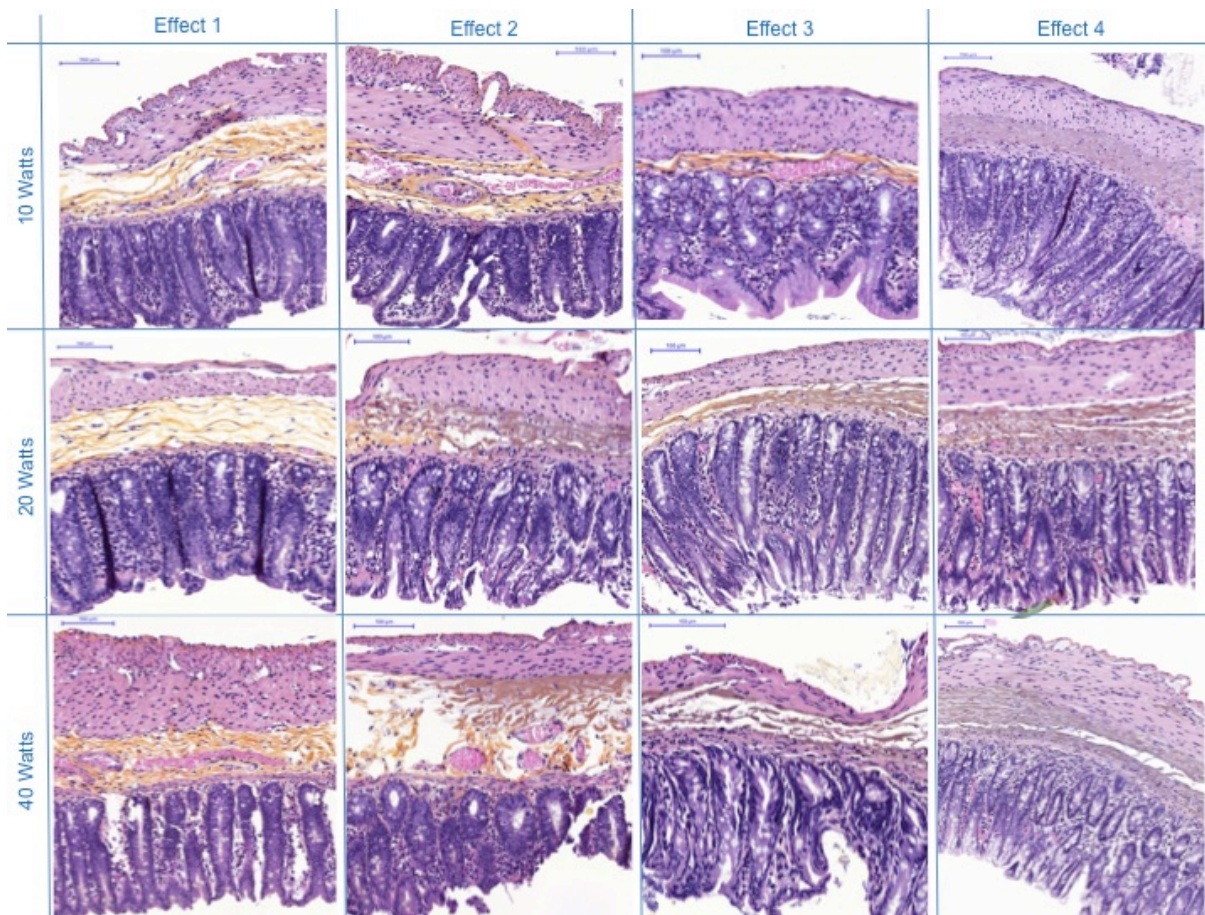


Figure 7: Immediate effect of bipolar electrocoagulation on the cecum, based on the power and strength settings of the generator (Valleylab™, Medtronic, Minneapolis, USA). In the first column, pictures of tissue treated with strength level 1 show damage to the serosa (epithelium is wrinkled), whereas the muscularis, connective tissue (orange), and the mucosa (glandules, crypts) are normal. In the second column, pictures of tissue treated with strength level 2 and 10 W of power had the same effects with edema in the muscular layer. In all the other pictures all the layers are damaged as indicated by the yellow brown color in the connective tissue and the elongated mucosa.

#### 2.1.3.1.2. Long-term tissue effects

No adhesion was reported in the group of animals treated with strength level 2, whereas in all the other groups, all the rats had dense adhesions stuck to the cecum, the abdominal wall, fat, omentum, or seminal vesicles (Figure 8).



Figure 8: Assessment of adhesion, macroscopic view on day 14 post operation: no adhesion in the strength level 2 group (a); adhesions in the strength level 3 group (b), strength level 4 group (c), and the strength level 5 group (d).

The median extent of the area covered by the adhesion was 13 % (11-23) in the strength level 3 group, 31 % (8-41) in the strength level 4 group, and 31 % (10-100) in the strength level 5 group (Figure 9a). The tendency of a smaller extent of the adhesion with strength level 3 did not reach statistical significance (Fig 9a). A rat from the strength level 4 groups died ten days after the surgery and was excluded from the adhesion assessment. The autopsy revealed a probable cecal perforation. We reported the death as a major adverse effect caused by cecal coagulation.

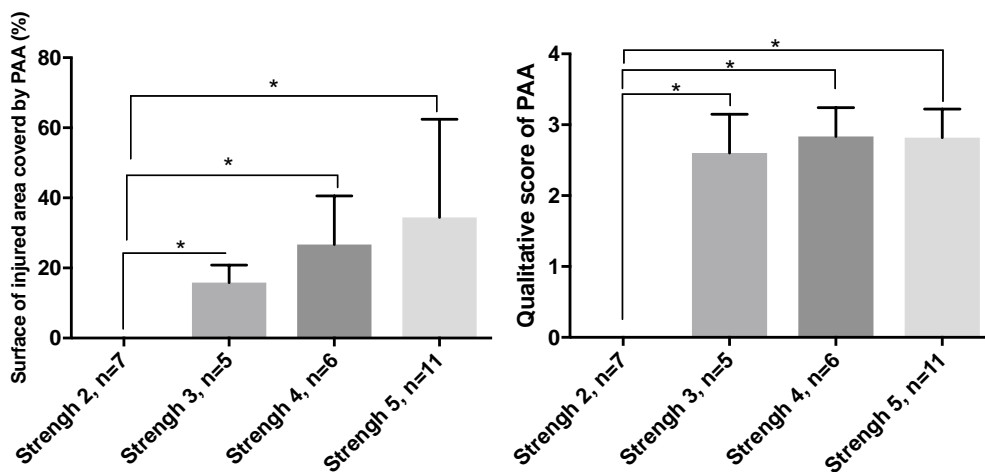


Figure 9: Extent (a) and severity (b) of the adhesions according to the setting of the strength of the bipolar forceps. \*  $p < 0.005$

The results of the pilot study on the immediate and long-term tissue effects convinced us to set the generator to strength level 4 and the power to 40 W in subsequent experiments. Changing the power seemed to be less important than the choice of the strength level in the induction of adhesion. Furthermore, no adhesions were induced with strength levels 1 and 2, even if some serosa damage

was immediately observed. Strength levels 3, 4 and 5 induced systematically dense and extended adhesions, causing damage to all the layers of the cecum. Strength level 3 seemed to provoke less extended adhesions. We chose the intermediate, strength level 4, to avoid the adverse effects caused by strength level 5, the maximal strength, even if adverse effects were rare in our studies.

### 2.1.3.1.3. Choice of the standardized peritoneal lesion

#### 2.1.3.1.3.1. Macroscopic assessment

Adhesions were systematically present in both the coagulation and suturing of the parietal peritoneum model and the coagulation of the cecum model. In the parietal peritoneum group, adhesions stuck to the abdominal flank with the intestine or the perigonadic fat pad. In all the cecum coagulation model groups, adhesions stuck to the injured intestine with the right flank abdominal wall, perigonadic fat pad, or seminal vesicle. The median qualitative score was 3 for all the groups (Table 3). The median extent of adhesions was 80% vs 100% vs 100% vs 31% vs 31% in the parietal peritoneum, visceral peritoneum (cecum, no injection), cecum NaCl low and high volume, and cecum DMEM groups, respectively (Table 3). Adhesions were significantly less extended in the Cecum NaCl high volume group compared with the Parietal Peritoneum, Cecum no injection and Cecum NaCl low volume groups (Figure 10).

Table 3: Qualitative and quantitative median (min, max) scores of the standardized peritoneal lesion groups. Adhesions were significantly less extended in the Cecum NaCl high volume group compared with the Parietal Peritoneum, Cecum no injection and Cecum NaCl low volume groups.

Group	Parietal Peritoneum	Cecum no injection	Cecum NaCl low volume	Cecum NaCl high volume	Cecum DMEM
Qualitative Score, Adhesion severity	3 (2-3)	3 (3-3)	3 (3-3)	3 (3-3)	3 (2-3)
Quantitative score Adhesion Extent	80% (40-100)	100% (50-100)	100% (31-100)	31% (8-41)	31% (10-100)

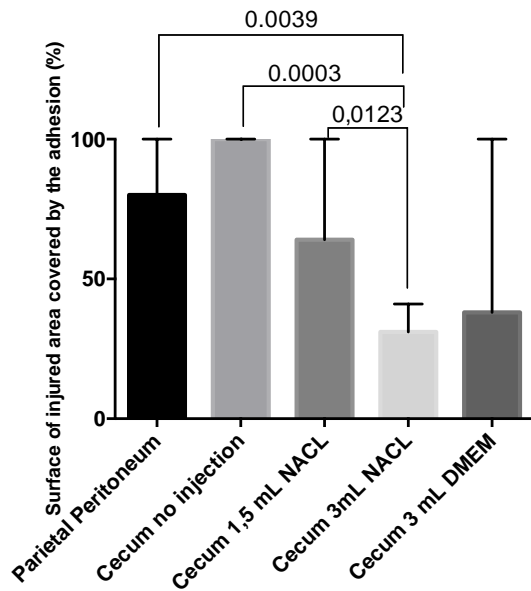


Figure 10: Quantitative median (range) scores of the different standardized peritoneal lesion groups. Adhesions were significantly smaller in the Cecum NaCl high volume group compared with the Parietal Peritoneum, Cecum no injection and Cecum NaCl low volume groups.

#### 2.1.3.1.3.2. Histological assessment

In the parietal peritoneum group the standardized peritoneal lesion damaged not only the peritoneum but also the subserosa and the underlying abdominal muscle. In addition to the infiltration by inflammatory cells, a granuloma formation and foreign body reaction were observed in the sutured tissues (Figure 11a).

In all the cecum coagulation model groups, the major reaction was an infiltration of the entire thickness of the cecum until the digestive lumen by inflammatory cells and fibroblasts (Figure 11b).

In all samples from all groups, adhesions were defined as multilayered fibrotic tissue sticking to the damaged area of the abdominal walls, to visceral fat or to the abdominal organs, including the liver or the intestines (Figure 11).

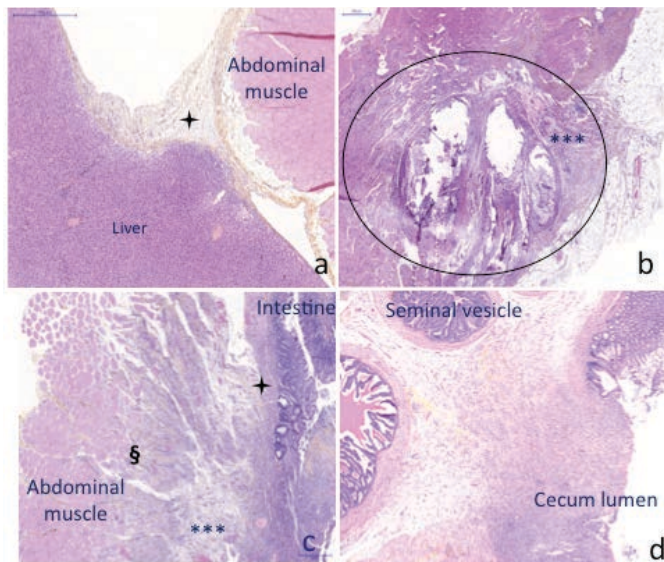


Figure 11: Tissues stained with hematoxylin phloxine saffron (HPS). Adhesions were defined as fibrotic tissue ( ) that stuck to at least two organs such as the liver (a), intestines (c) or seminal vesicle (d). Electrocoagulation led to leukocytic infiltration in the subserosa (\*\*), destruction of muscle cells in the underlying musculature (§) and early-stage fibrous organization ( ). Sutures led to granuloma formation (surrounded by a black circle) and foreign body reactions in the musculature (\*\*\*). Threats disappeared but empty spaces in the black circle indicate their initial location.

The review of the literature and this study permitted us to validate two rat models of postoperative adhesions. Both models were easy to perform, efficient, reproducible and clinically relevant. The first one was based upon a combined thermic and ischemic effect on the parietal peritoneum and the second one on a thermic effect on the visceral peritoneum. The second model allowed us to report a significant reduction of the extent of the adhesion after intraperitoneal injection (IP) of a large volume of NaCl solution. To schedule the next IP experiments by using our cell source as cell therapy, we were interested in adding this control group to assess the effect of a serum IP injection. In the literature, apart from Lucas, the intraperitoneal injection of isotonic saline serum, or buffers such as phosphate buffered serum (PBS) reduced adhesion formation (62,64,68,74,75).

#### 2.1.4. Conclusions

The results showed that increasing the strength level of the bipolar generator damaged the visceral peritoneum more, whereas changing the power damaged the tissue less. Strength levels 3, 4 and 5 induced systematically dense and extended areas of adhesion, causing damage to all layers of the visceral peritoneum.

The parietal and visceral models of adhesion were easy to perform, efficient, reproducible and clinically relevant according to the strategy of prevention studied. The parietal model offers a convenient support to fix a graft with sutures and the visceral cecal peritoneum model is convenient for lots of therapies because it is simple to perform. Adding an IP injection of a large volume of NaCl to the lesion models significantly reduced the extent of the adhesion area.

## 2.2. CHAPTER 2: CHOICE OF CELL SOURCE

The objective of the project was to develop an autologous cell-laden scaffold to prevent the formation of adhesions. An animal model was already available. The second step was to be able to isolate, culture, and expand autologous cells. Two cell candidates were selected based on their features: Mesothelial cells (MCs) were selected because they were already differentiated and functional, as required for peritoneum healing. Adipose stem cells (ASCs) were chosen for their stem cell capacities of expansion, self-renewal and differentiation as well as for their ready availability. Both types of cells were studied, and the methods and results are described below.

#### 2.2.1.1.1. Mesothelial cells (MCs)

#### 2.2.1.2. Method

##### 2.2.1.2.1. Anatomic Origin

Tunica vaginalis sampling was selected because it is less invasive than peritoneal sampling. In an attempt to transplant autologous cells into the rat adhesion model, it was necessary to obtain MCs without injuring the peritoneal cavity.

##### 2.2.1.2.2. Rats

Adult male Sprague-Dawley rats (350–400 g, Charles River, France) were housed in standard rodent cages under conventional laboratory conditions of a constant 22°C temperature with a 12 h light/dark cycle. They had free access to laboratory chow and tap water. The Ethics Review Committee for Animal Experimentation at the Lille Faculty of Medicine approved the experimental protocol (number APAFIS# 4623-2015112511478105).

##### 2.2.1.2.3. Tissue sampling

Under general anesthesia (an intraperitoneal injection of 130 mg/kg ketamine and 14 mg/kg xylazine or isoflurane inhalation), the inguinal and scrotal hair were shaved. The shaved areas were cleansed with Biseptine<sup>®</sup>, and a 2-cm midline incision was made on each side of the scrotum. Taking care to begin the dissection from the epididyme tuba to avoid contamination with subserosal tissue and trimming the marginal free tissue, particularly on the subserosal face, 3 cm<sup>2</sup> of the right side or both sides of the tunica vaginalis were sampled. Tissues were placed directly into a Petri dish with the peritoneal surface facing up between two pieces of gauze tissue soaked with iso serum for transport to the cell culture room.

The testis(es) were replaced inside the scrotum. Closure of the scrotum was carried out using a running suture of Vicryl 3.0<sup>®</sup> on the aponevrosis and by simple knots of Ethibond 2.0<sup>®</sup> on the skin. Postoperative analgesia was given by subcutaneous injection of buprenorphine (10 µg/kg) at 0 and 24 hours.

#### 2.2.1.2.4. MCs isolation

A pilot study was conducted to compare different tissue digestion protocols (data not shown). The better one, using 0.25% trypsin, is detailed below.

Each patch of excised tunica vaginalis was placed, peritoneal side facing up, directly on a 60-mm Petri-dish (Figure 12) and rinsed three times with PBS (pH 7.4). Irregular borders were cut and discarded to avoid contamination with fibroblasts (FBs). The enzymatic solution was discarded and 4 ml of stromal medium (DMEM supplemented with 10% fetal bovine serum (FBS) and gentamycin) was added to rinse and remove the contaminated cells. Next, each peritoneal tissue was placed in a clean Petri-dish in 3 ml of culture medium, and the MCs were separated by gently sliding a spatula over the surface of the enzyme-treated peritoneum and were then collected together into a flask. After homogenization, a cell count was carried out.

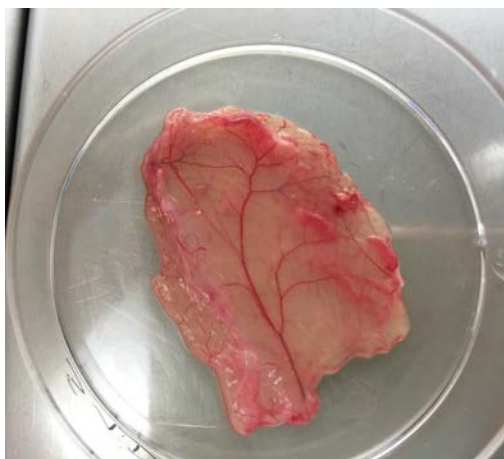


Figure 12: Macroscopic view of the tunica vaginalis

#### 2.2.1.2.5. MC culture

Freshly isolated cells were seeded at a density of  $6 \times 10^3$  cells/cm<sup>2</sup> in 6 well-plates or 6 cm Petri-dishes coated with stromal media and kept at 37°C (100% humidity, 5% CO<sub>2</sub>). At 48 h and after macroscopic observation, the cells were rinsed with Hanks' Balanced Salt solution (HBSS) and the cells were fed with DMEM enriched with 10 ng/ml epidermal growth factor (EGF), 2.5 µg/ml insulin, 400 ng/ml hydrocortisone, and 5% FBS, as proposed by Chen (100)). The media was changed every 48-72 h. The cells were passaged when they reached confluence; 0.05% trypsin was incubated with the cells for 3 min at 37°C until the cells were detached and floating. After neutralizing the trypsin with

media, the cells were pelleted in a centrifuge and the cell pellet was resuspended and counted using a Malassez square before being seeded at a density of  $6 \times 10^3$  cells/cm<sup>2</sup>. The purity of cell isolation in *in vitro* culture conditions was evaluated by observation of their typical polygonal or cobble-stone appearance with bright edges and their capacity for proliferation and survival duration was determined by calculating their doubling time according to the formula commonly described by Roth in 2006, <http://www.doubling-time.com/compute.php>.

#### 2.2.1.2.6. MC phenotype characterization

Mesothelial cells were identified by their phenotypic markers: cytokeratin 8, 18 and 19 and vimentin. MCs at the first passage were seeded at a density of  $2.5 \times 10^3$  cells/cm<sup>2</sup> on 12-mm glass coverslips pre-coated with FBS. Cellular proteins were localized after fixation with 4% formaldehyde, permeabilized with 0.3% Triton and blocked with PBS/2% BSA. The cells were incubated for 1 h in a humid and dark room at RT with a 1/100 concentration of an anti-vimentin antibody (Abcam ab 137321) and a 1/50 concentration of an anti-cytokeratin 8+18+19 antibody (Abcam ab 41825). The respective secondary antibodies used were a 1/400 concentration of a TRITC-conjugated anti-rabbit IgG antibody (Sigma T6778) and a 1/50 concentration of a FITC-conjugated anti-mouse IgG antibody (Sigma F9137). The negative controls consisted of cells stained without primary antibodies. For all samples, the cell nuclei were counterstained with DAPI (ThermoFisher Scientific). L142 epithelial cells were used as a positive control.

#### 2.2.1.2.7. Functional assessment of MCs *in vitro*

As we wanted to prove that we were able, through the construction of a peritoneal substitute, to graft functional MCs *in vitro* and *in vivo*, a functional assessment of MCs was required. Mesothelial cells are known to produce both the fibrinolytic enzyme tissue-type plasminogen activator (t-PA) and a specific t-PA inhibitor type 1 (PAI-1) that define the fibrinolytic activity in the peritoneal cavity. Enzyme-linked immunosorbent assay (ELISA) kits were used to measure the concentration of rat antifibrinolytic and fibrinolytic mediators produced by passage 1, 2 or 3 MCs in ten culture wells with five wells of FBs cultured for the negative controls. At 0, 1, 2, 4, 6, and 8 days, the culture medium was aspirated from

the well and stored at -80°C. Measurements of the amounts of tPA and PAI-1 were made according to the manufacturers' instructions (Molecular Innovations, Inc., Novi, MI, USA).

### 2.2.1.3. Results

#### 2.2.1.3.1. MC isolation

The surgical sampling of tunica vaginalis was convenient, feasible and well-tolerated by the rats. Only two of the forty-seven rats were diagnosed with complications: one with an intra-abdominal hematoma and the other with an adhesion sticking to the testis and intestine.

Digestion with 0.25% trypsin for 30 min, yielded between 32 to  $747 \times 10^3$  cells per isolation for one side of the tunica vaginalis (approximately  $3 \text{ cm}^2$ ). The mean cell yield was  $224 \pm 151 \times 10^3$  cells/isolation. The cell yield was unaffected by the experience level of the student performing the experiment (Figure 13) and cell yield was not correlated with the initial sampling of one or both sides (left and right) of the tunica vaginalis (Figure 14). We divided the isolation procedures into four categories using the first quartile, the median, and the third quartile values, 111, 192, and  $280 \times 10^3$  cells/isolation, respectively. The cell yield was defined as very low if less than  $111 \times 10^3$  cells were isolated; low if 111 to  $192 \times 10^3$  cells were isolated, moderate if 193 to  $280 \times 10^3$  cells were isolated and high if more than  $281 \times 10^3$  cells were isolated.

No statistically significant differences were found between the categories based on the weights of the rats (Figure 15).

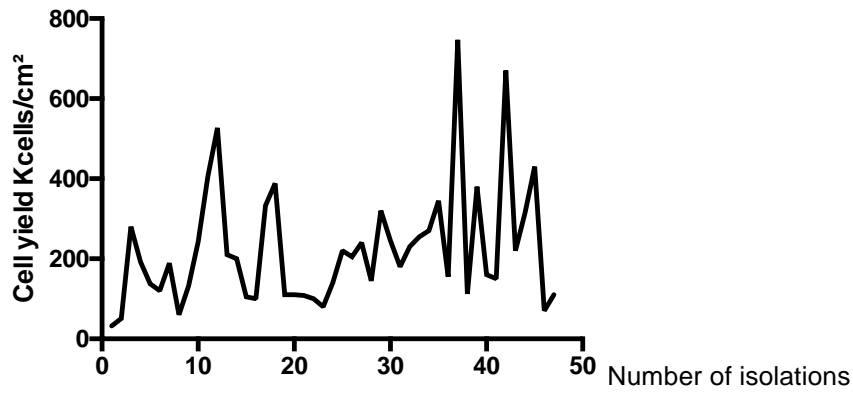


Figure 13: Chronological presentation of the number of MCs isolated per experiment. Experience did not impact the cell yield.

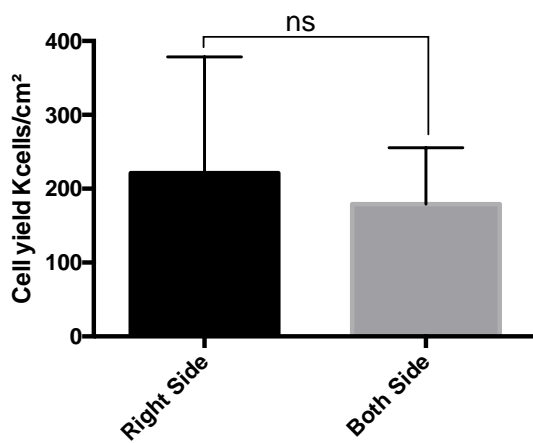


Figure 14: Correlation between cell yield and isolation of one or two (left and right) side(s) of the tunica vaginalis. No significant difference was found between the digestion of the right side and digestion of both sides.

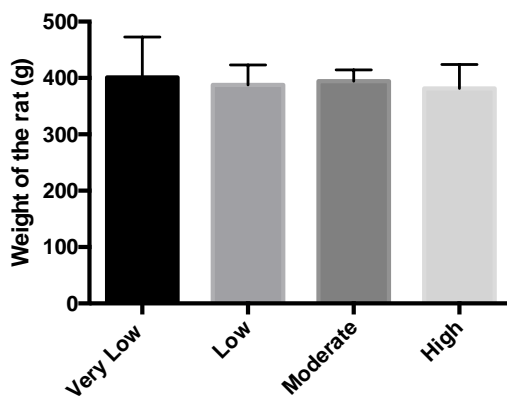


Figure 15: Correlation between rat weight and the cell yield category per isolation. No significant differences were found.

### 2.2.1.3.2. Mesothelial cell culture

MCs from the tunica vaginalis (n=47) were homogenous and healthy, but the success of harvesting MCs this way was variable and unpredictable (Picture 16a). Cell morphology and growth were either excellent with a typical polygonal or “cobble-stone” appearance with bright edges, good or heterogeneous. Heterogeneous colonies composed of a mixture of large, small or abortive mesothelial colonies, as well as fibroblastoid colonies were frequently observed (Picture 16b and c). MC morphology (excellent, good or inhomogeneous) during culture was not associated with the cell yield/isolation (Figure 17). Cell culture confluency was reached after  $6\pm 1$  days. The cell doubling time was 18 h for passage one, 28 h for passage two, and 51 h for passage 3. After only three passages, these adult, well-differentiated cells became senescent, demonstrating that they had a limited capacity for expansion.

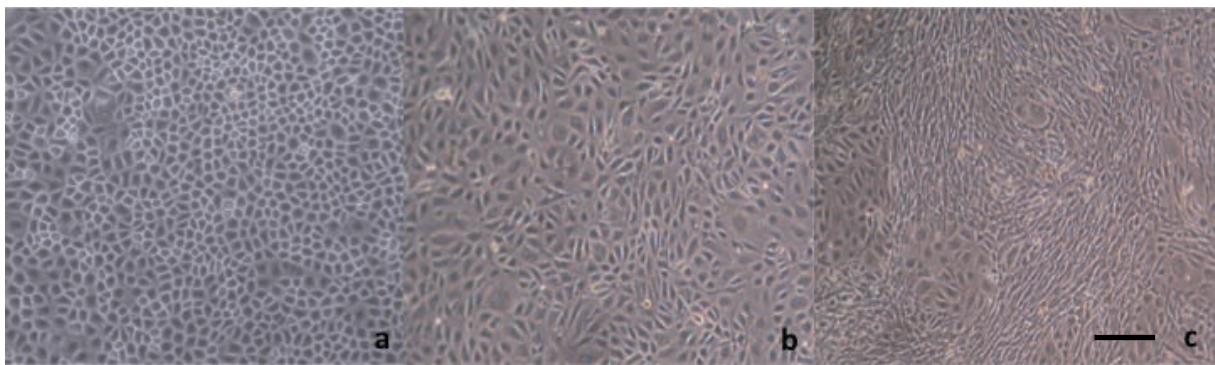


Figure 16: Microscopic observation of confluent mesothelial cell culture, first passage, Day 7: good morphology: homogenous and healthy (a); heterogeneous colonies (b and c). Bar, 200  $\mu$ m.

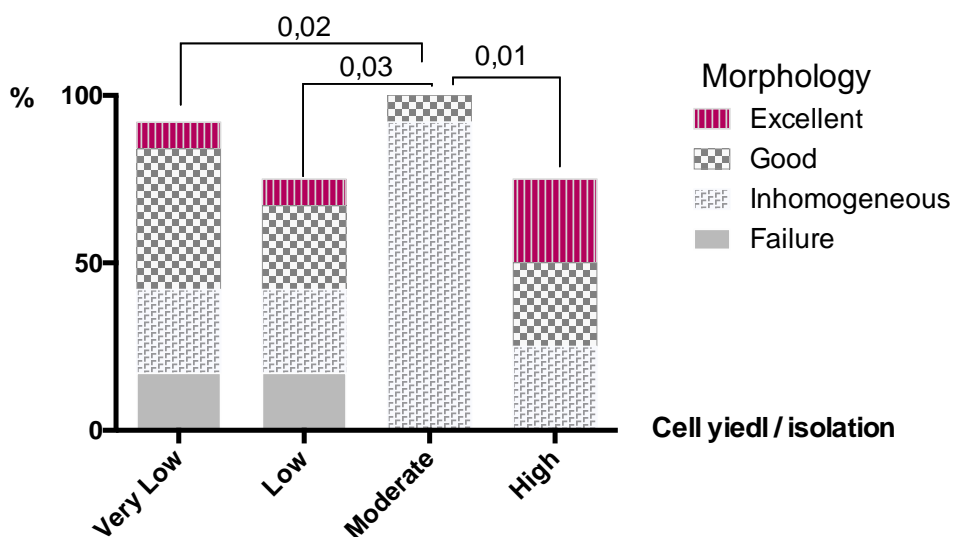


Figure 17: Cell morphology in culture versus cell yield/isolation, passage 0 cells. Fisher's Exact Test, two sided.

#### 2.2.1.3.3. MC characterization

Passage 1 MCs, which had the typical cobble-stone morphology and bright edges, were positively stained for vimentin and cytokeratin 8+18+19 (Figure 18).

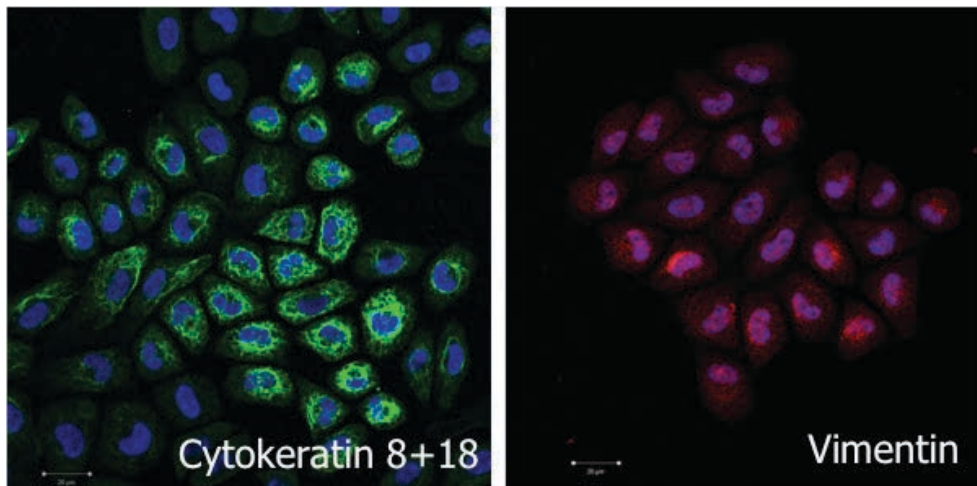


Figure 17: Immunocytochemistry of rat mesothelial cells: cells were stained with anti-cytokeratin 8+18+19 and anti-vimentin antibodies. Bar = 20 µm.

#### 2.2.1.3.4. Functional assessment of MCs *in vitro*

In the aspirated media samples stored at -80°C from previously described experiments, the levels of tPA and PAI-1 proteins produced at the following time points were quantified by ELISA (n = 4): 0–2 days, 2–4 days, 4–6 days and 6–8 days, but no signal was found for tPA and PAI-1 in both MCs (n= 2) and FB (n=1) supernatants.

#### 2.2.1.4. Conclusions

MCs were isolated from the tunica vaginalis without increasing rat morbidity. The cell yields after tissue digestion ranged from very low to high, MC morphology in culture ranged from excellent, with a typical polygonal or “cobble-stone” appearance with bright edges positively stained by cytokeratin and vimentin, good, or inhomogeneous. No factor was identified that explains these variations. After only three passages, these well-differentiated, adult cells, with a limited capacity for expansion, became senescent.

#### 2.2.1.5. Perspectives

The limited capacity of MCs for expansion has been proved by their senescence. Sampling of the tunica vaginalis in humans would be an invasive procedure, would yield a limited quantity of harvested cells and would only be possible in males. Moreover, the morbidity following the procedure is high and the harvested tissue is potentially cancerous. Finally, the number of cells isolated from the rats and the phenotype of the isolated cells in culture varied. The epithelial-to-mesenchymal transition (EMT) could explain the heterogeneous morphology of the cultured cells. EMT could be determined by measuring the reorganization of the cytoskeleton using morphological and immunocytochemical analysis, as it is defined by the loss of cell-cell junctions, reorganization of the cytoskeleton and disappearance of apical and basal cell surface polarity (4). EMT can be assessed by changes in the expression of cytokeratin (an epithelial intermediate filament protein), vimentin (a mesenchymal cell-specific intermediate filament protein), cell-surface glycoproteins such as podoplanin, mesothelin, and proteins of intercellular attachments such as  $\beta$ -catenin and ZO-1 (55,101,102). Lachaud used EMT as a quality to support the use of adult human MCs as a possible surrogate for damaged corneal endothelium (5). Moreover, EMT appears in a variety of normal physiological processes but also in peritoneal pathologies (102). Menstrual effluent induced EMT in MCs; the changes were reversible, revealed by a disruption in cell-cell contact and an increase in MC motility (103).

On another hand, fibroblast contamination could also explain the heterogeneity of the MC cultures, as lots of FBs were present in the submesothelial stroma of the initial tissue samples. Tissue digestion, MC separation with a spatula and MC collection are sources of FB contamination.

Nextly, the functional assessment of MCs is the ultimate characterization of functional MCs *in vitro* or *in vivo*. The fibrinolysis pathway or glycocalyx secretions are two pathways that can be used to explore the functions of the peritoneum. We need to work more on the fibrinolysis pathway to prove the functionality of our MCs at the moment of their use for cell- or tissue- therapy.

## 2.2.2. Adipose stem cells (ASCs)

### 2.2.2.1. Methods

#### 2.2.2.1.1. Rats

Male adult Sprague-Dawley rats (350-400 g, Charles River, France) were housed under conventional laboratory conditions in standard rodent cages at a constant temperature of 22°C with a 12 h light/dark cycle. The rats had free access to laboratory chow and tap water. The Ethics Review Committee for Animal Experimentation at the Lille Faculty of Medicine approved the experimental protocols (number APAFIS# 4623-2015112511478105).

#### 2.2.2.1.2. Choice of anatomic origin of the fat biopsy

Both human and rat fat tissue depots have distinct intrinsic features and adipose stem cells with phenotypes specific to their location and fat type. Two rat sample sources, subcutaneous inguinal white fat and perigonadic visceral white fat, were compared in terms of their cell isolation yields, morphology, phenotype and capacity for self-renewal and expansion.

##### 2.2.2.1.2.1. Inguinal rASC isolation from subcutaneous fat pads

Under general anesthesia (as previously described), the inguinal area was shaved and cleansed with Biseptine<sup>®</sup>. A short skin incision of the inguinal area permitted the removal of a subcutaneous white fat pad (1,8 g - 2,9 g) from the inguinal region. Closures were carried out by simple knots of Vicryl 3.0<sup>®</sup> on the subcutaneous tissues and by simple knots of Vicryl 2.0<sup>®</sup> on the skin. The tissue samples were soaked in cold PBS.

##### 2.2.2.1.2.2. Gonadic rASC isolation from visceral fat

Under general anesthesia, the ventral hair was shaved, the abdomen cleansed with Biseptine<sup>®</sup> and a 2–3 cm midline incision was made on the inferior part of the abdominal wall to harvest a piece of perigonadic fat (1-4 g). The digestive organs were gently replaced. Closures were carried out by simple knots of Vicryl 3.0<sup>®</sup> on the subcutaneous tissues and by simple knots of Vicryl 2.0<sup>®</sup> on the skin. Tissue samples were soaked in cold PBS.

### 2.2.2.1.3. ASC isolation

#### 2.2.2.1.3.1. Tissue digestion

Adipose tissue was washed in PBS, placed in a Petri-dish, minced into small pieces using scissors (Figure 19), and digested with a mixture of collagenase A (Roche, 2 mg/ml) in 20 mg/ml BSA (3 ml/g of fat tissue) for 60 min in a water bath at 37°C under strong, manual agitation every 10 min. Digestion was stopped with FBS (final concentration 10%).

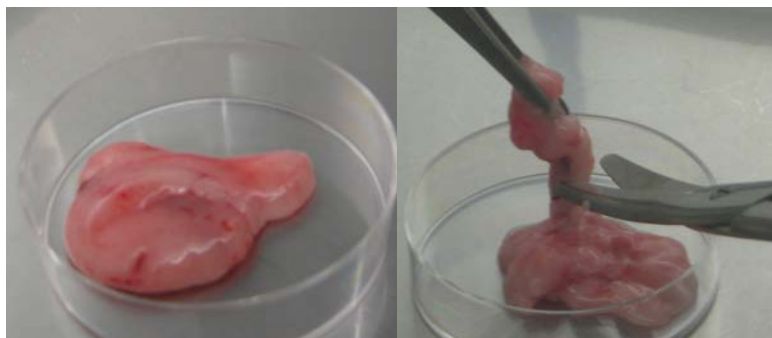


Figure 19: Inguinal fat pad on a Petri-dish, minced into small pieces using scissors before digestion

#### 2.2.2.1.3.2. Stromal vascular fraction (SVF) isolation

The cell suspension was filtered through a 250  $\mu\text{m}$  nylon mesh and centrifuged for 10 min at 500 g RT to discard free lipids and the supernatant and isolate the stromal vascular fraction (SVF). After a second filtration with a 100  $\mu\text{m}$  mesh filter and centrifugation at 500 g for 10 min at RT, the SVF pellet was resuspended in stromal media and seeded.

### 2.2.2.1.4. Optimization of the culture medium

#### 2.2.2.1.4.1. rASCs culture

Cells from the freshly isolated SVF were seeded at a density of  $1 \times 10^3$  cells/cm<sup>2</sup> in DMEM supplemented with stromal medium or MSC Growth Medium (Promocell®) and incubated at 37°C with 5% CO<sub>2</sub>. One rinse was performed after 48 h to eliminate undesired cells such as red blood cells. The media was changed every 48-72 h. The cells were passaged when they reached confluence by incubating them with 0.05% trypsin for 2 to 3 min at 37°C, until the cells were detached and floating. After neutralizing the trypsin with media, the cells were pelleted, resuspended and counted using a

Malassez square before being seeded at a density of  $5 \times 10^3$  cells/cm<sup>2</sup>. The purity of cell isolation in *in vitro* culture condition was evaluated by observation of their typical thin spindle-like shape and their capacity for proliferation and survival duration was determined by calculating the doubling time according to the formula commonly described by Roth in 2006 <http://www.doubling-time.com/compute.php>.

#### 2.2.2.1.4.2. Proliferation assay for the comparison of media types

ASCs at first passage were seeded at a density of  $7 \times 10^3$  cells/well in 24 WP in stromal media (n=3/medium/rat). Six hours after seeding, the media was removed and replaced with MSC Growth Medium (Promocell®) in half of the wells and stromal media in the other half. The cells were counted after 48 h of proliferation by using an automated counter.

#### 2.2.2.1.5. Stem cell capacities

##### 2.2.2.1.5.1. Self-renewal capacity or clonogenicity

In a 25 cm<sup>2</sup> dish, ASCs at passage 0, 1, or 2 were seeded at a density of  $1 \times 10^3$  cell/well. The effect of growing cells in DMEM supplemented with 20% FCS or MSC Growth Medium (Promocell®) was compared. Media was changed after 5 days. Colony-forming efficiency was assessed after 9 days, after two rinses with warm, non-sterile PBS by staining with 2-3 ml/well of Crystal Violet for 5 min. Several rinses with water were used to discard the unfixed stain. After drying, colonies with 50 cells or more were counted, and the frequency of the colonies was expressed per  $1 \times 10^3$  plated cells.

##### 2.2.2.1.5.2. Osteogenic differentiation

Cells were seeded at a density of  $20 \times 10^3$  cells/well in 96-well plates. After reaching confluence, half of the wells were induced and the other halves were non-induced. In the induced wells the media was replaced with 15 µL of a solution composed of dexamethasone  $10^{-2}$  M (1 µL in 1 ml of media), ascorbic acid (5 mg in 1 ml of media), βGP (216 mg in 1 ml of media prepared the day before, as it requires a long time to dissolve) in  $2 \times 725$  µL of stromal medium. In the non-induced wells, non-

inducing stromal medium was used. Twice a week for 30 days, the media from each well was discarded and replaced with 125 µL of inducing or non-inducing media.

Osteogenic assessment at day 30 consisted of observing the presence of trabecular lines and calcium deposits (stained with Alizarin red for qualitative assessment) in the induced wells. To prepare Alizarin red solution, Alizarin red powder (Sigma A 5533) at a concentration of 40 mM was diluted in 20 ml of milli Q water and the pH of the fresh solution (pH=2.3) was adjusted to a pH of 4.1 or 4.2 with 0.5 mM NaOH. The solution was filtered through a 45 µm cellulose strainer to discard debris.

In the induced and non-induced wells, media was discarded and the cells were rinsed with 125 µl/well of 10% formalin for 5 min. Then, the same volume of formalin was added to each well, incubated for one hour and discarded. The wells were rinsed with 200 µl/well of milli Q water. When the wells were dry, 75 µl/well of the AZR solution was added and incubated for 20 min at room temperature (RT) on a shaker at 80 rpm. The AZR solution was then discarded, and four successive rinses were done with 200 µl of milliQ water, at RT on the shaker at 80 rpm, for 5 min/rinse. Pictures were taken during the last rinse to have the best contrast.

#### 2.2.2.1.5.3. Adipogenic differentiation

Cells were seeded and induced for osteogenic differentiation as previously described. Induced cells were fed using a StemPro® Adipogenesis Differentiation Kit A10070-01 (for 1.5 ml, 0.15 ml of supplement media was added to 1.35 ml of base media). The inducing medium contained insulin, dexamethasone, IBMX, indomethacin and hydrocortisone to promote the proliferation and differentiation of preadipocytes.

Adipogenic assessment at day 14 consisted of looking for the presence of lipid droplets in the induced wells. Briefly, the inducing media was discarded, and the cells rinsed with 125 µl/well of 10% formalin for 5 min. Then, the formalin was discarded and the same volume of fresh formalin was added and incubated with the cells for one hour. During this time the Red Oil Solution was diluted in milliQ water at a ratio of 6:4 and filtered with a 0.2 µm cellulose strainer. After 20 min, the solution was filtered through a 45 µm PTFE φ13 mm strainer. In the 96 WP, the formalin was discarded, and the cells were rinsed with 125 µL of 60% isopropanol. When the wells were dried, 50 µl/well of Red Oil Solution was added for 10 min. Then, the Red Oil Solution was discarded, and four successive rinses were done

with 50 than 100 then 150 and 200 µl of milliQ-water. Pictures were taken keeping some water in each well to have a better contrast for qualitative comparisons.

Lipid production was quantified by measuring the absorbance of Red Oil Solution at 492 nm. The water was removed and the wells were dried. Then 200 µl/well of 100% isopropanol were added to dissolve the dye. After pipetting, 150 µl of the solution in each well was placed in a 96 WP. Two controls were used: a well with 100% isopropanol and a well with 3.3% Red Oil Solution in 100% isopropanol.

#### 2.2.2.1.5.4. Differentiation toward the mesothelial phenotype: cultures using conditioned media (CM)

To study the paracrine effect of MCs or the effect of the culture medium on ASCs,  $10 \times 10^3$  cells/well of ASCs were seeded on 24-well plates and supplemented with 500 µl of MSC Growth Medium (Promocell®) one day before the experiment (day -1). After 24 h, on day 0, differentiation was initiated using a conditioned media (CM) and the media was changed every day.

CM preparation: MCs were seeded in a Petri-dish at a density of  $10 \times 10^3$  cell/cm<sup>2</sup>. The medium in the dish was discarded every 24 h. Then, the media was centrifuged to eliminate cells (1000 g, 5 min). The supernatant was filtered through a 0.22 µm filter.

The MC media was diluted with an equal volume of MSC Growth Medium (Promocell®) to obtain the CM. Control 1 was ASCs cultured in medium 1, which consisted of half DMEM and half MSC Growth Medium (Promocell®) and control 2 was ASCs cultured in medium 2, MSC Growth Medium (Promocell®).

The difference between the CM and control 1 was the factors secreted by the MCs and their extracellular matrix. The difference between CM and control 2 was the FCS and other supplements in DMEM.

For the first experiment, only the proliferation rate was assessed on day 2, 4 and 6 using Alamar Blue®.

### 2.2.2.2. Results and discussion

#### 2.2.2.2.1. Choice of anatomic origin of the mesothelium biopsy

The mean number of cells isolated was  $1200 \pm 285 \times 10^3$  cell/g of subcutaneous fat vs  $704 \pm 162 \times 10^3$  cell/g of visceral fat (Figure 20).

The cultured ASC morphology consisted of well-elongated, connected, stellar cells (Figure 21). Confluency was reached in 5 to 6 days. ASCs isolated from subcutaneous fat were easily passaged four or five times and had a mean doubling time that ranged from 20 to 29 hours. ASCs isolated from visceral fat did not survive longer than the third passage. Subcutaneous fat-derived ASCs showed a clonogenicity of  $14 \pm 3\%$  (Figure 22a, c) compared with visceral fat-derived ASCs, which had a clonogenicity of  $4.5 \pm 3.5\%$  (Figure 22b, c).

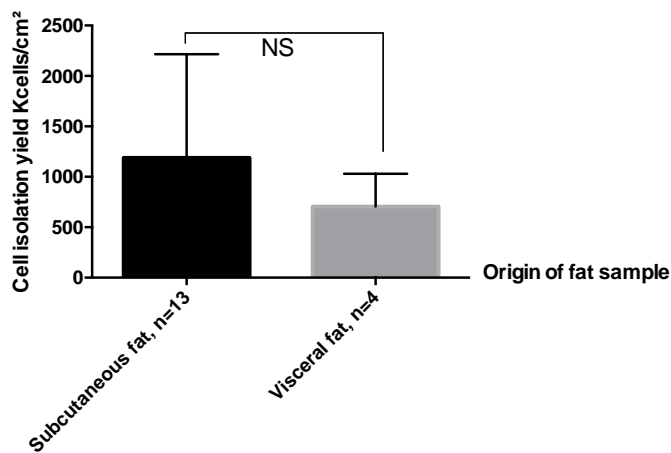


Figure 20: Number of freshly isolated cells from the SVF according to the anatomic origin of the rat fat pad:  $1200 \pm 285 \times 10^3$  cell/g of subcutaneous fat vs  $704 \pm 162 \times 10^3$  cell/g of visceral fat. There was no significant difference.

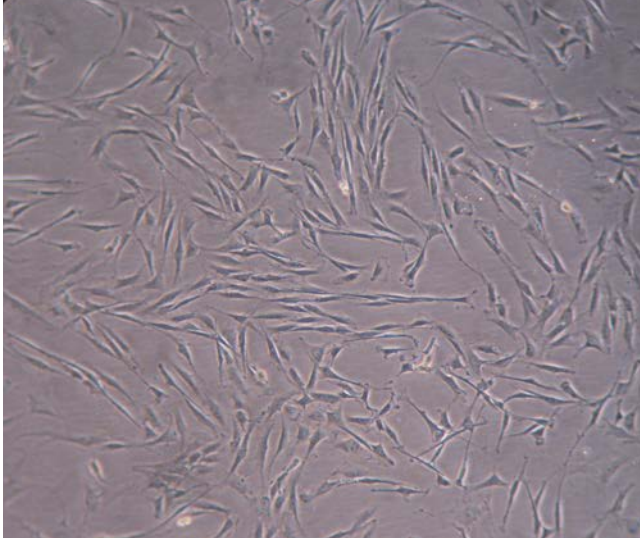
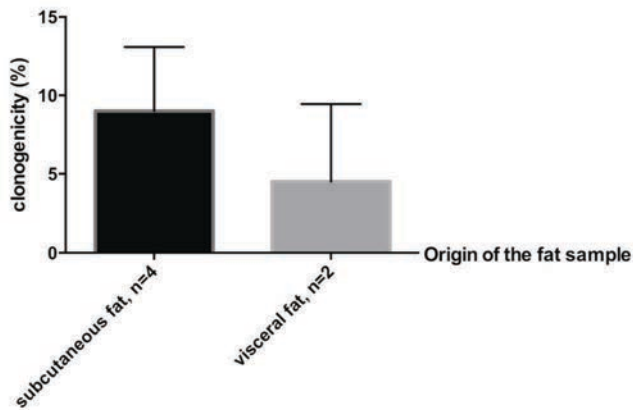
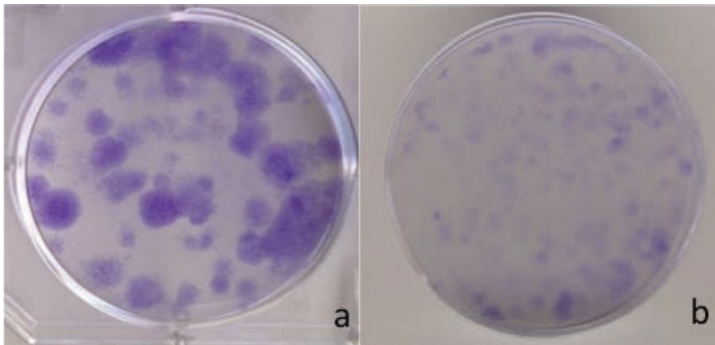


Figure 21: rASCs isolated from the subcutaneous inguinal fat pad, first passage, Day 6: elongated spindle-shaped and stellar cells. Confluency 80%.



C

Figure 22: Clonogenicity of the isolated adipose stem cells according to the anatomic origin of the rat fat pad: subcutaneous white inguinal fat-derived adipose stem cells showed a clonogenicity of  $14 \pm 3\%$  (a, c) in comparison with visceral fat-derived ASCs which had a clonogenicity of  $4.5 \pm 3.5\%$  (b, c). No significant differences were found.

#### 2.2.2.2.2. Optimization of the culture media

#### 2.2.2.2.1. rASC culture

After 48 h, passage 2 subcutaneous fat-derived ASCs had a good morphology: thin spindle shaped and branched out cells (Figure 23a,c) compared with cells grown in stromal media, which had fewer, flatter, and larger spindle-shaped cells (Figure 23b,d).

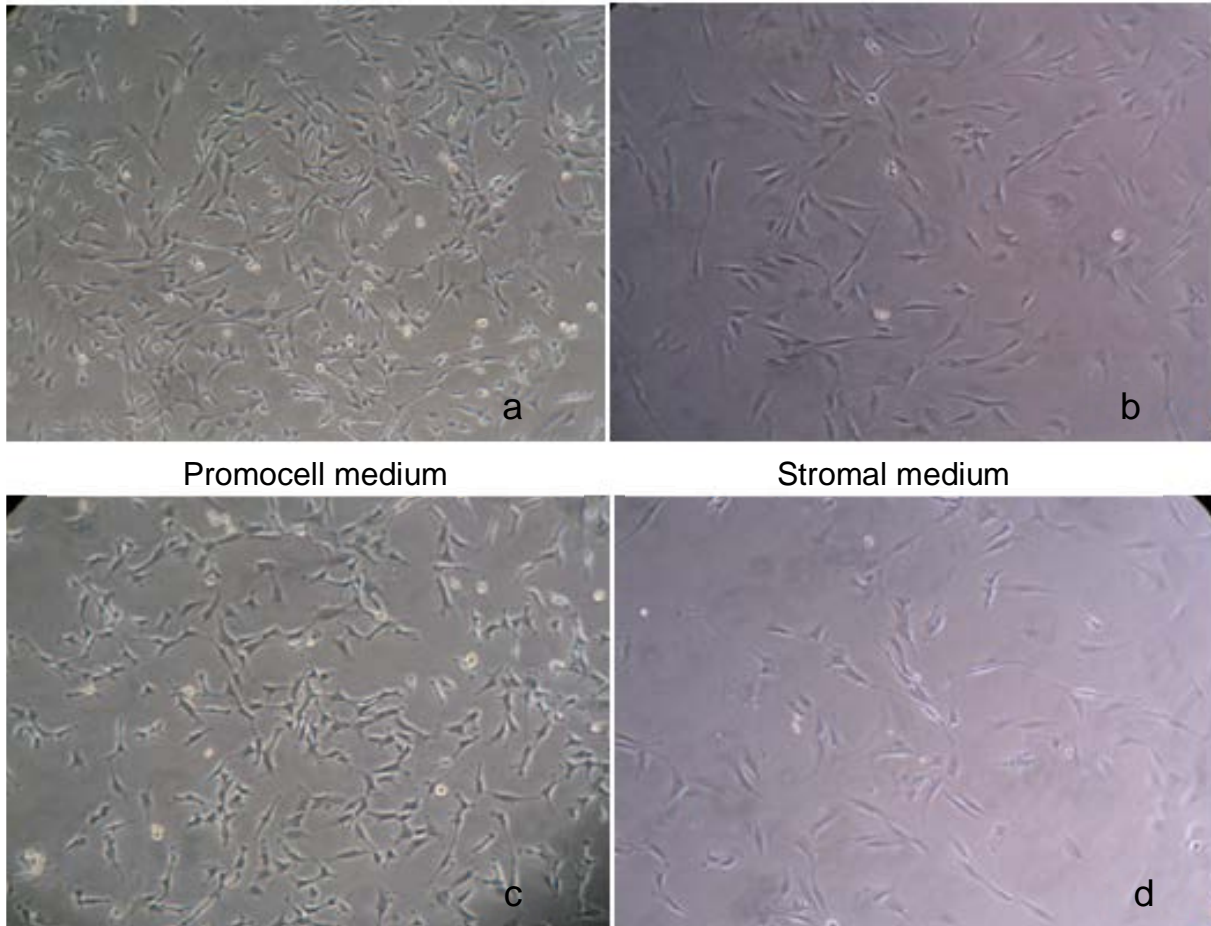


Figure 23: Subcutaneous fat-derived ASCs, passage 2, 48 h, seeding density:  $7 \times 10^3$  cell/well in 24 WP grown in MSC Growth Medium (Promocell®) had very good morphology, thin spindle-shaped and branched-out cells in (a, c) in comparison with cells grown in stromal media which had fewer, flatter, and larger spindle-shaped cells (b, d).

#### 2.2.2.2.2. Proliferation assay for media comparison

The doubling time for ASCs grown in stromal media ( $n=3$ /group) was  $28 \pm 0.7$  h and  $11 \pm 0.5$  h for ASCs grown in MSC Growth Medium,  $p=0.0031$ .

#### 2.2.2.2.3. Clonogenicity based on media type

ASCs ( $n=2$ /group) grown in MSC Growth Medium were more efficient at forming colonies (27%) than were those grown in stromal media (12%),  $p=0.003$ .

### 2.2.2.2.3. Stem cell capacities

#### 2.2.2.2.3.1. Colony forming efficiency

Rat ASCs seeded at a very low density had a mean clonogenicity of  $14 \pm 9\%$ .

#### 2.2.2.2.3.2. Osteogenic differentiation

Only two of the five osteogenic differentiation experiments succeeded. Calcium deposits in induced cells were stained with Alizarin red (Figure 24a, c), in contrast to the non-induced cells. The three other experiments failed because of unexpected adipogenic differentiation in the MSC Growth Medium or because the cell sheets detached from the bottom of the well during differentiation.

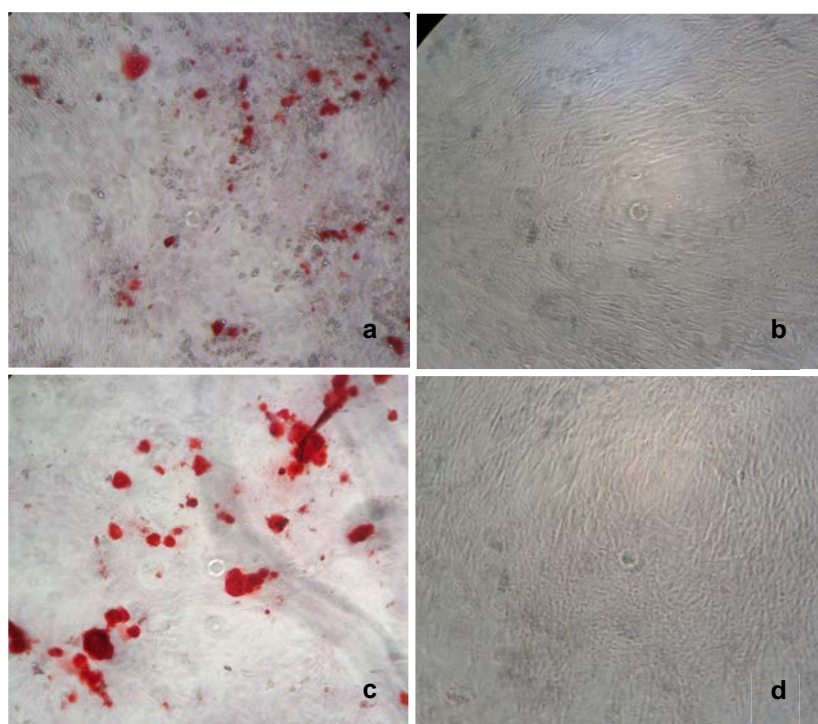


Figure 24: Macroscopic observation after 30 days of osteogenic differentiation in induced rASCs (a, c) in contrast with non-induced rASCs (b, d).

#### 2.2.2.2.3.3. Adipogenic differentiation

The adipogenic differentiation experiments succeeded, and lipids were stained with Red Oil Solution. Induced ASCs contained a significantly higher amount of Red Oil Solution than did non-induced cells (Figure 25). Semi-quantitative evaluation by microscopic observation showed red deposits in the induced cells and no staining in the non-induced cells (Figure 25c).

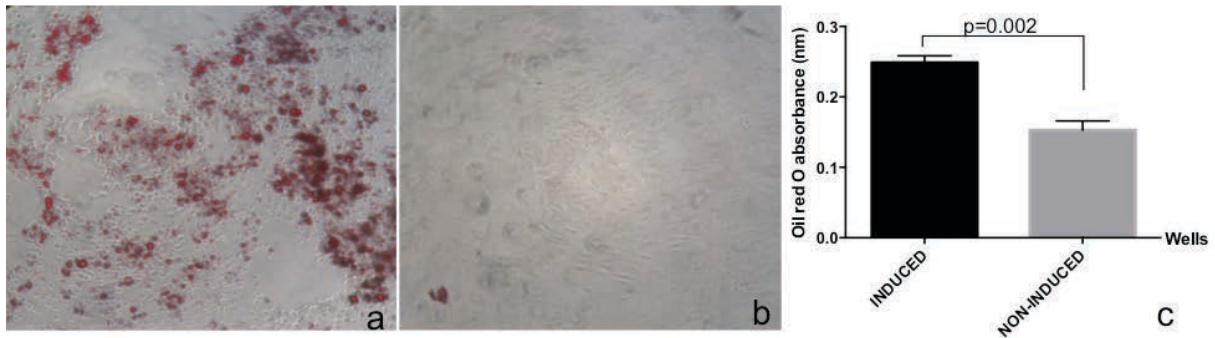


Figure 25: Qualitative and semi-quantitative assessment of adipogenic differentiation after 14 days: Induced cells contained a significantly higher count of Red Oil Solution (a, c) than non-induced cells (b, c).

#### 2.2.2.2.3.4. ASC differentiation towards a MC phenotype

Cell counts, doubling time and viability assays showed that ASCs cultured in CM were able to survive and proliferate (Figure 26). No significant differences were calculated because only one experiment was performed. Conditioned media improved ASC proliferation and viability because of the factors secreted by MCs and their extracellular matrix and the presence of FCS and other supplements in DMEM.

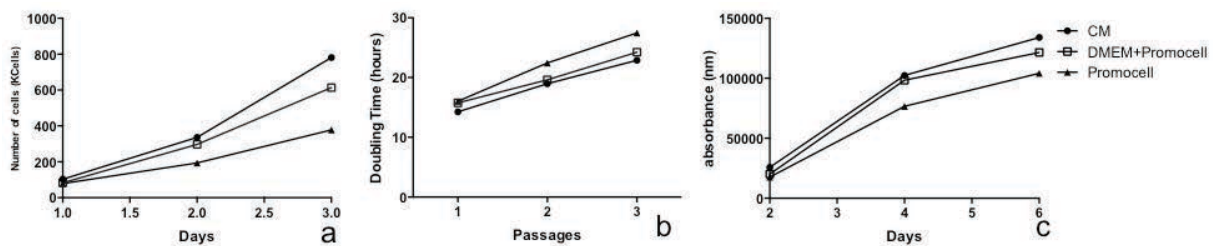
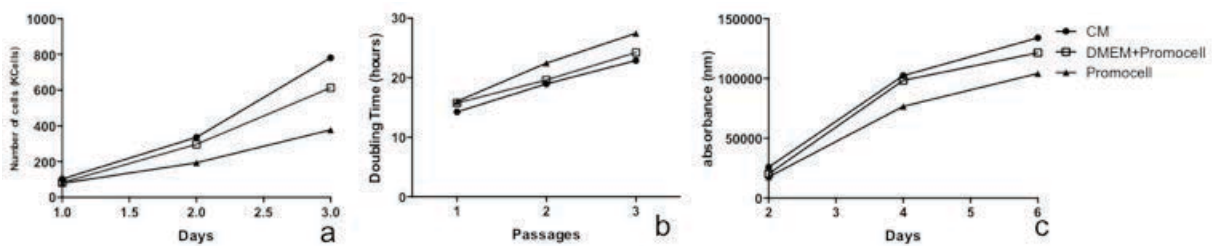


Figure 26: Assessment of ASC proliferation using conditioned media using cell counts (a), doubling times (b) and the Blue Alamar® vitality assay (c). n=1, no statistical analyses were performed.



#### 2.2.2.3. Conclusions

ASC self-renewal and long-term proliferation capacity and their multipotent differentiation potential toward adipose and osteogenic phenotypes were confirmed. Subcutaneous white fat tissue seemed to provide more cells than visceral white fat did. MSC Growth Medium enabled cell culture, expansion and renewal.

#### 2.2.2.4. Perspectives

To complete the description of the ASC phenotype, we were interested in characterizing freshly isolated cells from the SVF to confirm the ratio of stem cells in SVF (approximately 2-3%) using cell-sorting and based upon generally accepted and published definitions of adipose stem cells: CD34+CD31-CD45-CD146- (43,50,52,104–108). After the first passage and selection of ASCs based on their capacity to adhere to a plastic surface, the same characterization informed us of the expansion capacity and of selection of our primary isolates. This characterization of the ASCs transplanted *in vivo* confirmed the nature of the engrafted cells.

The differentiation of ASCs toward a mesothelial phenotype has yet to be proven. Differentiation to the ectoderm phenotype has been published; ASCs have been differentiated into keratinocyte-like cells, to engineer a stratified epidermis (109). Differentiation to the endoderm phenotype has also been proven; ASCs were differentiated into urothelial cells *in vitro* (110). There has also been a possible differentiation of rat ASCs into contractile smooth myocytes (111). rASCs attenuated peritoneal injuries in a rat model of peritonitis through a paracrine effect on MC proliferation; the ASCs were colocalized with peritoneal cells close to the injured MCS (112). To prove that ASCs could differentiate into MCs, three experiments were performed and compared *in vitro*: direct co-culture to study direct cell interactions, culture using conditioned medium (CM) to study the influence of the media or paracrine effects of MCs on ASCs, and co-culture using Transwell® inserts, to study cell interactions and active cell crosstalk or autocrine effects of MCs.

MC- and ASC-labeling strategies for *in vivo* cell-tracking experiments would permit us to study biological processes involving engrafted cell interactions with their scaffold or with bystander cells such as MCs or macrophages to study the adhesion of transplanted ASCs to the injured surface and finally to give us key points to optimize the cell delivery strategy.

Attention could also be given to the use of another stem cell source: endometrial and menstrual blood mesenchymal stem cells as described by D Ulrich and her team (113).

Further experiments on human cell cultures are required to learn more about storage, isolation, culture, and characterization of human MCs and ASCs. This knowledge represents a milestone in our regenerative medicine project before we can think about a clinical study. Comparative studies similar to those performed with rat tissues have been started with human tissues to demonstrate the feasibility of our concept for future clinical application. The regional ethics committee, the hospital and a patients' committee accepted a clinical study, titled Meso-Patch 1408, promoted by the Centre Oscar Lambret. The inclusion of patients undergoing reconstructive breast surgery (n= 20) to get lipoaspirate residues and patients undergoing abdominal surgery (n=10) to get peritoneal biopsies was scheduled. Finally, we were able to include only 5 patients in the arm breast surgery to isolate human adipose stem cells (hASCs).



**PROTOCOLE D'ETUDE**  
**N° du protocole : 2014-08**

**PATCH ANTI ADHERENTIEL DE CELLULES MESOTHELIALES DANS  
UNE MATRICE D'HYDROGEL :**  
Analyse exploratoire évaluant l'expression du morphotype et du phénotype  
mésothélial après culture à partir de deux sources cellulaires d'origine  
humaine.

Code de l'étude : MESO-PATCH-1408  
N° ID RCB : 2014-A01866-41

**Promoteur :** Centre Oscar Lambret  
3, rue Frédéric Combemale  
BP307 59020 Lille Cedex

Five healthy female patients, aged 37-62 years, undergoing lipofilling for breast reconstructive surgery from June to October 2015 were included in the study based on the following inclusion criteria: >18 years old, received and gave signed, informed consent, belonged to a social security scheme, and were operated on in our hospital. Exclusion criteria for the study: were being pregnant or nursing, or under guardianship. None of the participants presented comorbidity. Their BMI ranged from 18 to 30 kg/m<sup>2</sup>.

The fat tissue was harvested from the abdomen or thighs using a liposuction machine after infusing iso saline serum with adrenaline into the tissue. The adipose tissue was centrifuged at 3,000 rpm for 5

min. After centrifugation, the bottom cell debris and supernatant were removed. The middle layer of adipose aspirates (Figure 27) was transferred to the laboratory in an isotherm box for immediate digestion or was stored in a fridge at 4°C. Immediate isolation was performed on two fresh lipoaspirates (patients 3 and 4), and delayed isolation was performed on the other samples after 2 hours (n=1, patient 2), 8 hours (n=1, patient 5), 18 hours (n=1, patient 1) and 24 hours (n=1, patient 5).



Figure 27: Intact lipoaspirate

The number of isolated cells in the SVF ranged from 41 to  $498 \times 10^3$  cells/g of fat. Fridge storage seemed to influence the cell yield (Figure 28). Freshly digested samples from patient 3 and 4 permitted the isolation of 298 and  $498 \times 10^3$  cells/g of fat. The other samples were kept for 2 to 24 hours and the cell yield ranged from 41 to  $129 \times 10^3$  cells/g of fat. Cells were seeded at a density of  $1 \times 10^3$  cells/cm<sup>2</sup> and did not reach confluency. Confluency was reached after 4 or 5 days in cultures with a seeding density of  $8 \times 10^3$  cells/cm<sup>2</sup>.

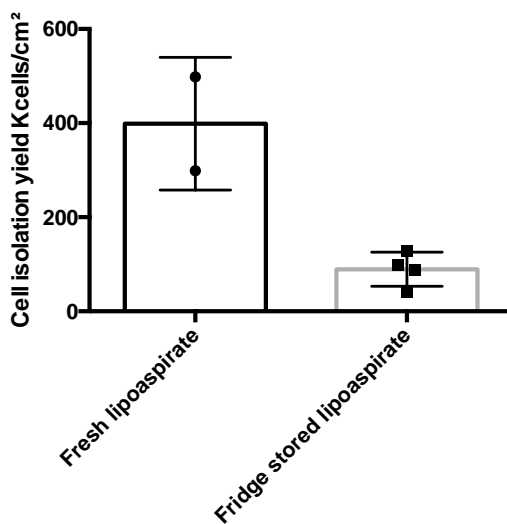


Figure 28: Consequences of lipoaspirate storage at 4°C on the number of isolated cells in the SVF: fridge storage seemed to decrease the capacity of cells isolation.

Further experiments on human cell cultures are required to be able to make conclusions about storage, isolation, culture, and characterization of human MCs and ASCs

## 2.3. CHAPTER 3: COMPARISON BETWEEN CELL-THERAPY AND CELL-LADENED SCAFFOLDS OR TISSUE-THERAPY

### 2.3.1.1.1. Introduction

Two cell sources were isolated, characterized and expanded, presenting complementary advantages and disadvantages. We were interested in cell transplantations to repair damaged peritoneum and prevent peritoneal adhesions, but the transplantation strategy had to be proven. The goal of this chapter was to choose between two strategies of regenerative medicine: cell therapy (without a scaffold) and tissue therapy (with a scaffold). The most simple cell therapy technique was to inject free cells into the abdominal cavity. Improving the cell therapy strategy, cell-sheet technology was also tested in order to develop a scaffold-free sheet composed of an upper layer of mesothelial cells and an underlying layer of fibroblasts, similar to the peritoneum *in vivo*. We compared these two cell therapies to the tissue therapy, following a *proof of concept* study, to determine if the scaffold improved peritoneum healing and adhesion prevention.

### 2.3.2. Cell therapy using IP injection of MCs

#### 2.3.2.1. Method

MCs were isolated and cultured as previously described. The viability and homogeneity of each MC culture was confirmed by daily cell observations. To control for heterogeneity or culture failure, we randomized the rats in the control group. After reaching confluency, autologous MCs were trypsinized and resuspended in 1.5 ml of culture media and injected into the abdominal cavity of rats in the cecal coagulation model. Each graft of cells was performed subsequently to preserve the viability of the cell suspension. Cell suspension was quickly transferred to the animal room; the rat, under general anesthesia, was ready, and cecum coagulation was done just before the graft.

Two cell densities were compared  $0.4 \times 10^6$  MCs/100 mg body weight in a volume of 1.5 ml and  $0.8 \times 10^6$  MCs/100 mg body weight in a volume of 3 ml, n=3/group.

The control group with  $0.4 \times 10^6$  MCs/100 mg body weight in 1.5 ml received an IP injection of 1.5 ml of NaCl and the control group with  $0.8 \times 10^6$  MCs/100 mg body weight in 3 ml received an IP injection of 3 ml of NaCl.

### 2.3.2.2. Results and discussion

All rats were diagnosed with dense adhesions and no statistically significant reductions in the extent of adhesion were found (Figure 29).

We did not succeed in reproducing the results of Bertram, Lucas or Foley. Foley used the same density of cells injected into the testis cavity, which is a very small cavity; so fewer cells were lost or dispersed. Bertram and Lucas grafted  $1 \times 10^6$  MCs/100 mg body weight into the abdominal cavity and both succeeded in reducing adhesion formation, but they used different animal models from ours. Bertram used a model of simple cecum abrasion, which is less convincing because abrasion is less effective for adhesion creation. Lucas used a parietal peritoneal excision and suture model and the 3 ml NaCl injection in his control group did not change adhesion formation, in opposition to our results.

Moreover, IP injections of MCs required a large number of cells; a possible limitation for its clinical application. Several explanations such as the loss of cells or their partial recruitment to the area of interest, rapid cell destruction, or an inflammatory response as a side effect could explain this failure.

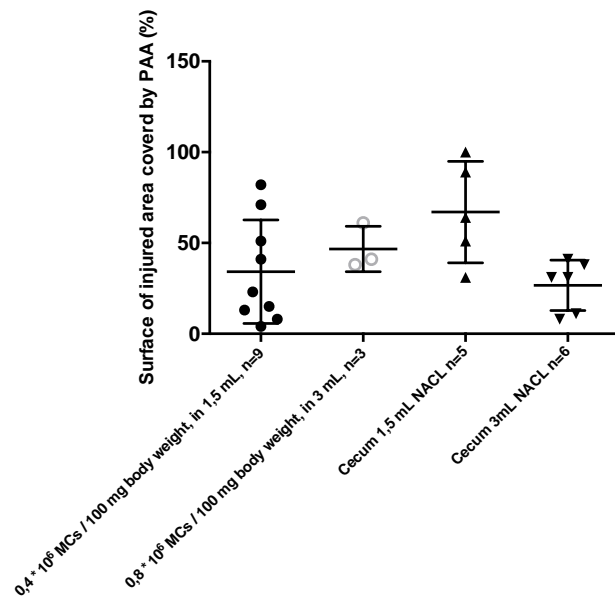


Figure 29: Effect of IP injections of MCs on the extent of adhesion. No significant differences were found.

### 2.3.2.3. Conclusions

IP MC therapy did not reduce or prevent adhesion formation in the visceral electrocoagulation rat model.

### 2.3.3. Comparison between cell-sheet therapy and tissue therapy (peritoneal graft)

#### 2.3.3.1. Introduction

Using a rat model of standardized and clinically relevant peritoneal lesions, this study evaluated the contribution of autologous peritoneal grafts to both reperitonealization of the deperitonealized lesions and prevention of postoperative abdominal adhesions. We also attempt to reveal the conditions necessary for the survival of transplanted mesothelial cells by modifying the position of the autologous peritoneal graft and by referring to the case of a bilayer cell sheet that consists of a layer of mesothelial cells on another layer of fibroblasts.

#### 2.3.3.2. Method

##### 2.3.3.2.1. Rats

Characteristics of the rats and laboratory conditions were similar to those previously described in the previous animal experiments.

##### 2.3.3.2.2. Experimental design and induction of standardized peritoneal lesion

Twenty rats were allocated randomly into four groups (5 rats in each). Group abbreviations indicated if mesothelial cells (MC) or fibroblasts (FB) were exposed to the abdominal cavity, as well as whether cell or tissue therapy was used. The groups are denoted as follows: (1) rats received autologous peritoneal grafts with the mesothelium side exposed to the abdominal cavity (MC/FB graft); (2) rats received autologous peritoneal grafts with the subserosa side containing fibroblasts exposed to the abdominal cavity (FB/MC graft); (3) rats received a cell sheet consisting of mesothelial cells and fibroblasts (MC/FB sheet); and (4) rats received no treatment (Control) (Figure 30).

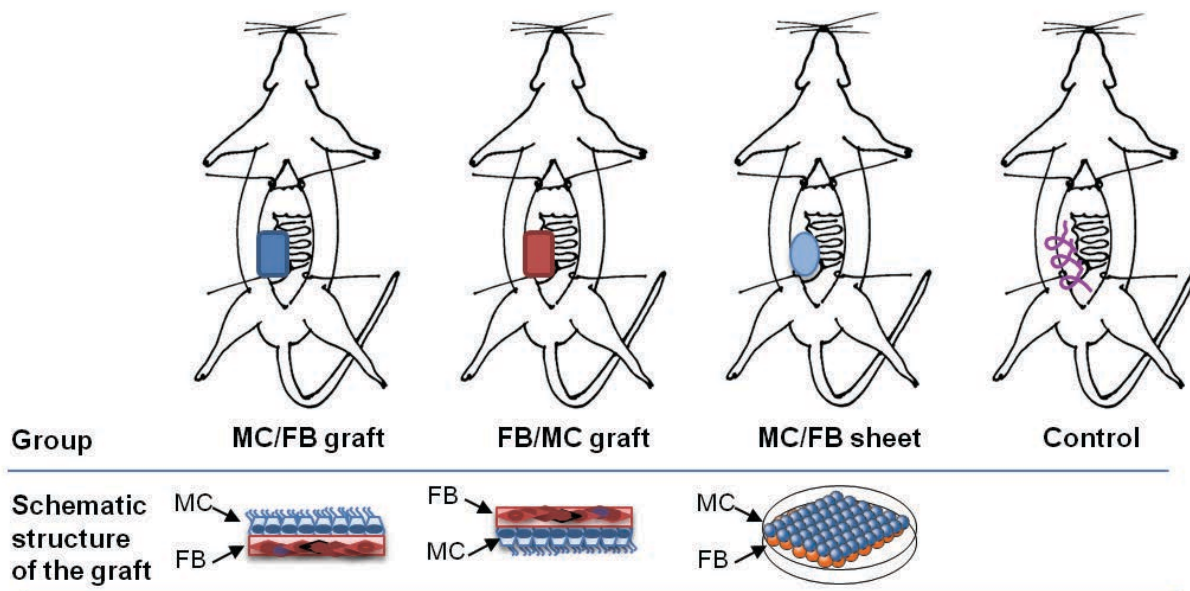


Figure 30: Twenty rats were randomized to four groups (n= 5 / group) to undergo a transplant surgery of different grafts: peritoneal graft with direct exposure of MC side to the abdominal cavity (MC/FB graft); peritoneal graft with direct exposure of subserosa side to the abdominal cavity (FB/MC graft), MC-FB bi-layered -sheet (MC/FB sheet) and sham group without any graft (Control).

All animals underwent standardized parietal right flank peritoneum lesion associating coagulation and suture (20). As previously described, after skin preparation, abdomen was opened on the inferior part of the abdominal wall. The peritoneum of the right abdominal wall was exposed, and a standardized burn lesion was inflicted 1.5 cm dorsal to and parallel with the midline incision on the peritoneal surface in an area of 0.5 x 1.0 cm. The lesion was inflicted by sweeping bipolar forceps (Valleylab™, Medtronic, Minneapolis, USA) with a setting of 40 W and effect 4. To further induce ischemia to this electrocautery burn area, three interrupted Vicryl® 3.0 sutures (Ethicon, Somerville, USA) were placed at regular intervals on the cranial, caudal, and middle parts of this burn area (Figure 31d). Thereafter, rats of the MC/FB graft and FB/MC graft groups were transplanted with the prepared graft and rats of the MC/FB sheet were transplanted with the cell sheet. The controls did not undergo any transplantation. Subsequently, the midline incision was closed in two layers using a running Vicryl® 3.0 suture (Ethicon, Somerville, USA) on the muscle and by simple knots with Ethibond® 2.0 (Ethicon, Somerville, USA) on the skin. For analgesia, all the animals received buprenorphine (Vetergesic®, CEVA santé animale, Libourne, France) at a dose of 10 µg/kg by subcutaneous injection postoperatively and every 24 hours for the following two days.

#### 2.3.3.2.3. Preparation and transplantation of autologous peritoneal graft

As an autologous peritoneal graft, the tunica vaginalis was procured from all the rats allocated to the MC/FB graft and FB/MC graft groups. This was performed according to a previous paper (4), which reported that the tunica vaginalis is a proper and practical source for autologous peritoneal graft in rats. During embryonic development, it originated from the peritoneum and descended with the testes into the scrotum during the fetal period. Additionally, accessing the tunica vaginalis is surgically convenient, without causing abdominal complications.

The procurement procedure was as follows. Through a 2-cm incision made on the right scrotum, the testicle was exposed and the parietal lamina of the tunica vaginalis was explanted. The testis was replaced inside the scrotum with caution and the incision was closed in two layers. First, the subcutaneous layer was closed by a running suture using Vicryl® 3.0 (Ethicon, Somerville, USA), and the skin layer was closed with simple knots using Ethibond® 2.0 (Ethicon, Somerville, USA). Thereafter, the borders of the procured tunica vaginalis were trimmed to make it a rectangle of size 1.5 x 2.0 cm and the graft was maintained in a phosphate buffered saline (PBS)-soaked cotton gauze until transplantation.

Transplantation of the autologous peritoneal graft was performed immediately after the grafts were prepared using all the rats of the MC/FB graft and FB/MC graft groups that had already undergone induction of the standardized peritoneal lesions. The transplantation procedure was as follows. The graft, namely the procured and trimmed rectangular-shaped tunica vaginalis, was used to cover the entire peritoneal lesion and was immobilized by four Prolene® 5.0 (Ethicon, Somerville, USA) stitches at each corner (Fig. 31a,b). The suture material was placed beneath the graft to avoid subsequent adhesion formation caused by the suture material. When the grafts were placed over the lesions, MC/FB and FB/MC grafts differed in the amount of graft surface that would be exposed to the abdominal cavity. When the grafts were placed over the lesions, MC/FB and FB/MC grafts differed in the graft surfaces that would be exposed to the abdominal cavity: in MC/FB graft, mesothelial cells were located on the surface, and in FB/MC graft, fibroblasts and the subserosal surface were located on the surface.

#### 2.3.3.2.4. Preparation and implantation of bilayer cell sheet

The bilayer cell sheet was prepared through two sequential steps. The first step was the isolation of both the mesothelial cells and fibroblasts from all the rats allocated to the MC/FB sheet group and the second step was the construction of a bilayer cell sheet by applying cell sheet technology using these autologous cells for each rat (5).

At the animal facility, the tunica vaginalis was procured from the rat, and the parietal lamina was expanded from the tunica vaginalis, trimmed to be a rectangle with a size of 2.5 x 3.0 cm, placed directly on PBS-soaked cotton gauze, and immediately transported to the laboratory. At the laboratory, the cell isolation step was performed. First, to isolate the mesothelial cells, the inner surface of the parietal lamina was rinsed using pH 7.4 phosphate-buffered saline (PBS) and exposed to 0.25% trypsin with 2 mM EDTA solution (2.5 mL/cm<sup>2</sup>) at 37°C for 30 min. After the trypsin-EDTA solution was discarded, the culture medium (DMEM supplemented with 10% fetal bovine serum and 20 µ/mL gentamycin) was added to neutralize the remaining enzyme. The parietal lamina was transferred to another Petri-dish containing culture medium and single mesothelial cells were released by gently sliding a spatula over the inner surface of the parietal lamina. The cells were harvested, counted and plated in a 60-mm Petri-dish at a density of  $6 \times 10^3$  cells/cm<sup>2</sup>. Second, to isolate the fibroblasts, the parietal lamina lacking mesothelial cells was rinsed with Hank's balanced salt solution (HBSS), cut into small pieces using scissors of a few millimeters square and further soaked with frequent manual agitation in 6 mL of a solution containing 0.25% trypsin with 2 mM EDTA at 37°C for 10 min. After neutralization using complete medium, the supernatant was filtered through a cell strainer with a mesh size of 100 µm (Falcon®, Corning, NY, USA) and centrifuged at 300 g for 5 min. The pellet was re-suspended and the cells were counted and plated in a 60-mm Petri-dish at the density of  $1 \times 10^4$  cells/cm<sup>2</sup>. For both these cells, the culture media was changed every 48 to 72 h. Based on observation and immunostaining, the mesothelial cells exhibited a typical cobble-stone appearance and were positive for cytokeratin and vimentin, whereas the fibroblasts, which had a spindle shape, were larger than the mesothelial cells and were positive for vimentin but negative for cytokeratin.

The construction of the bilayer cell sheets using these autologous cells started after 5 days of culture of the fibroblasts. The fibroblasts were detached and seeded at a density of  $8 \times 10^5$  cells per well on a 6-well temperature-responsive culture plate (UpCell®; Cell Seed, Tokyo, Japan) pre-coated with fetal bovine serum. When the fibroblasts became confluent one to two days later, the cultured mesothelial

cells were detached and seeded over the fibroblast sheet at a density of  $9 \times 10^5$  cells per well and co-cultured for another 5 days, resulting in the formation of a bilayer cell sheet consisting of over-confluent mesothelial cells and fibroblasts, which were ready for implantation.

The bilayer cell sheets were implanted into the rats of the MC/FB sheet group after they underwent the standard lesion formation. Ten minutes before implantation, the bilayer cell sheet was detached by reducing the temperature to 20°C. After discarding the entire medium, approximately 50 µL of fresh medium was added to the cell layer, and a polyvinylidene fluoride (PVDF) transfer membrane was gently placed on top of the cell sheet. Macroscopically, when the border of the cell sheet became whitish and thick, both the cell sheet and the PVDF membrane were held with forceps and cut into a small round piece of 1.5 cm in diameter to fit the peritoneal lesion area on the right flank. The implantation procedure was performed as follows: the cell sheet attached to the PVDF transfer membrane was gently placed on the traumatized area, pressed through the PVDF transfer membrane using warm PBS-soaked cotton gauze for 3 to 5 min, and the PVDF transfer membrane was then peeled away (Fig. 31c).

#### 2.3.3.2.5. Macroscopic and Histological assessment of postoperative peritoneal adhesion

As previously described we assessed on post operative day 14 the adhesion of formation by macroscopical and histological observations.

#### 2.3.3.2.6. Statistical analysis

Data are presented as the absolute numbers or the median (range) values. Each group was compared to the control group to assess differences in the quality and quantity of the adhesions. The scores of the postoperative abdominal adhesions were compared using the chi-squared test with a Yates's correction. The surfaces of the injured areas covered by the adhesion were compared using a non-parametric Wilcoxon-Mann-Whitney test.  $P < 0.017$  was considered to be statistically significant using the Bonferroni correction (3 comparisons). GraphPad Prism version 6.0 for Windows XP (GraphPad Software Inc., La Jolla, CA, USA) was used for statistical analysis.

### 2.3.3.3. Results

#### 2.3.3.3.1. Macroscopic evaluation

At the second-look laparotomy performed in 3 rats, we observed adhesions on the laparotomy and their incidence had no relation to a specific group. No interloop adhesions other than intra- or postoperative complications were found in any of the rats.

In the MC/FB graft group, there was no adhesion on the surface of the autologous peritoneal graft that covered the entire area damaged by the standardized peritoneal lesion (Figure 31e). Limited, thin and filmy adhesions were observed at the corners of three grafts where the stitches were placed to immobilize the grafts. These adhesions were included for quantitative and qualitative assessment but were considered to be adverse effects induced by the threat.

In the Control, FB/MC graft, and the MC/FB sheet groups, all the rats showed adhesions that were located on the peritoneal lesion surface (Figure 31f,g,h). These adhesions were either filmy vascular or dense vascular and were sticking to the omentum, seminal vesicle, perigonadic fat pad or the liver in the area of the standardized lesions.

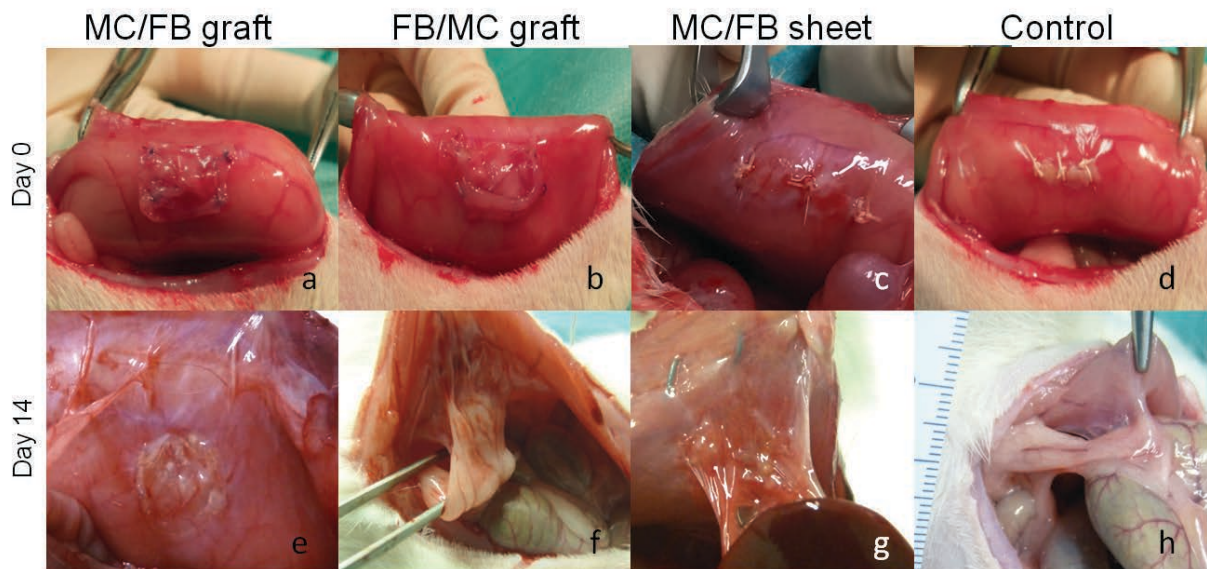


Figure 31: Intra-operative view of the graft, Day 0, (a-d) and of the day of macroscopic assessment after 14 days during the sacrifice (e-h); e: no adhesion on the graft; different organs stuck on the graft like, f: liver, g: perigonadic fat pad, h: cecum.

Regarding the adhesion quality scores, the value of the MC/FB graft group was inferior to that of the FB/MC graft, MC/FB sheet and control groups (2 (0-3) vs. 3 (3-3), 3 (2-3), 3 (2-3),  $p=0,18$ , Figure 32a). Moreover, regarding the quantitative evaluation of the adhesion using the ratio of the area covered with adhering tissue to the entire area of the standardized peritoneal lesion, the value of the MC group was significantly lower than that of the FB/MC graft, MC/FB sheet and control groups (4%(0-14) vs. 100%(60-100), 50% (30-100), 60 (30-100),  $p<0.005$ , Figure 32b). Additionally, there was no significant difference found between the FB, cell sheet and control groups.

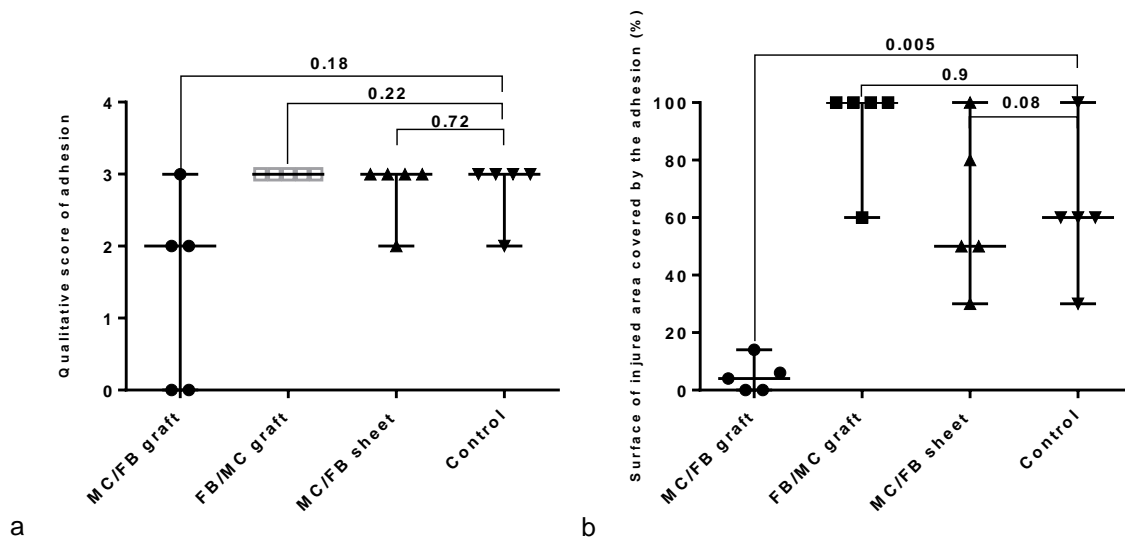


Figure 32: Quantitative and qualitative assessment of adhesion: (a) the quality or severity of adhesion expressed by a score given for each adhesion, (b) the extent of adhesion defined by the proportion of adhesion covered injured surface area.

#### 2.3.3.3.2. Histological evaluation

We found that in the abdominal wall, the standardized peritoneal lesion damaged not only the peritoneum but also the subserosa and the underlying abdominal muscle. In all the samples of the FB, CS, and control groups, we found that the adhesions defined as multilayered fibrotic tissue were sticking to the damaged area of the abdominal walls, to visceral fat tissue or to the abdominal organs, including the liver and intestines (Figure 33b,c,d). In contrast, in the MC group, we observed peritoneal grafts on the abdominal muscle without any fibrotic tissue attaching these grafts (Figure 33a). We also found mesothelial cells lining the surface of the transplanted peritoneum by immunohistochemical staining for cytokeratin AE1/AE3 (Figure 33e). The mesothelial cells were indistinguishable from the adjacent ones on the intact peritoneum (Figure 33f,g,h).

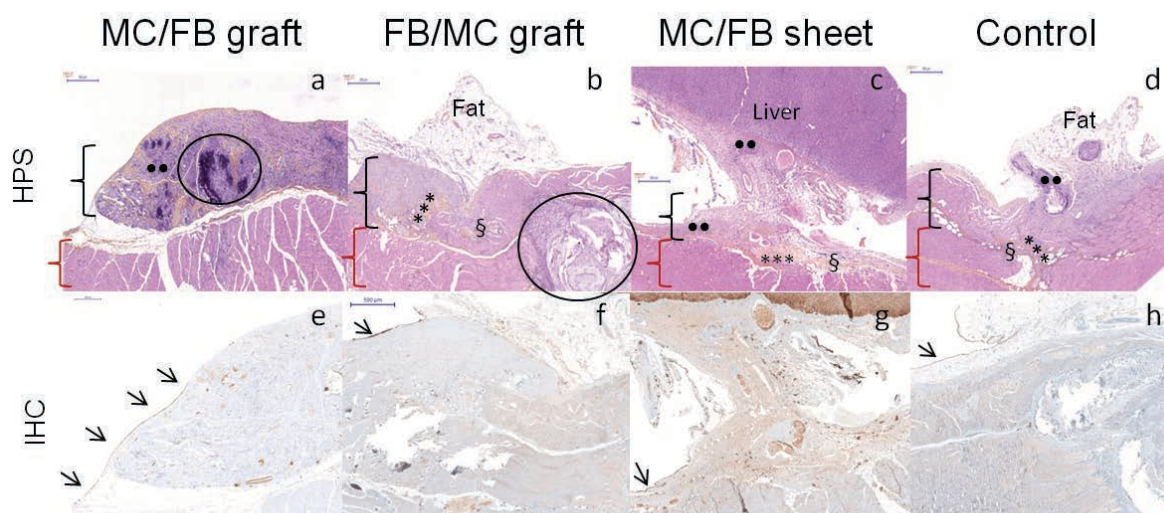


Figure 33: Histological analysis of tissue samples: muscle (red parenthesis) and graft (black parenthesis). Adhesions were defined as fibrotic tissue (✦) sticking at least two organs such as liver (c), or fat (b, d). Electrocoagulation led to leukocytic infiltration into the subserosa (\*\*), destruction of muscle cells in the underlying musculature (§) and early-stage fibrous organization (✦). Sutures led to granuloma formation (surrounded by a black circle) and foreign body reaction in the musculature (\*\*). Threats disappeared but empty spaces into black circle indicated their initial location. MC/FB graft lied on the abdominal muscle structure; and both hematoxylin phloxine saffron (HPS) (a) and immunohistochemical (IHC) (e) staining revealed a thin top layer of MCs (↗) lining on the induced peritoneal damage area, which is indistinguishable from adjacent normal peritoneum. In the others groups, the thin MCs (↗) layer stained by cytokeratin IHC was disrupted by the adhesion (f,g,h).

#### 2.3.3.4. Discussion

In the present study, using rats that had sustained adhesion induction through the standardized deperitonealized lesion, we demonstrated that autologous peritoneal grafts prevent postoperative abdominal adhesions and contribute to reperitonealization of the deperitonealized lesions. Through macroscopic observations and histological assessment, all the rats receiving the autologous peritoneal grafts did not have adhesions on the surface of the grafts, while all the rats that did not receive a graft showed severe adhesions on the lesions (Figures 31, 33). This provided evidence that autologous peritoneal grafts prevent postoperative abdominal adhesions.

Regarding the conditions for the transplanted mesothelial cells to survive on the standardized deperitonealized lesions and to achieve reperitonealization, we found that the mesothelial cells need

to be exposed to the abdominal cavity and that a fibroblast sheet created by cell sheet technology does not work as a scaffold for the mesothelial cells. The former finding is based on observations that the mesothelial cells were detected 14 days after autologous peritoneum grafts were transplanted with the mesothelial cell side exposed to the abdominal cavity, while they were not detected when the subserosa side containing fibroblasts was exposed to the abdominal cavity (Figure 33).

In selecting an animal model for this study that involved adhesion induction through a standardized deperitonealized lesion, we considered two critical characteristics: clinical relevance and stable reproducibility. In the model chosen, which was established by Walwiener et al. and had 100% adhesion incidence and 64% severe adhesions, the deperitonealized lesion is caused by electrocoagulation and suturing (6). To be clinically relevant and to improve the effectiveness (7), different effects were combined. Both burning and suturing, which reinforce ischemia, damaged the peritoneum, subserosa, and muscular layer, and reproduced surgical dissections, such as uterine myomectomy, rectal shaving, gastrectomy, etc. Furthermore, simple peritonectomy or abrasion have been reproduced by models of limiting deperitonealized lesion to a mechanical denuding and led to fewer adhesions (8,9).

Regarding the effects of autologous peritoneal grafts, contrasting findings were reported by two researchers in the 1970s (22, 23). First, they used only mechanical denuding to deperitonealize the abdominal wall in their rats, and they found that the peritonealized lesions ended by self-healing without adhesion. Then, they concluded that reperitonealization using the autologous peritoneal grafts was a harmful practice, probably because the grafts they used were peritoneal grafts that included the underlying muscular layer. Muscle is known to be extremely vulnerable to ischemia (11) and ischemic muscle could have accelerated the adhesion formation. In contrast, the autologous peritoneal grafts in the present study were procured from the tunica vaginalis and contained no muscular layer.

Finally, in one of these two studies, a running suture was used to fix the peritoneal graft. This suture, which was exposed in the abdominal cavity, could have been a strong stimulus for adhesion formation (6,7).

Our study clearly shows that reperitonealization is related to the absence of adhesion formation since all the rats reaching reperitonealization did not form postoperative abdominal adhesions, while the rats that did not reach reperitonealization did form adhesions (Figure 31d). Moreover, adhesion prevention requires functional mesothelial cells that would be able to (i) provide a protective barrier or slippery

and non-adhesive surface (10) and (ii) secrete soluble factors that lyse fibrin deposits, leading to the formation of postoperative abdominal adhesions.

Although it is obvious that autologous peritoneal grafts can prevent adhesion formation through the preserved function of the transplanted mesothelial cells, using peritoneal grafts minimized any adverse biological reaction. Additionally, through using a clinically relevant and stably reproducible animal model, we believe that we have succeeded in providing the first proof of the concept that mesothelium reconstruction prevents adhesion formation.

When considering the clinical applications, an autologous peritoneal graft would be efficient for preventing adhesion formation. This graft could be harvested at the time of the surgery to cover the surface of the deperitonealized lesions caused by the procedure. The sampling technique should be very gentle to avoid adhesion formation and to result in self-healing, as mentioned above. To promote complete self-healing of the sampled area, a mechanical denuding should be used for the peritonectomy and abdominal cavity spaces that would not be in contact with the small intestine should be selected, such as subdiaphragmatic space or lateral flank. However, there are still limitations, such as the potential adverse effects of graft sampling, the limited quantity of peritoneum available and the potential tumor tissue.

These limitations in using the patient's own peritoneum motivate us to create an alternative to the peritoneum. In planning strategies to reconstruct the microstructure of mesothelial cells and to transplant the peritoneum alternative, we believe the scaffold for the mesothelial cells is crucial and should offer good mechanical features. In fact, we found that the mesothelial cells survived when they were located within the peritoneal grafts, but they did not survive when they were located on the fibroblast sheets, which contained extracellular matrix but were very frail. Even by adding fibroblasts to reproduce the subserosa layer, transplantations of cell sheets were difficult because they lacked resistance, were fragile and lacked an extracellular matrix. For example, the sheets could have been damaged or partially transplanted.

#### 2.3.3.5. Conclusion

We used autologous peritoneal grafts procured from the tunica vaginalis and a clinically relevant and stably reproducible rat model. This allowed us to demonstrate that autologous peritoneal grafts

contributed to the prevention of postoperative abdominal adhesions through rapid reperitonealization and mesothelial reconstruction on standardized deperitonealized lesions. This was possible only when these grafts were transplanted with the appropriately positioned polarity of their mesothelial cells. In addition, our findings demonstrated that the mesothelium needs to be located on the scaffold containing the extracellular matrix, which may contribute to planning and creating a microstructure alternative to the peritoneum by applying tissue-engineering technologies.

## 2.4. CHAPTER 4: CHOICE OF SCAFFOLD MATERIALS

### 2.4.1. Introduction

The *proof of concept* study showed that a scaffold mimicking the extracellular matrix and the microstructure of the peritoneum was required for the success of our therapy, which involved finding a good biomaterial with qualities that will be detailed later. This scaffold would be associated with the cell sources using tissue-engineering technologies.

Biomaterials for tissue engineering provide a three-dimensional environment that allows cells to develop new tissues with appropriate structure and function. These materials are usually designed to replicate the biological and physical function of the native ECM found in the body to enhance tissue formation. Thus, the ideal biomaterial should be biocompatible and support cell and tissue growth without inducing severe inflammatory processes that lead to foreign-body reactions or fibrous deposits that induce adhesion (114). In the long term, it is often preferable to use a biodegradable material scaffold so that all the implanted materials will disappear, leaving behind only the generated tissue.

Traditionally, two main classes of biomaterials have been utilized in the abdominal cavity: cellular matrices derived from animals and synthetic polymers (39). Research in this area has identified several natural biodegradable materials. Hydrogels retain a great quantity of water, have good biocompatibility, have low interfacial tension, and cause minimal mechanical and frictional irritation. Hard materials such as synthetic polymers (poly(lactic acid) (PLA), poly(glycolic acid) (PGA), and poly(lactic-co-lycolide) (PLGA)) provide compressive and torsional strength. However, hydrogels more effectively promote cell expansion and tissue formation(115).

Moreover, to ensure the clinical relevancy of our cell-laden scaffold, the biomaterial would be used during open or mini-invasive surgeries on damaged areas such as uterine horns in order to prevent adhesion. The cell-laden scaffold had to be deliverable through a small incision made during a laparoscopy through the 0.3-12 mm transcutaneous ports. The material had to be fixed easily without sutures because threads and sutures are known to enhance adhesion formation.

Therefore, we selected a hydrogel that was injectable, auto-adherent, biocompatible, degradable, and similar to ECM components to offer a good 3D environment to transport and deliver cells for cell growth and cell differentiation.

#### 2.4.2. BD-Purastat® choice

3D Matrix Laboratory collaborated with us and provided us with samples of BD-Purastat®, a commercially available peptide sold at a concentration of 1% as a hemostatic agent for surgery. This self-assembling peptide is used to create defined three-dimensional (3D) microenvironments for a variety of cell culture experiments in research. BD-Purastat® was selected because its composition is similar to that of collagen, which is the most abundant component of the peritoneal ECM. BD-Purastat® is a synthetic peptide consisting of standard amino acids (2.5% w/v) in 99% water. It is acidic (pH=2.3) and under physiological conditions (saline buffer addition and pH = 7) the peptide component of BD-Purastat® self-assembles into a 3D hydrogel that exhibits a nanometer-scale fibrous structure with an average pore size of 50-200 nm. BD-Purastat® is biocompatible, resorbable, and injectable. It does not contain any animal-derived materials and/or pathogens, thanks to its synthetic production.

BD-Purastat® is non-cytotoxic to neurons and promotes adhesion and neurite sprouting of neurons (116,117), osteoblasts (118), and fibroblasts (119). It reduces hemorrhaging with only minimal tissue responses (120). BD-Purastat® permits the adhesion, growth and differentiation of dental pulp stem cells (121).

Based on the literature and product data sheet, BD-Purastat® was a good candidate for supporting the expansion and differentiation of cells to prevent postoperative adhesion, as it met all our required criteria: it is injectable for clinical application by open or mini invasive surgery, can be manipulated into any shape, is auto-adherent, biocompatible, degradable, and offers a 3D environment for cell growth and cell differentiation.

#### 2.4.3. BD-Purastat® dilution and gelation assays

##### 2.4.3.1. Method

The viscosity of the stock solution of BD-Purastat® (2.5%) was decreased by 30 min of sonication.

Several concentrations (0.02%, 0.1%, 0.5%, and 1%) of BD-PuraMatrix® were prepared in 2 ml centrifuge tubes by gently pipetting the appropriate volumes of sterile water and stock solution together.

Then, 240 µL of each of the sample concentrations of BD-PuraMatrix® solution were injected into 24 well plates, (n=2). The viscous solution was injected slowly into each well to avoid introducing bubbles.

Next, 700  $\mu\text{L}$  of culture medium was added on top of the BD-PuraMatrix® by slowly pipetting down the sides of the well to induce gelation. Plates were incubated at 37°C.

Gel formation was assessed after 1 h and 24 h.

#### 2.4.3.2. Results and discussion

Dilutions needed a gentle and repeated pipetting, as shown in Figure 34. The same results were reported after one or twenty-four hours for all concentrations. The 1% and 0.5% solutions gelled but the gel broke when it was removed from the plastic well. The 0.02% and 0.1% solutions were liquid and easier to inject into the wells, but the degree of gelation was difficult to assess by simple observation. It seemed to still be liquid when removed from the well.

The dilution of BD-PuraMatrix® was possible after a good pipetting to obtain a homogeneous gel. Lower concentrations (0.02% and 0.1%) were injectable but were not solid enough and were thus inappropriate for our application because of an important loss of solution beyond the area that needed to be covered. The intermediate concentration, 0.5% BD-PuraMatrix®, solidified and stayed on the area to be covered. The literature shows that cell viability, migration and proliferation increase in lower BD-PuraMatrix® concentrations (122–126). Therefore, we eliminated the 1% concentration and decided to perform the next experiments with 0.5% BD-PuraMatrix®.

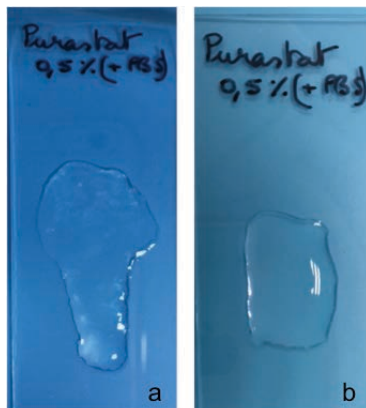


Figure 34: Homogenization after sonication and addition of diluent needed regular, gentle and repeated pipetting; 10 times (a) versus 30 times (b).

#### 2.4.4. Viability of *in vitro* encapsulated cells

##### 2.4.4.1. Method

3D cell encapsulation into BD-Purastat® was performed using a 0.5% final gel concentration and a final concentration of  $5 \times 10^6$  cells/ml using the MC3T3 and MC cell lines (n=4/group).

After decreasing the viscosity of BD-Purastat® stock by sonication for 30 min, BD-Purastat® was centrifuged for a short time to eliminate bubbles. The appropriate volume of the desired concentration of BD-Purastat® was prepared in Eppendorf tubes by diluting the stock solution with sterile 20% sucrose to generate a 2X concentration of 1% BD-Purastat®. The control group was cells in culture medium.

The cells were trypsinized and rinsed in a sterile 10% sucrose solution. Then, the cells were pelleted by centrifugation and resuspended in a 10% sucrose solution at 2X the final desired cell concentration.

Equal volumes (100 µl) of 2X BD-Purastat® and 2X cells in sucrose were mixed together and then carefully added to the center of a well, avoiding introducing bubbles.

Gelation was initiated by gently adding culture media (100 µl) along the wall of each well. The media was changed twice over the following 60 min by removing only half of the media per change (50 µl) to further equilibrate the pH. Culture plates were placed in a 37°C cell culture incubator.

After 48 h, the control group was visually checked for cell density and morphology and the homogeneity of the gel was visually assessed in the other groups. In practice, the cells were not visible throughout the hydrogel. The Alamar Blue® test was used to assess cell viability in the gel. Briefly, 75 µL of media was discarded and 175 µL of Alamar Blue® was added and incubated with the cells for 3 hours at 37°C. The gel and the supernatant were homogenized by pipetting, and 150 µL from each well was used to read the absorbance at 540 nm. Medium was used as a blank. The percent difference in reduction between the signal of encapsulated cells and control cells was reported to reflect the survival.

##### 2.4.4.2. Results and discussion

At 48 h, the cells were over-confluent in the control group. The observation of cells within the gel was difficult. In the 0.5% gel, there were bubbles in half of the wells or lateral holes where the medium was

added. MC3T3 cells had a median survival of 82% (66%-89%) after 48 h encapsulated in the gel. MCs had a median survival of 111% (92%-136%) after 48 h encapsulated in the gel (Figure 35).

Thus, MCs grown in 0.5% BD-PuraMatrix® *in vitro* survived, proving that we could use 0.5% BD-PuraMatrix® to construct a cell-laden hydrogel sheet.

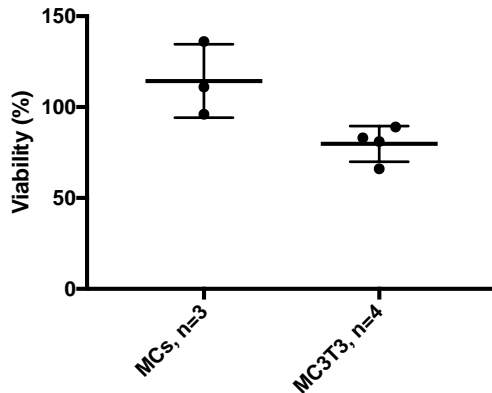


Figure 35: MC3T3 and MC viability in 0.5% BD- Purastat® after 48 h: MC3T3 and MCs showed good survival.

#### 2.4.5. *In vivo* transplantation of 0.5% BD-Purastat® into an animal model of adhesion

##### 2.4.5.1. Method

A 0.5% solution of BD-Purastat® was prepared and used in a simple bipolar cecum coagulation (effect 4, 40 W) animal model (10 rats). . When the cecum was coagulated, 100 µL of the viscous solution was dispersed onto the traumatized area to cover it (Figure 36a). We added drops of blood taken from the tail of the rat to ensure a good gelation of the BD-Purastat® solutions. For each animal, we waited for 30 s to ensure gelation. The cecum was carefully replaced in the abdominal cavity, and the abdominal wall was closed. Postoperative care and adhesion assessment were performed as previously described. The test groups were compared with the control group (cecum coagulation with no injection and effect 4 and 40 W, n=5).



Figure 36: Macroscopic aspects of the *in vivo* transplantation of BD-Purastat® on a rat adhesion model (a) and the assessment of a filmy vascular adhesion during rat sacrifice (b).

#### 2.4.5.2. Results and discussion

##### 2.4.5.2.1. Transplantation observations

The results of the *in vivo* manipulation and data from the literature confirmed our choice of 0.5%. At this concentration, the hydrogel was injectable, adhesive to the area of interest, ensured minimal losses of solution by dispersion beyond the area of interest; and enabled good cell survival and proliferation.

##### 2.4.5.2.2. Adhesion assessment

All of the rats presented one adhesion sticking to the injured cecum and abdominal wall, visceral fat, or seminal vesicle. All adhesions were filmy, vascularized, or dense. In the 0.5% BD-Purastat® group, the mean adhesion extent was  $35 \pm 11\%$  ( $n=10$ ) and in the control group,  $90 \pm 10\%$  ( $n=5$ ). Compared with the control grafts, grafts from the 0.5% BD-Purastat® solution significantly decreased ( $p=0.009$ ) the extent of the adhesions in the cecum coagulation model (Figure 36b, 37).

Data from the *in vitro* viability assays of encapsulated cells showed that BD-Purastat® was biocompatible and able to significantly reduce the extent of the adhesion in our rat model of visceral peritoneum electrocoagulation. Adhesions were still dense, but their extent on the injured surface was reduced by 50%.

A thin layer of blood was added to the cecal burn to help BD-Purastat® gelation because blood is known to increase adhesion formation by adding fibrin onto the burned surface, thus creating an imbalance in fibrinolysis. The addition of blood to the visceral peritoneum model only increased the

severity of the model, so the comparisons with the visceral peritoneum model as validated in the first part of our work were still possible.

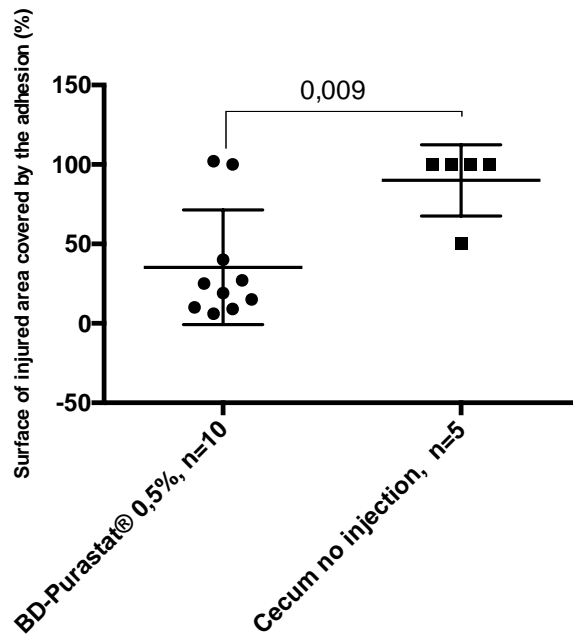


Figure 37: Assessment of the extent of adhesion after 0.5% BD-Purastat® grafts: significant reduction in the extent of adhesion compared with the control group,  $p=0,009$ .

#### 2.4.6. Conclusions

BD-Purastat® demonstrated its biocompatibility and its capacity to reduce adhesion formation in our rat model of visceral peritoneum electrocoagulation.

At a 0.5% concentration, this hydrogel presented good mechanical properties: injectability, adhesion to the area of interest, minimal loss of solution by dispersion beyond the area of interest; and good survival and proliferation of the cells.

## 2.5. Chapter 5: IN VIVO APPLICATION OF CELL-LADENED BD-PURASTAT® GELS

The previous experiments identified and provided an animal model to test our cell-laden scaffold, autologous cells, and a promising biomaterial. Adding cells to 0.5% BD-Purastat® should improve the previously reported adhesion prevention with 0.5% BD-Purastat® alone, thanks to the autocrine and paracrine effect of the cells and their function. Furthermore, MCs were already differentiated, but ASCs had to differentiate toward a mesothelial phenotype. Both cell sources were used in the cell-laden hydrogel. Then, as a large range of cell concentrations was reported in similar experimental studies, different MC concentrations were tested.

### 2.5.1. Cell type comparisons

#### 2.5.1.1. Method

MCs and ASCs encapsulated in 0.5% BD-Purastat® were used. The volume of cell-laden hydrogel or hydrogel alone applied to the visceral peritoneum model (cecal coagulation) was 100 µL. The control group did not receive hydrogel after cecal coagulation. Rats were randomized into one of the following groups:

- ASCs in BD-Purastat®, n=3
- MCs in BD-Purastat®, n=4
- BD-Purastat®, n=4
- Control group, n=5

First, 100 µL of BD-Purastat® was sonicated for 30 min. During that time, cells were trypsinized, counted, rinsed in 10% sucrose and resuspended at double the expected concentration in 10% sucrose. The expected concentration was  $10 \times 10^6$  cells/ml. In the animal room, 100 µL of the 2X cell suspension was mixed by pipetting with 100 µL of BD-Puramatrix® solution. Each rat was already ready, under general anesthesia, with the median opening performed. After cecum coagulation, a thin layer of blood from the tail was added to the area. Then, 100 µL of the cell-encapsulated mixture was slowly dispersed onto the injured surface. Closure and postoperative care were performed as previously described. Assessment was performed as usual, and comparisons were made with the simple 0.5% BD-Purastat® group and the control group.

### 2.5.1.2. Results

All the rats were diagnosed with dense adhesions. The median (min-max) extent of these adhesions was 100% (100-100), 31% (25-100), 28% (6-100), and 100% (50-100), respectively, in the ASCs in BD-Purastat<sup>®</sup>, MCs in BD-Purastat<sup>®</sup>, BD-Purastat<sup>®</sup>, and control groups (Figure 38). No significant differences in the amount were found in adding MCs or ASCs on the reduction of the extent of the adhesion, but ASC addition seemed to decrease the protective effect of BD-Purastat<sup>®</sup> alone.

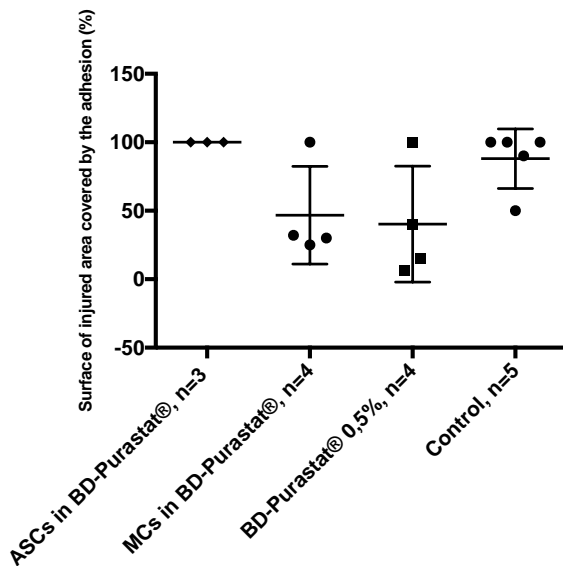


Figure 38: Extent of adhesion after application of cell-laden 0,5% BD-Purastat<sup>®</sup> grafts, according to the cell type and compared with no application of the hydrogel. No significant differences to the reduction of the extent of the adhesion were found by adding MCs or ASCs, but the addition of ASCs seemed to decrease the protective effect of BD-Purastat<sup>®</sup> alone.

### 2.5.2. MC density comparison for MCs laden 0,5% BD-Purastat<sup>®</sup> applications

#### 2.5.2.1. Method

Then, using the same method of cell encapsulation, we compared different cell densities of MCs in 0.5% BD-Purastat<sup>®</sup> grafts and assigned rats randomly to the following groups:

- $10 \times 10^6$  MCs/ml, n=4
- $2 \times 10^6$  MCs/ml, n=4
- $1 \times 10^6$  MCs/ml, n=4

### 2.5.2.2. Results

All the rats were diagnosed with dense adhesions. The median (min-max) extent of these adhesions were 31% (25-100), 47, 5% (13-160), 21, 5% (13-46), and 22% (6-100) in the groups with  $10 \times 10^6$  MCs/ml in BD-Purastat<sup>®</sup>,  $2 \times 10^6$  MCs/ml in BD-Purastat<sup>®</sup>,  $1 \times 10^6$  MCs/ml in BD-Purastat<sup>®</sup>, and BD-Purastat<sup>®</sup>, respectively (Figure 39). No significant differences were found.

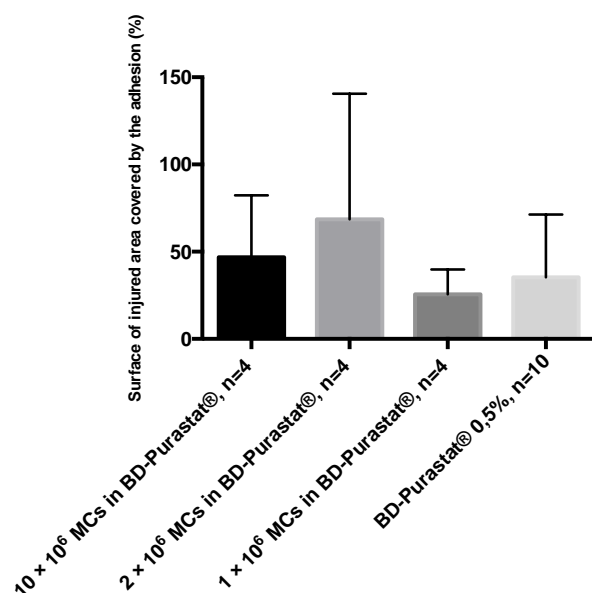


Figure 39: Extent of adhesion after MC in 0.5% BD-Purastat<sup>®</sup> grafts, according to the cell density in comparison with the gel alone. No significant differences were found.

### 2.5.3. Discussion

Unfortunately, we were unable to demonstrate that cell-laden BD-Purastat<sup>®</sup> improved the effect of BD-Purastat<sup>®</sup> alone in preventing adhesion formation. The time of the graft after the peritoneal injury, the density of cells in the hydrogel, the method of hydrogel delivery, and the quantity of hydrogel delivered could explain our failure.

Authors using BD-Purastat<sup>®</sup> *in vivo* in experimental animal studies reported promising effects on mucosal regeneration in the rat middle-ear (127), improvement of cardiac function after myocardial infarction (125,126), and dental pulp regeneration (122). Injection and surface plating methods enhanced cell survival, proliferation and differentiation of neural stem cells in brain injury (123) and spinal cord repair (124). Except for the Guo study, the gel concentration ranged from 0.1 to 0.5% and

the cell density ranged from 0.1 to  $10 \times 10^6$ /ml. The method of delivery changed with the model. For example, Akiyama, after surgical elimination of the middle-ear mucosa, replaced the missing tissue with a direct injection of epithelial cells encapsulated in BD-Purastat<sup>®</sup> (100  $\mu$ L) in the cavity (127). Similarly, Dissanayaka injected encapsulated dental pulp stem cells and endothelial cells to fill a dental root (122). Tokunaga first encapsulated cells in a low-concentration hydrogel (0.1%), injected this suspension directly into the border zone of the myocardial infarction area and subsequently dispersed cells that had been encapsulated at the same density but in a high-concentrated hydrogel (0.5%) onto the infarction. He probably wanted to avoid leakage around the infarction area by using the 0.5% gel, which offers a better viscosity and ensures good cell mobility and expansion inside the tissue due to the 0.1% gel (125). Similarly, Moradi injected a high density of cells ( $10 \times 10^6$ /ml) encapsulated in a 0.1% gel into rat spinal cords in a rat model of spinal cord injury. Guo encapsulated a high density of mesenchymal stem cells ( $60 \times 10^6$ /ml) in a concentrated gel (1%) and injected this suspension into the myocardia in a myocardial repair model (126).

Moreover, the methods of cell and scaffold construction are also discussed in the literature. Aligholi compared encapsulation and injection of cells into the hydrogel and showed that cell injection 3 hours after gel deposition improved neural cell viability, proliferation, and differentiation in brain injuries (123).

Finally, the time of cell delivery after the trauma impacts the result. Kanda show that the paracrine effect of transplanted mesothelial cells during peritoneal repair is associated with the conditions of its surroundings. It is important to determine the most appropriate time for developing peritoneal repair through mesothelial transplantation (55).

#### 2.5.4. Conclusions

MC- and ASC-laden BD-Purastat<sup>®</sup> did not prevent adhesion formation even with changes of MCs concentration in hydrogel. Cell encapsulation in hydrogel did not improve the positive effect of BD-Purastat<sup>®</sup> alone in preventing adhesion formation.

### 2.5.5. Perspectives

As reported in the literature and to improve our results, different methods of application of the cell-laden hydrogel were compared. Dispersion, injection into the serosa, or associations of dispersion and injection have been used.

Next, the duration of time from the trauma to the application of the cell-laden hydrogel application varied from several minutes to hours. For our clinical transfer, transplantation had to be performed during the initial surgery. A second procedure includes increased risks of both morbidity and adhesion formation and would not be acceptable for the patient. Based on the operating time, several minutes or hours after the trauma would be the maximal delay that could be proposed before the transplantation of the encapsulated cells.

Cell labeling strategies for *in vivo* cell-tracking experiments could help us understand our results better. The goal of *in vivo* microscopy is to study the biological interactions of cells with surrounding cells such as other mesothelial cells and macrophages and to follow the cells and study their location and their interaction with the injured surface.

### 3. Part 3

#### CONCLUSIONS and PERSPECTIVES

### 3.1. Conclusions

The aim of this work was to develop a new therapeutic method of preventing intra-abdominal adhesions by a technique of regenerative medicine using previously isolated autologous cells and to test its efficiency in an animal model.

After preliminary studies on the effects of the settings of the bipolar coagulation generator on tissues, two rat models of adhesion were validated. These models were complementary, easy to perform, efficient, reproducible and clinically relevant. The parietal model offered a convenient support to fix a graft with sutures, whereas the visceral cecal peritoneum model was convenient for lots of therapies because it was very easy to perform.

In parallel, cell sources were studied, and cells were isolated, expanded and characterized. MCs were isolated from the tunica vaginalis without increasing rat morbidity. The MC yield after tissue digestion and MC morphology in culture were irregular. Senescence arrived quickly for these adult well-differentiated cells that had a limited expansion capacity. Promising ASCs were isolated from subcutaneous fat tissue efficiently. Their stem cells' self-renewal and long-term proliferation capacities as well as their multipotent differentiation potential have been confirmed.

The strategy to construct the therapeutic required the use of a scaffold, as demonstrated by the *proof of concept* study, which showed that autologous peritoneal grafts prevented postoperative abdominal adhesions only if the polarity of the mesothelial cells was respected. The presence of a scaffold was required, whereas cell therapy techniques: intraperitoneal injection and cell-sheet technology failed. A biomaterial for the scaffold and a tissue therapy technique to construct the cell-laden scaffold were required.

BD-Purastat<sup>®</sup>, a synthetic hydrogel similar to the collagen, demonstrated its biocompatibility and its capacity to reduce adhesion formation in our rat model of visceral peritoneum electrocoagulation. At a concentration of 0.5%, this hydrogel presented good mechanical properties and was able to reduce the extent of the adhesion. However, MCs and ASCs laden BD-Purastat<sup>®</sup> did not prevent adhesion formation, and cell addition to the scaffold did not improve the positive effect of BD-Purastat<sup>®</sup> alone.

## 3.2. Perspectives

### 3.2.1. Animal model

The rat model that we validated is clinically relevant to the human issue of postoperative abdominal adhesions and is reproducible and efficient. Small animal models are convenient for demonstrating the effectiveness of an adhesion prevention therapy.

#### 3.2.1.1. *Ex vivo* Model

To conduct a detailed study of cell function or pathways of interaction, we would like to reproduce a model for *ex vivo* development of adhesions according to the 3R guidelines of animal experimentation, i.e., replacement, reduction and refinement. This *ex vivo* model would be convenient for part of the experiments. The model is cost-effective and reproducible. Peritoneal tissue strips from rats underwent abrasion by scraping with a scalpel. After incubation in a special medium, visible adhesion bands were observed as early as 24 hours (99).

#### 3.2.1.2. Heterologous small animal model

Before clinical studies, the characterization of the safety of our cell-based product (i.e., biodistribution and tumorigenicity) was performed on heterologous small animal models, especially immunodeficient mouse strains, which are favorable due to their tolerance to the human cell therapy product.

#### 3.2.1.3. Large animal models

During the subsequent product development phase, large animal models (i.e., sheep, mini pigs, dogs) must be considered because they may better reflect the anatomy and/or physiology of humans. In addition to their efficacy, these may be suitable models for proving some of the safety aspects of our product, e.g., optimizing the dosage and local tolerance or identifying the undesired interactions and effects of the administered cells on the target tissue.

### 3.2.2. Regenerative Medicine

#### 3.2.2.1. Our cell-based regenerative therapy

Mason and Dunnill proposed a brief definition, "Regenerative medicine replaces or regenerates human cells, tissue, organs to restore or establish normal function." (128). The central focus of our project is human cells and so we could label our project regenerative medicine. We were interested in functional adult mesothelial cells or adipose stem cells as cell sources. We hope to reprogram adult stem cells based on their pluripotency. These cells are conveniently collected by a simple subcutaneous biopsy

under local anesthesia. We showed that cells alone cannot succeed, and we wanted to develop a therapy associating cells and the temporary scaffold. It is an exciting perspective to ask the biomaterial community interested in nanotechnology to include advanced cell approaches in their practice. In contrast, we tend to use a minimum of artificial material and enhance the natural capacities of the cells.

Applications have already been found: a peritoneal graft after surgical trauma is feasible and would be effective, as demonstrated by our *proof of concept* study. Furthermore, by extension, our cell-based regenerative therapy can also restore peritoneum function after different types of trauma, especially the prevention of adhesion after surgical trauma. We could restore filtration in cases of peritoneal fibrosis induced by chronic peritoneal dialysis, restore lymphatic drainage and resorption after extended lymphadenectomies or, in other clinical fields, provide a semi-permeable slippery membrane to replace the damaged cornea.

#### 3.2.2.2. Clinical requests

We still keep in mind that clinical transfer is possible but requires some specifications. In the context of oncology or emergencies, cells would be harvested and expanded in a short time or possibly immediately. An extemporaneous cell expansion medical device called Celution® has already been designed. This automatic processing of adipose tissue to obtain SVF is planned to be used immediately as a therapy for a number of conditions, including nonhealing wounds resulting from radiation damage (129). The SVF use instead of ASCs as a cell source is one option that should be tested in future experiments (130).

In all clinical contexts, from oncology to the preservation of fertility in young women, we need to ensure that our cell-based regenerative therapy is safe and we need to evaluate two prominent endpoints, i.e., biodistribution and tumorigenicity in heterologous small animal models, especially immunodeficient mouse strains because of their tolerance of human cell therapy products (131).

#### 3.2.2.3. Managing Innovation in Regenerative Medicine

The stem cell field has gone global, with increasing numbers of trials outside of North America and Europe. Bubela and McCabe conducted a comprehensive analysis of 4,102 stem cell clinical trials published up to the end of 2012 in ClinicalTrials.gov and the WHO metaRegister of Controlled Trials and classified 860 as novel stem cell clinical trials. In spite of ongoing challenges, a substantial

volume of stem cell therapies are moving into late-stage clinical development (132). Corbett reminds us that innovative regenerative medicines include great expenses and difficulties involved in planning how individual therapies will be developed, manufactured to commercial levels and ultimately successfully delivered to patients. Specific challenges also exist when evaluating the safety, efficacy and cost-effectiveness of these therapies. Collaboration between publicly funded researchers and the pharmaceutical industry could be key to the future development of regenerative medicine in clinical practice; such collaborations might also offer a possible antidote to the innovation crisis in the pharmaceutical industry (133). In France, our project would be referred as a “médicament combiné de thérapie innovante” and laws regulate its development (i.e., 90/385/CEE, 93/42/CEE, 2006/86/CE, 2006/17/CE, and 2004/23/CE) under the guidance of the French national agency of safety of medicine and health products, “Agence nationale de sécurité du médicament et des produits de santé” (ANSM).

#### 3.2.2.4. A great opportunity of collaboration and translational research

Moved by the desire to improve my surgical practice, I needed to find scientific guidance to enable me to engage in translational research. I was welcomed into the U1008 Inserm laboratory by Dr Chai, who provided me with resources, structure, technical support and scientific guidance. My work started three years ago under the impetus of my hospital and the Seeding Microsystems in Medicine In Lille (SMMIL-E project). I was supported by a fruitful interaction with Pr Okitsu, Project Professor on the SMMIL-E project. The SMMIL-E project regroups scientific activities that encompass microsystems developed in a joint international unit between CNRS and the Institute of Industrial Science of the University of Tokyo. As an original interdisciplinary approach, bridging fundamental and clinical research, four work packages were related to the scale of transferred biotechnologies. Our work package was titled “Biological adhesives and neo-tissues: cellular fibers and post-surgery recovery”.

In these three years, many questions have been asked and remain unanswered. The existing collaboration needs to be strengthened. The location of the laboratories close to our hospital and its medical teams is a keypoint. Moreover, the capacity of scientists and clinicians to work together and to learn from each other is also a guarantee of success and of long-term partnership.

## REFERENCES

1. De Wilde RL, Brölmann H, Koninckx PR, Lundorff P, Lower AM, Wattiez A, et al. Prevention of adhesions in gynaecological surgery: the 2012 European field guideline. *Gynecol Surg*. 2012 Nov;9(4):365–8.
2. Miller A, Hong MK-H, Hutson JM. The broad ligament: a review of its anatomy and development in different species and hormonal environments. *Clin Anat N Y N*. 2004 Apr;17(3):244–51.
3. Mutsaers SE. The mesothelial cell. *Int J Biochem Cell Biol*. 2004 Jan;36(1):9–16.
4. van Baal JOA., Van de Vijver KK, Nieuwland R, van Noorden CJF, van Driel WJ, Sturk A, et al. The histophysiology and pathophysiology of the peritoneum. *Tissue Cell*. 2017 Feb;49(1):95–105.
5. Lachaud CC, Soria F, Escacena N, Quesada-Hernández E, Hmadcha A, Alió J, et al. Mesothelial Cells: A Cellular Surrogate for Tissue Engineering of Corneal Endothelium. *Investig Ophthalmology Vis Sci*. 2014 Sep 23;55(9):5967.
6. Ferrandez-Izquierdo A, Navarro-Fos S, Gonzalez-Devesa M, Gil-Benso R, Llombart-Bosch A. Immunocytochemical typification of mesothelial cells in effusions: in vivo and in vitro models. *Diagn Cytopathol*. 1994;10(3):256–62.
7. Di Paolo N, Sacchi G, Del Vecchio MT, Nicolai GA, Brardi S, Garosi G. State of the art on autologous mesothelial transplant in animals and humans. *Int J Artif Organs*. 2007 Jun;30(6):456–76.
8. Lachaud CC, López-Beas J, Soria B, Hmadcha A. EGF-induced adipose tissue mesothelial cells undergo functional vascular smooth muscle differentiation. *Cell Death Dis*. 2014 Jun 26;5(6):e1304.
9. Foley-Comer AJ, Herrick SE, Al-Mishlab T, Prêle CM, Laurent GJ, Mutsaers SE. Evidence for incorporation of free-floating mesothelial cells as a mechanism of serosal healing. *J Cell Sci*. 2002 Apr 1;115(Pt 7):1383–9.
10. Mutsaers SE. Mesothelial cells: their structure, function and role in serosal repair. *Respirol Carlton Vic*. 2002 Sep;7(3):171–91.
11. Mesothelial cells and peritoneal homeostasis- ClinicalKey [Internet]. [cited 2017 Apr 4]. Available from: <https://www.clinicalkey.fr/#!/content/journal/1-s2.0-S0015028216627954>
12. Mutsaers SE, Birnie K, Lansley S, Herrick SE, Lim C-B, Prêle CM. Mesothelial cells in tissue repair and fibrosis. *Front Pharmacol [Internet]*. 2015 Jun 9 [cited 2015 Sep 8];6. Available from: <http://journal.frontiersin.org/Article/10.3389/fphar.2015.00113/abstract>

13. Yelian FD, Shavell VI, Diamond MP. Early demonstration of postoperative adhesions in a rodent model. *Fertil Steril*. 2010 May;93(8):2734–7.
14. Hirschelmann A, Tchartchian G, Wallwiener M, Hackethal A, De Wilde RL. A review of the problematic adhesion prophylaxis in gynaecological surgery. *Arch Gynecol Obstet*. 2012 Apr;285(4):1089–97.
15. Mavros MN, Velmahos GC, Lee J, Larentzakis A, Kaafarani HMA. Morbidity related to concomitant adhesions in abdominal surgery. *J Surg Res*. 2014 Dec;192(2):286–92.
16. Ellis H. The clinical significance of adhesions: focus on intestinal obstruction. *Eur J Surg Suppl Acta Chir Suppl*. 1997;(577):5–9.
17. Parker MC, Ellis H, Moran BJ, Thompson JN, Wilson MS, Menzies D, et al. Postoperative adhesions: ten-year follow-up of 12,584 patients undergoing lower abdominal surgery. *Dis Colon Rectum*. 2001 Jun;44(6):822-829-830.
18. ten Broek RPG, Issa Y, van Santbrink EJP, Bouvy ND, Kruitwagen RFPM, Jeekel J, et al. Burden of adhesions in abdominal and pelvic surgery: systematic review and met-analysis. *BMJ*. 2013 Oct 3;347:f5588.
19. Ouaiïssi M, Gaujoux S, Veyrie N, Denève E, Brigand C, Castel B, et al. Post-operative adhesions after digestive surgery: their incidence and prevention: review of the literature. *J Visc Surg*. 2012 Apr;149(2):e104-114.
20. Lower AM, Hawthorn RJS, Clark D, Boyd JH, Finlayson AR, Knight AD, et al. Adhesion-related readmissions following gynaecological laparoscopy or laparotomy in Scotland: an epidemiological study of 24 046 patients. *Hum Reprod Oxf Engl*. 2004 Aug;19(8):1877–85.
21. Monk BJ, Berman ML, Montz FJ. Adhesions after extensive gynecologic surgery: clinical significance, etiology, and prevention. *Am J Obstet Gynecol*. 1994 May;170(5 Pt 1):1396–403.
22. Ellis H, Moran BJ, Thompson JN, Parker MC, Wilson MS, Menzies D, et al. Adhesion-related hospital readmissions after abdominal and pelvic surgery: a retrospective cohort study. *Lancet Lond Engl*. 1999 May 1;353(9163):1476–80.
23. Ellis H. The magnitude of adhesion related problems. *Ann Chir Gynaecol*. 1998;87(1):9–11.
24. Swank DJ, Swank-Bordewijk SCG, Hop WCJ, van Erp WFM, Janssen IMC, Bonjer HJ, et al. Laparoscopic adhesiolysis in patients with chronic abdominal pain: a blinded randomised controlled multi-centre trial. *Lancet Lond Engl*. 2003 Apr 12;361(9365):1247–51.
25. Van Der Krabben AA, Dijkstra FR, Nieuwenhuijzen M, Reijnen MM, Schaapveld M, Van Goor H. Morbidity and mortality of inadvertent enterotomy during adhesiotomy. *Br J*

Surg. 2000 Apr;87(4):467–71.

26. Wilson MS, Menzies D, Knight AD, Crowe AM. Demonstrating the clinical and cost effectiveness of adhesion reduction strategies. *Colorectal Dis Off J Assoc Coloproctology G B Irel.* 2002 Sep;4(5):355–60.
27. Wei G, Chen X, Wang G, Fan L, Wang K, Li X. Effect of Resveratrol on the Prevention of Intra-Abdominal Adhesion Formation in a Rat Model. *Cell Physiol Biochem.* 2016;33–46.
28. Bayhan Z, Zeren S, Kocak FE, Kocak C, Akcilar R, Kargı E, et al. Antiadhesive and anti-inflammatory effects of pirfenidone in postoperative intra-abdominal adhesion in an experimental rat model. *J Surg Res.* 2016 Apr;201(2):348–55.
29. Yan S, Yue Y, Zeng L, Yue J, Li W, Mao C, et al. Effect of intra-abdominal administration of ligustrazine nanoparticles nano spray on postoperative peritoneal adhesion in rat model: LNNS postoperative peritoneal adhesion. *J Obstet Gynaecol Res.* 2015 Dec;41(12):1942–50.
30. Jamshidi-Adegani F, Seyedjafari E, Gheibi N, Soleimani M, Sahmani M. Prevention of adhesion bands by ibuprofen-loaded PLGA nanofibers. *Biotechnol Prog [Internet].* 2016 Apr [cited 2016 Jun 24]; Available from: <http://doi.wiley.com/10.1002/btpr.2270>
31. Topal E, Ozturk E, Sen G, Yerci O, Yilmazlar T. A comparison of three fibrinolytic agents in prevention of intra-abdominal adhesions. *Acta Chir Belg.* 2010 Feb;110(1):71–5.
32. Xia Q, Liu Z, Wang C, Zhang Z, Xu S, Han CC. A Biodegradable Trilayered Barrier Membrane Composed of Sponge and Electrospun Layers: Hemostasis and Antiadhesion. *Biomacromolecules.* 2015 Sep 14;16(9):3083–92.
33. Hinoki A, Saito A, Kinoshita M, Yamamoto J, Saitoh D, Takeoka S. Polylactic acid nanosheets in prevention of postoperative intestinal adhesion and their effects on bacterial propagation in an experimental model: Polylactic acid nanosheets in prevention of postoperative intestinal adhesion and bacterial propagation. *Br J Surg.* 2016 May;103(6):692–700.
34. Bang S, Lee E, Ko Y-G, Kim WI, Kwon OH. Injectable pullulan hydrogel for the prevention of postoperative tissue adhesion. *Int J Biol Macromol.* 2016 Jun;87:155–62.
35. Zhu L, Zhang Y-Q. Postoperative anti-adhesion ability of a novel carboxymethyl chitosan from silkworm pupa in a rat cecal abrasion model. *Mater Sci Eng C.* 2016 Apr;61:387–95.
36. Chiang SC, Cheng CH, Moulton KS, Kasznica JM, Moulton SL. TNP-470 inhibits intraabdominal adhesion formation. *J Pediatr Surg.* 2000 Feb;35(2):189–96.
37. Greene AK, Alwayn IPJ, Nose V, Flynn E, Sampson D, Zurakowski D, et al. Prevention

of intra-abdominal adhesions using the antiangiogenic COX-2 inhibitor celecoxib. *Ann Surg*. 2005 Jul;242(1):140–6.

38. Becker JM, Dayton MT, Fazio VW, Beck DE, Stryker SJ, Wexner SD, et al. Prevention of postoperative abdominal adhesions by a sodium hyaluronate-based bioresorbable membrane: a prospective, randomized, double-blind multicenter study. *J Am Coll Surg*. 1996 Oct;183(4):297–306.

39. Dabrowski A, Lepère M, Zaranis C, Coelio C, Hauters P. Efficacy and safety of a resorbable collagen membrane COVA+™ for the prevention of postoperative adhesions in abdominal surgery. *Surg Endosc*. 2016 Jun;30(6):2358–66.

40. Brustia R, Scatton O, Soubrane O. Variation on a Theme: Alternative to Plastic Bag in ALPPS Procedures: Feasibility and Clinical Safety of COVA+™ Membrane in ALPPS Procedures. *World J Surg*. 2015 Dec;39(12):3023–7.

41. Kawanishi K, Nitta K, Yamato M, Okano T. Therapeutic Applications of Mesothelial Cell Sheets. *Ther Apher Dial Off Peer-Rev J Int Soc Apher Jpn Soc Apher Jpn Soc Dial Ther*. 2014 Sep 4;

42. Hwang JH, Kim IG, Lee JY, Piao S, Lee DS, Lee TS, et al. Therapeutic lymphangiogenesis using stem cell and VEGF-C hydrogel. *Biomaterials*. 2011 Jul;32(19):4415–23.

43. Kim Y-D, Jun YJ, Kim J, Kim CK. Effects of human adipose-derived stem cells on the regeneration of damaged visceral pleural mesothelial cells: a morphological study in a rabbit model. *Interact Cardiovasc Thorac Surg*. 2014 Sep;19(3):363–7.

44. Xu Y, Guan R, Lei H, Li H, Wang L, Gao Z, et al. Therapeutic Potential of Adipose-Derived Stem Cells-Based Micro-Tissues in a Rat Model of Postprostatectomy Erectile Dysfunction. *J Sex Med*. 2014 Jul 15;

45. Boquest AC, Shahdadfar A, Frønsdal K, Sigurjonsson O, Tunheim SH, Collas P, et al. Isolation and transcription profiling of purified uncultured human stromal stem cells: alteration of gene expression after in vitro cell culture. *Mol Biol Cell*. 2005 Mar;16(3):1131–41.

46. De Rosa A, De Francesco F, Tirino V, Ferraro GA, Desiderio V, Paino F, et al. A new method for cryopreserving adipose-derived stem cells: an attractive and suitable large-scale and long-term cell banking technology. *Tissue Eng Part C Methods*. 2009 Dec;15(4):659–67.

47. Berry DC, Stenesen D, Zeve D, Graff JM. The developmental origins of adipose tissue. *Dev Camb Engl*. 2013 Oct;140(19):3939–49.

48. Caserta F, Tchkonja T, Civelek VN, Prentki M, Brown NF, McGarry JD, et al. Fat depot origin affects fatty acid handling in cultured rat and human preadipocytes. *Am J Physiol Endocrinol Metab*. 2001 Feb;280(2):E238–247.

49. Tang W, Zeve D, Suh JM, Bosnakovski D, Kyba M, Hammer RE, et al. White fat progenitor cells reside in the adipose vasculature. *Science*. 2008 Oct 24;322(5901):583–6.
50. Yamamoto N, Akamatsu H, Hasegawa S, Yamada T, Nakata S, Ohkuma M, et al. Isolation of multipotent stem cells from mouse adipose tissue. *J Dermatol Sci*. 2007 Oct;48(1):43–52.
51. Rodeheffer MS, Birsoy K, Friedman JM. Identification of white adipocyte progenitor cells in vivo. *Cell*. 2008 Oct 17;135(2):240–9.
52. Baer PC. Adipose-derived mesenchymal stromal/stem cells: An update on their phenotype in vivo and in vitro. *World J Stem Cells*. 2014;6(3):256.
53. Bertram P, Tietze L, Hoopmann M, Treutner KH, Mittermayer C, Schumpelick V. Intraperitoneal transplantation of isologous mesothelial cells for prevention of adhesions. *Eur J Surg Acta Chir*. 1999 Jul;165(7):705–9.
54. Lucas PA, Warejcka DJ, Zhang L-M, Newman WH, Young HE. Effect of rat mesenchymal stem cells on development of abdominal adhesions after surgery. *J Surg Res*. 1996;62(2):229–232.
55. Kanda R, Hamada C, Kaneko K, Nakano T, Wakabayashi K, Hara K, et al. Paracrine effects of transplanted mesothelial cells isolated from temperature-sensitive SV40 large T-antigen gene transgenic rats during peritoneal repair. *Nephrol Dial Transplant Off Publ Eur Dial Transpl Assoc - Eur Ren Assoc*. 2014 Feb;29(2):289–300.
56. Hekking LH, van den Born J. Feasibility of mesothelial transplantation during experimental peritoneal dialysis and peritonitis. *Int J Artif Organs*. 2007 Jun;30(6):513–9.
57. Asano T, Takazawa R, Yamato M, Takagi R, Iimura Y, Masuda H, et al. Transplantation of an autologous mesothelial cell sheet prepared from tunica vaginalis prevents post-operative adhesions in a canine model. *Tissue Eng*. 2006 Sep;12(9):2629–37.
58. Asano T, Takazawa R, Yamato M, Kihara K, Okano T. Mesothelial cells from tunica vaginalis, a practical source for mesothelial transplantation. *Int J Artif Organs*. 2007 Jun;30(6):495–500.
59. Asano T, Takazawa R, Yamato M, Kageyama Y, Kihara K, Okano T. Novel and simple method for isolating autologous mesothelial cells from the tunica vaginalis. *BJU Int*. 2005 Dec;96(9):1409–13.
60. Rodbell M. LOCALIZATION OF LIPOPROTEIN LIPASE IN FAT CELLS OF RAT ADIPOSE TISSUE. *J Biol Chem*. 1964 Mar;239:753–5.
61. Hoffman AS. Hydrogels for biomedical applications. *Adv Drug Deliv Rev*. 2012 Dec;64:18–23.

62. Javaherzadeh M, Shekarchizadeh A, Kafaei M, Mirafshrieh A, Mosaffa N, Sabet B. Effects of Intraperitoneal Administration of Simvastatin in Prevention of Postoperative Intra-abdominal Adhesion Formation in Animal Model of Rat. *Bull Emerg Trauma*. 2016 Jul;4(3):156–60.
63. Bayhan Z, Zeren S, Kocak FE, Kocak C, Akcilar R, Kargı E, et al. Antiadhesive and anti-inflammatory effects of pirfenidone in postoperative intra-abdominal adhesion in an experimental rat model. *J Surg Res*. 2016 Apr;201(2):348–55.
64. Sahbaz A, Aynioglu O, Isik H, Gun BD, Cengil O, Erol O. Pycnogenol prevents peritoneal adhesions. *Arch Gynecol Obstet*. 2015 Dec;292(6):1279–84.
65. Diken Allahverdi T, Allahverdi E, Yayla S, Deprem T, Merhan O, Vural S, et al. Effects of alpha lipoic acid on intra-abdominal adhesion: an experimental study in a rat model. *Ulus Travma Ve Acil Cerrahi Derg Turk J Trauma Emerg Surg TJTES*. 2015 Jan;21(1):9–14.
66. Lee M-TG, Lee C-C, Wang H-M, Chou T-H, Wu M-C, Hsueh K-L, et al. Hypothermia Increases Tissue Plasminogen Activator Expression and Decreases Post-Operative Intra-Abdominal Adhesion. *PLoS One*. 2016;11(9):e0160627.
67. De Clercq K, Schelfhout C, Bracke M, De Wever O, Van Bockstal M, Ceelen W, et al. Genipin-crosslinked gelatin microspheres as a strategy to prevent postsurgical peritoneal adhesions: In vitro and in vivo characterization. *Biomaterials*. 2016 Jul;96:33–46.
68. Bianchi E, Boekelheide K, Sigman M, Lamb DJ, Hall SJ, Hwang K. Ghrelin Inhibits Post-Operative Adhesions via Blockage of the TGF- $\beta$  Signaling Pathway. *PLoS One*. 2016;11(4):e0153968.
69. Bove GM, Chapelle SL. Visceral mobilization can lyse and prevent peritoneal adhesions in a rat model. *J Bodyw Mov Ther*. 2012 Jan;16(1):76–82.
70. Whang SH, Astudillo JA, Sporn E, Bachman SL, Miedema BW, Davis W, et al. In Search of the Best Peritoneal Adhesion Model: Comparison of Different Techniques in a Rat Model. *J Surg Res*. 2011 May;167(2):245–50.
71. Gaertner WB, Hagerman GF, Felemovicius I, Bonsack ME, Delaney JP. Two Experimental Models for Generating Abdominal Adhesions. *J Surg Res*. 2008 May;146(2):241–5.
72. Lauder CIW, Garcea G, Strickland A, Maddern GJ. Use of a modified chitosan-dextran gel to prevent peritoneal adhesions in a rat model. *J Surg Res*. 2011 Dec;171(2):877–82.
73. Kawanishi K, Yamato M, Sakiyama R, Okano T, Nitta K. Peritoneal cell sheets composed of mesothelial cells and fibroblasts prevent intra-abdominal adhesion formation in a rat model: Peritoneal cell sheets prevent abdominal adhesions. *J Tissue Eng Regen Med*. 2013 Dec;n/a-n/a.

74. Cassidy MR, Sherburne AC, Heydrick SJ, Stucchi AF. Combined intraoperative administration of a histone deacetylase inhibitor and a neurokinin-1 receptor antagonist synergistically reduces intra-abdominal adhesion formation in a rat model. *Surgery*. 2015 Mar;157(3):581–9.
75. Sakai S, Ueda K, Taya M. Peritoneal adhesion prevention by a biodegradable hyaluronic acid-based hydrogel formed in situ through a cascade enzyme reaction initiated by contact with body fluid on tissue surfaces. *Acta Biomater*. 2015 Sep;24:152–8.
76. Kutuk MS, Ozgun MT, Batukan C, Ozcelik B, Basbug M, Ozturk A. Oral tadalafil reduces intra-abdominal adhesion reformation in rats. *Hum Reprod Oxf Engl*. 2012 Mar;27(3):733–7.
77. Tahmasebi S, Tahamtan M, Tahamtan Y. Prevention by rat amniotic fluid of adhesions after laparotomy in a rat model. *Int J Surg Lond Engl*. 2012;10(1):16–9.
78. Wallwiener CW, Kraemer B, Wallwiener M, Brochhausen C, Isaacson KB, Rajab TK. The extent of adhesion induction through electrocoagulation and suturing in an experimental rat study. *Fertil Steril*. 2010 Mar;93(4):1040–4.
79. Kraemer B, Scharpf M, Planck C, Tsaousidis C, Enderle MD, Neugebauer A, et al. Randomized experimental study to investigate the peritoneal adhesion formation of conventional monopolar contact coagulation versus noncontact argon plasma coagulation in a rat model. *Fertil Steril*. 2014 Oct;102(4):1197–202.
80. Agacayak E, Tunc SY, Icen MS, Alabalik U, Findik FM, Yuksel H, et al. Honokiol decreases intra-abdominal adhesion formation in a rat model. *Gynecol Obstet Invest*. 2015;79(3):160–7.
81. Karatas A, Ozlu T, Ozyalvacli G, Tosun M, Cetinkaya A, Donmez ME, et al. Intraperitoneal *Nigella sativa* for Prevention of Postoperative Intra-Abdominal Adhesions in Rats. *J Invest Surg*. 2014 Dec;27(6):319–26.
82. Keskin HL, Sirin YS, Keles H, Turgut O, Ide T, Avsar AF. The aromatase inhibitor letrozole reduces adhesion formation after intraperitoneal surgery in a rat uterine horn model. *Eur J Obstet Gynecol Reprod Biol*. 2013 Apr;167(2):199–204.
83. Kelekci S, Yilmaz B, Oguz S, Zergeroğlu S, Inan I, Tokucoglu S. The efficacy of a hyaluronate/carboxymethylcellulose membrane in prevention of postoperative adhesion in a rat uterine horn model. *Tohoku J Exp Med*. 2004 Nov;204(3):189–94.
84. Oncel M, Remzi FH, Connor J, Fazio VW. Comparison of cecal abrasion and multiple-abrasion models in generating intra-abdominal adhesions for animal studies. *Tech Coloproctology*. 2005 Apr;9(1):29–33.
85. bipolar electrocoagulation [Internet]. *TheFreeDictionary.com*. [cited 2017 Mar 28].

Available from: <http://medical-dictionary.thefreedictionary.com/bipolar+electrocoagulation>

86. Link WJ, Incropera FP, Glover JL. The plasma scalpel. *Med Prog Technol.* 1976;4(3):123–31.
87. Foley-Comer AJ, Herrick SE, Al-Mishlab T, Prêle CM, Laurent GJ, Mutsaers SE. Evidence for incorporation of free-floating mesothelial cells as a mechanism of serosal healing. *J Cell Sci.* 2002 Apr 1;115(Pt 7):1383–9.
88. Ellis H. The hazards of surgical glove dusting powders. *Surg Gynecol Obstet.* 1990 Dec;171(6):521–7.
89. Jagelman DG, Ellis H. Starch and intraperitoneal adhesion formation. *Br J Surg.* 1973 Feb;60(2):111–4.
90. van den Tol MP, Haverlag R, van Rossen ME, Bonthuis F, Marquet RL, Jeekel J. Glove powder promotes adhesion formation and facilitates tumour cell adhesion and growth. *Br J Surg.* 2001 Sep;88(9):1258–63.
91. Topcu O, Kuzu I, Karayalcin K. Effects of peritoneal lavage with scolicalid agents on survival and adhesion formation in rats. *World J Surg.* 2006 Jan;30(1):127–33.
92. Laufman H, Rubel T. Synthetic absorbable sutures. *Surg Gynecol Obstet.* 1977 Oct;145(4):597–608.
93. Chelala E, Baraké H, Estievenart J, Dessily M, Charara F, Allé JL. Long-term outcomes of 1326 laparoscopic incisional and ventral hernia repair with the routine suturing concept: a single institution experience. *Hernia J Hernias Abdom Wall Surg.* 2016 Feb;20(1):101–10.
94. Tandon A, Shahzad K, Pathak S, Oommen CM, Nunes QM, Smart N. Parietex<sup>TM</sup> Composite mesh versus DynaMesh<sup>(®)</sup>-IPOM for laparoscopic incisional and ventral hernia repair: a retrospective cohort study. *Ann R Coll Surg Engl.* 2016 Nov;98(8):568–73.
95. Binda MM, Molinas CR, Hansen P, Koninckx PR. Effect of desiccation and temperature during laparoscopy on adhesion formation in mice. *Fertil Steril.* 2006 Jul;86(1):166–75.
96. Butz N, Müller SA, Treutner K-H, Anurov M, Titkova S, Oettinger AP, et al. The influence of blood on the efficacy of intraperitoneally applied phospholipids for prevention of adhesions. *BMC Surg.* 2007 Jul 25;7:14.
97. De Iaco PA, Muzzupapa G, Bigon E, Pressato D, Donà M, Pavesio A, et al. Efficacy of a hyaluronan derivative gel in postsurgical adhesion prevention in the presence of inadequate hemostasis. *Surgery.* 2001 Jul;130(1):60–4.
98. Leach RE, Burns JW, Dawe EJ, SmithBarbour MD, Diamond MP. Reduction of postsurgical adhesion formation in the rabbit uterine horn model with use of

hyaluronate/carboxymethylcellulose gel. *Fertil Steril*. 1998 Mar;69(3):415–8.

99. Saed GM, Fletcher NM, Diamond MP. The Creation of a Model for Ex Vivo Development of Postoperative Adhesions. *Reprod Sci*. 2016 May 1;23(5):610–2.

100. Experience in Primary Culture of Human Peritoneal Mesothelial Cell. *Chin J Physiol* [Internet]. 2012 [cited 2017 May 5]; Available from: <http://www.cps.org.tw/docs/Vol55%20No4%20Article%207.pdf>

101. Aroeira LS, Loureiro J, González-Mateo GT, Fernandez-Millara V, del Peso G, Sánchez-Tomero JA, et al. Characterization of epithelial-to-mesenchymal transition of mesothelial cells in a mouse model of chronic peritoneal exposure to high glucose dialysate. *Perit Dial Int J Int Soc Perit Dial*. 2008 Nov;28 Suppl 5:S29-33.

102. Katz S, Balogh P, Nagy N, Kiss AL. Epithelial-To-Mesenchymal Transition Induced by Freund's Adjuvant Treatment in Rat Mesothelial Cells: A Morphological and Immunocytochemical Study. *Pathol Oncol Res*. 2012 Jul;18(3):641–9.

103. Demir AY, Groothuis PG, Nap AW, Punyadeera C, de Goeij AFPM, Evers JLH, et al. Menstrual effluent induces epithelial-mesenchymal transitions in mesothelial cells. *Hum Reprod Oxf Engl*. 2004 Jan;19(1):21–9.

104. Dhanasekaran M, Indumathi S, Kanmani A, Poojitha R, Revathy KM, Rajkumar JS, et al. Surface antigenic profiling of stem cells from human omentum fat in comparison with subcutaneous fat and bone marrow. *Cytotechnology*. 2012 Oct;64(5):497–509.

105. Iyyanki TS, Dunne LW, Zhang Q, Hubenak J, Turza KC, Butler CE. Adipose-Derived Stem-Cell-Seeded Non-Cross-Linked Porcine Acellular Dermal Matrix Increases Cellular Infiltration, Vascular Infiltration, and Mechanical Strength of Ventral Hernia Repairs. *Tissue Eng Part A*. 2015 Feb;21(3–4):475–85.

106. Yu G, Wu X, Kilroy G, Halvorsen Y-DC, Gimble JM, Floyd ZE. Isolation of Murine Adipose-Derived Stem Cells. In: Gimble JM, Bunnell BA, editors. *Adipose-Derived Stem Cells* [Internet]. Totowa, NJ: Humana Press; 2011 [cited 2015 Mar 24]. p. 29–36. Available from: [http://link.springer.com/10.1007/978-1-61737-960-4\\_3](http://link.springer.com/10.1007/978-1-61737-960-4_3)

107. Ghorbani A, Jalali SA, Varedi M. Isolation of adipose tissue mesenchymal stem cells without tissue destruction: a non-enzymatic method. *Tissue Cell*. 2014 Feb;46(1):54–8.

108. Colleoni S, Bottani E, Tessaro I, Mari G, Merlo B, Romagnoli N, et al. Isolation, growth and differentiation of equine mesenchymal stem cells: effect of donor, source, amount of tissue and supplementation with basic fibroblast growth factor. *Vet Res Commun*. 2009 Dec;33(8):811–21.

109. Chavez-Munoz C, Nguyen KT, Xu W, Hong S-J, Mustoe TA, Galiano RD. Transdifferentiation of Adipose-Derived Stem Cells into Keratinocyte-Like Cells: Engineering

a Stratified Epidermis. Pant AB, editor. PLoS ONE. 2013 Dec 2;8(12):e80587.

110. Zhang M, Xu M, Zhou Z, Zhang K, Zhou J, Zhao Y, et al. The differentiation of human adipose-derived stem cells towards a urothelium-like phenotype in vitro and the dynamic temporal changes of related cytokines by both paracrine and autocrine signal regulation. PLoS One. 2014;9(4):e95583.

111. Wang C, Yin S, Cen L, Liu Q, Liu W, Cao Y, et al. Differentiation of adipose-derived stem cells into contractile smooth muscle cells induced by transforming growth factor-beta1 and bone morphogenetic protein-4. Tissue Eng Part A. 2010 Apr;16(4):1201–13.

112. Kim H, Mizuno M, Furuhashi K, Katsuno T, Ozaki T, Yasuda K, et al. Rat adipose tissue-derived stem cells attenuate peritoneal injuries in rat zymosan-induced peritonitis accompanied by complement activation. Cytotherapy. 2014 Mar;16(3):357–68.

113. Ulrich D, Muralitharan R, Gargett CE. Toward the use of endometrial and menstrual blood mesenchymal stem cells for cell-based therapies. Expert Opin Biol Ther. 2013 Oct;13(10):1387–400.

114. Atala A, Kasper FK, Mikos AG. Engineering complex tissues. Sci Transl Med. 2012 Nov 14;4(160):160rv12.

115. Asti A, Gioglio L. Natural and synthetic biodegradable polymers: different scaffolds for cell expansion and tissue formation. Int J Artif Organs. 2014 Apr 15;37(3):187–205.

116. Zou Z, Zheng Q, Wu Y, Guo X, Yang S, Li J, et al. Biocompatibility and bioactivity of designer self-assembling nanofiber scaffold containing FGL motif for rat dorsal root ganglion neurons. J Biomed Mater Res A. 2010 Dec 15;95A(4):1125–31.

117. Guo J, Su H, Zeng Y, Liang Y-X, Wong WM, Ellis-Behnke RG, et al. Reknitting the injured spinal cord by self-assembling peptide nanofiber scaffold. Nanomedicine Nanotechnol Biol Med. 2007 Dec;3(4):311–21.

118. Horii A, Wang X, Gelain F, Zhang S. Biological Designer Self-Assembling Peptide Nanofiber Scaffolds Significantly Enhance Osteoblast Proliferation, Differentiation and 3-D Migration. Isalan M, editor. PLoS ONE. 2007 Feb 7;2(2):e190.

119. Dégano IR, Quintana L, Vilalta M, Horna D, Rubio N, Borrós S, et al. The effect of self-assembling peptide nanofiber scaffolds on mouse embryonic fibroblast implantation and proliferation. Biomaterials. 2009 Feb;30(6):1156–65.

120. Song H, Zhang L, Zhao X. Hemostatic Efficacy of Biological Self-Assembling Peptide Nanofibers in a Rat Kidney Model. Macromol Biosci. 2010 Jan 11;10(1):33–9.

121. Cavalcanti BN, Zeitlin BD, Nör JE. A hydrogel scaffold that maintains viability and supports differentiation of dental pulp stem cells. Dent Mater. 2013 Jan;29(1):97–102.

122. Dissanayaka WL, Hargreaves KM, Jin L, Samaranayake LP, Zhang C. The interplay of dental pulp stem cells and endothelial cells in an injectable peptide hydrogel on angiogenesis and pulp regeneration in vivo. *Tissue Eng Part A*. 2015 Feb;21(3–4):550–63.
123. Aligholi H, Rezayat SM, Azari H, Ejtemaei Mehr S, Akbari M, Modarres Mousavi SM, et al. Preparing neural stem/progenitor cells in PuraMatrix hydrogel for transplantation after brain injury in rats: A comparative methodological study. *Brain Res*. 2016 Jul 1;1642:197–208.
124. Moradi F, Bahktiari M, Joghataei MT, Nobakht M, Soleimani M, Hasanzadeh G, et al. BD PuraMatrix peptide hydrogel as a culture system for human fetal Schwann cells in spinal cord regeneration. *J Neurosci Res*. 2012 Dec;90(12):2335–48.
125. Tokunaga M, Liu M-L, Nagai T, Iwanaga K, Matsuura K, Takahashi T, et al. Implantation of cardiac progenitor cells using self-assembling peptide improves cardiac function after myocardial infarction. *J Mol Cell Cardiol*. 2010 Dec;49(6):972–83.
126. Guo H, Cui G, Wang H, Tan Y. Transplantation of marrow-derived cardiac stem cells carried in designer self-assembling peptide nanofibers improves cardiac function after myocardial infarction. *Biochem Biophys Res Commun*. 2010 Aug 13;399(1):42–8.
127. Akiyama N, Yamamoto-Fukuda T, Takahashi H, Koji T. In situ tissue engineering with synthetic self-assembling peptide nanofiber scaffolds, PuraMatrix, for mucosal regeneration in the rat middle-ear. *Int J Nanomedicine*. 2013;8:2629–40.
128. Mason C, Dunnill P. A brief definition of regenerative medicine. *Regen Med*. 2008 Jan;3(1):1–5.
129. Fraser JK, Hicok KC, Shanahan R, Zhu M, Miller S, Arm DM. The Celution® System: Automated Processing of Adipose-Derived Regenerative Cells in a Functionally Closed System. *Adv Wound Care*. 2014 Jan 1;3(1):38–45.
130. Quentin Denost. Ingénierie tissulaire en chirurgie colorectale : du défaut pariétal au remplacement d'organe : étude in vitro et in vivo. *Biologie cellulaire*. Université de Bordeaux, 2014. Français. <NNT : 2014BORD0188>. <tel-01165145>.
131. Lehmann J, Schulz RM, Sanzenbacher R. [Strategic considerations on the design and choice of animal models for non-clinical investigations of cell-based medicinal products]. *Bundesgesundheitsblatt Gesundheitsforschung Gesundheitsschutz*. 2015 Nov;58(11–12):1215–24.
132. Bubela T, McCabe C. Value-Engineered Translation for Regenerative Medicine: Meeting the Needs of Health Systems. *Stem Cells Dev*. 2013 Dec 1;22(Suppl 1):89–93.
133. Corbett MS, Webster A, Hawkins R, Woolacott N. Innovative regenerative medicines in the EU: a better future in evidence? *BMC Med*. 2017 Mar 8;15(1):49.



## COMMUNICATIONS

### Oral presentation

- 2015-07-02: "BioMEMS and Cancer - Progress with SMMiL-E", Lille, France
- 2016-05-20: Canceropole Nord Ouest, Deauville, France
- 2016-10-24: 2nd European Workshop on Regenerative Medicine, Bordeaux, France
- 2016-09-15: Journées André Verbert, Ecole doctorale de Lille, Lille, France
- 2016-12-10: LIMMS and SMMIL'E workshops, Tokyo, Japan
- 2017-09-08: 28th annual conference of the European Society for Biomaterials, Athens

### Poster presentation

- 2015 09 28: LIMMS Workshop "Beyond the Frontiers of Nanoscience and Biosystems" and the "EUJO-LIMMS Final Workshop : Paving the Way for a Sustainable EU laboratory in Japan", Lille, France
- 2015 10 12: BIOMAT 2015, Ile de Ré, France
- 2016-12-09: Annual congress of CNGOF, collège national des gynécologues et obstétriciens français, Montpellier, France
- 2017-06-26: European chapter meeting of the Tissue Engineering and Regenerative Medicine International Society, Davos, Switzerland

## PUBLICATIONS

- [Surgery](#). 2017 Jun 27. pii: S0039-6060(17)30323-9.

Autologous peritoneal grafts permit rapid reperitonealization and prevent postoperative abdominal adhesions in an experimental rat study.

[Bresson L](#)<sup>1</sup>, [Leblanc E](#)<sup>2</sup>, [Lemaire AS](#)<sup>2</sup>, [Okitsu T](#)<sup>3</sup>, [Chai F](#)<sup>4</sup>.

- Submitted in Journal of Surgical Research.

"Review of animal models of post-operative abdominal adhesions"

[Bresson L](#)<sup>1</sup>, [Lemaire AS](#)<sup>2</sup>, [Chai F](#)<sup>4</sup>.